Analysis and Modeling of Coal Softening and Resolidification under Rapid Heating

Koichi MATSUOKA

(1)

Analysis and Modeling of Coal Softening and Resolidification under Rapid Heating

Koichi Matsuoka

Hokkaido University

1997

CONTENTS

Chapter 1 General Introduction

1.1 Background

The annual domestic production of steel amounts to *ca.* 90-100 Mt which is roughly equivalent to 1 ton/person. Steel is produced from iron ore (main components; Fe_2O_3 and Fe_3O_4) by reduction in either blast furnace processes or electric furnace processes. The former processes produce 70 % of the total production while the latter 30 %. In the former processes coke is used not only as a reductant and heat source to promote the ore reduction but also as a mechanically structural material to control the flow of ore pellets in the moving-bed furnace. Thus, coke consumption is approximately 32 Mt/Y for the above-mentioned steel production, as shown in **Fig.1.1**. Demand for coke in future is predicted to decrease slowly to 25 Mt/Y in 2020. On the other hand, a sharp decrease of coke production is also predicted in the early next century and a shortage of coke is due to take place in 2003 when the demand exceed the production, as described in **Fig.1.2**.

In conventional processes, coke is produced from expensive caking coals in a batch oven. The average life of the ovens is about 30 to 40 years and, now, most of the ovens which were constructed after the World War II in Japan are facing to their shut-down at the beginning of the next century. In addition, the existing processes have the following defects[1-3] to be overcome towards the next century:

1) The batchwise production is not flexible enough to meet the fluctuation of consumption.

2) Their feedstock is strictly limited to expensive caking coals.

3) They are operated at high temperatures with uneconomical energy consumption.

To overcome these defects there have so far been proposed three different ideas. The smelting reduction processes,[2] which employ non-caking coal as a reductant, are expected to replace the blast furnace processes. Efforts have been made to increase the amount of pulverized non-caking coal injected to the blast furnace as a reductant. Both aims to suppress the coke consumption. However, at present, the smelting reduction processes seem to have difficulties in their scale-up and the pulverized coal injection contributes to reducing coke consumption to a limit extent.

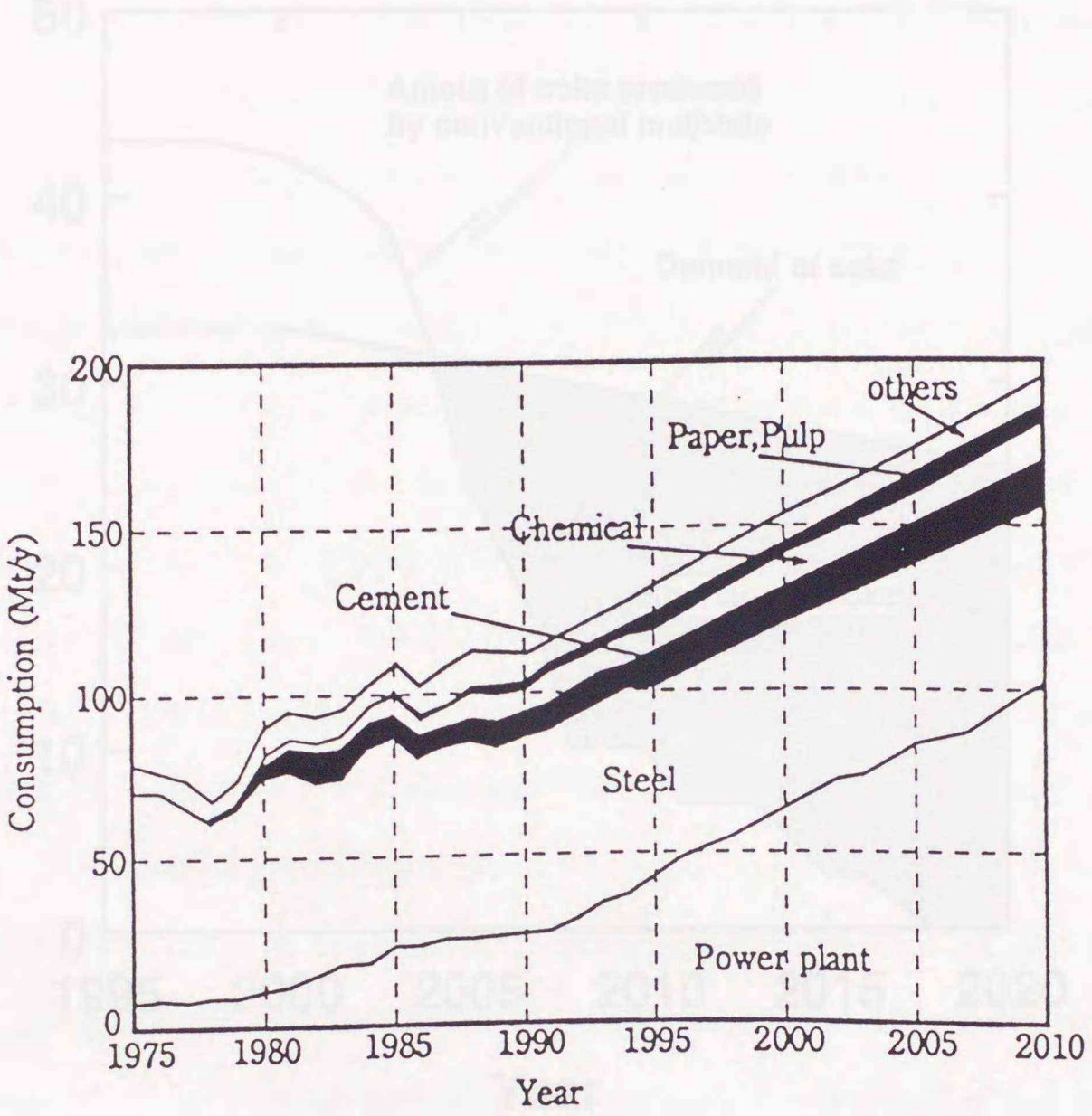

Fig. 1.1 Trend of coal consumption in Japan.[1)]

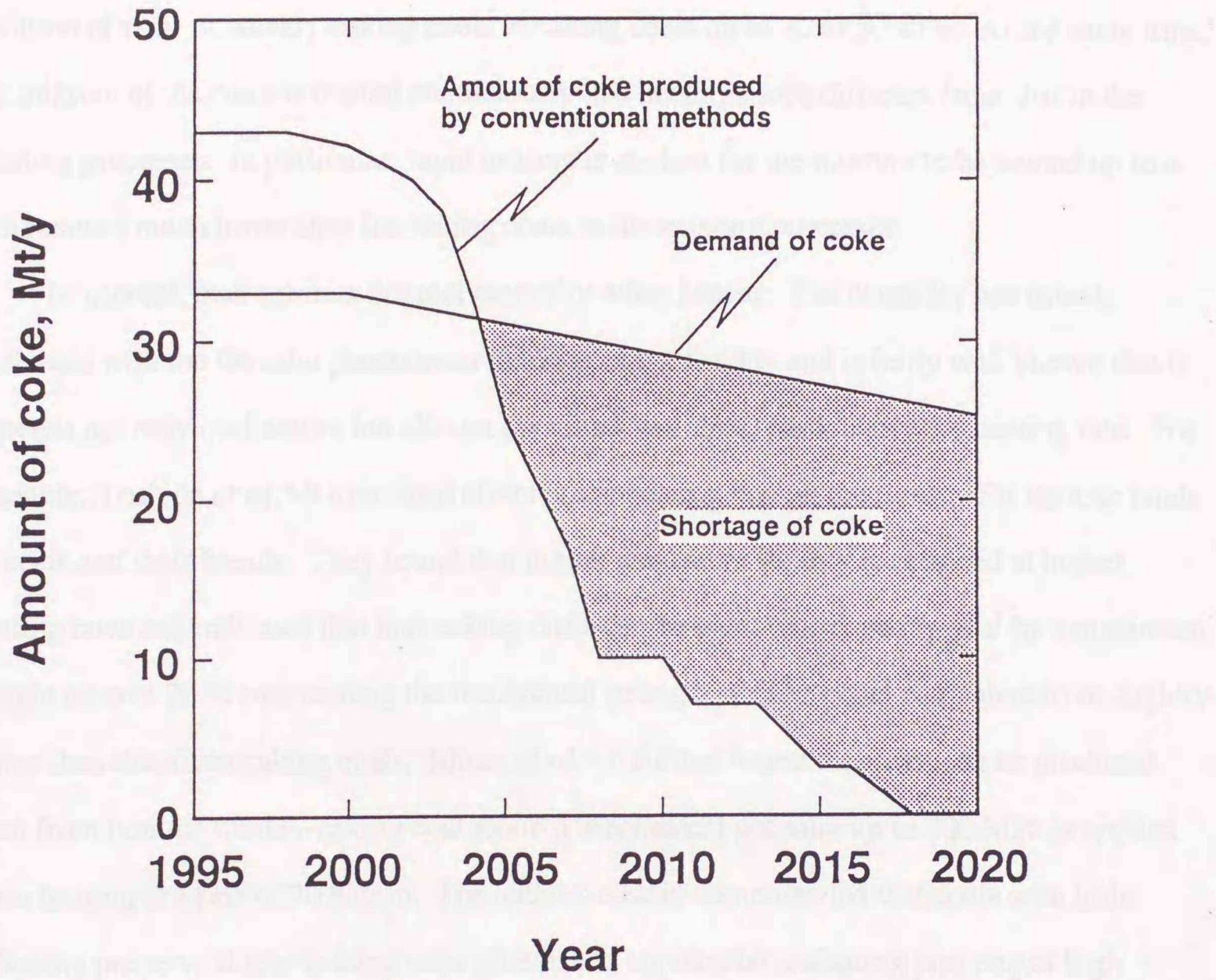

Fig. 1.2 Prediction of coke demand toward next century in Japan.[1,3)]

On the other hand, there has recently been initiated a national research project called "SCOPE 21 (Super Coke Oven for Productivity and Environment Enhancement toward the 21st Century) " by MITI which aims to develop a novel cokemaking process to overcome the above defects in the existing cokemaking processes. The process under development considers addition of non- or weakly-caking coals to caking coals up to 20 to 50 wt%. At the same time, the mixture of the coals is treated continuously in a heating mode different from that in the existing processes. In particular, rapid heating is applied for the mixture to be heated up to a temperature much lower than for caking coals in the existing processes.

In general, coal exhibits thermal plasticity when heated. The plasticity has usually evaluated with the Gieseler plastometer in terms of the fluidity and is fairly well known that it depends not only coal nature but also on operating variables, particularly the heating rate. For example, Yoshida *et al.*[4,5] examined effect of the heating rate on the fluidity for various kinds of coals and their blends. They found that higher maximum fluidity is obtained at higher heating rates and indicated that non-caking coals can be blent with a caking coal by a maximum weight ratio of 20 % maintaining the mechanical strength of coke pellet equivalent to or slightly lower than that from caking coals. Miura *et al.*[6-9] further found that coke can be produced even from non- or weakly-caking coal alone if mechanical pressure up to 100 MPa is applied upon heating at a rate of 20 K/min. The authors clearly demonstrated that coals with little softening property at low heating rates give rise to appreciable softening property at high heating rates.[10] All of these experimental findings imply that non- or weakly-caking coals can be used for coke production under rapid heating. In the novel process, coal is supposed to be rapidly heated up to a temperature of 723 to 773 K and to be pelletized before further heating at a slower rate up to *ca.* 1073 K for carbonization.

1.2 Previous Studies

1.2.1 Viscosity Model

When heated beyond *ca.* 600 K, coal undergoes pyrolysis and carbonization reactions. For caking coals the former reaction extensively promotes softening of the bulk of coal while the latter resolidification, accompanying volatiles release. As mentioned in the preceding

section, the softening and resolidification processes have long been evaluated on the basis of the fluidity defined by the Gieseler plastometry.

Van Kreveren and co-workers[11-13] measured the fluidity of coals with the Gieseler plastometer and assumed that the following consecutive reaction would occur.

$$\text{coal} \rightarrow \text{metaplast} \rightarrow \text{semicoke}$$

Fitzgerald[14,15] analyzed the fluidity by a model based on the above reaction. Considering increase of the fluidity due to the formation of the metaplast, which behaves as a liquid, the fluidity was described by the following equation:

$$f_r = (1-\phi_S)^{\lambda}$$

where f_r, ϕ_S and λ mean the relative fluidity, the concentration of solids, *i.e.*, unreacted coal, semicoke and ash, and the Einstein coefficient (= 2.5), respectively. They found that the fluidity changes with temperature through a maximum in its time or temperature history and that the equation is applicable only for explanation of the fluidity data for a narrow range of temperature beyond the temperature at the maximum, where the fluidity decreases monotonously. Fong *et al.*[16,17] also measured the fluidity of bituminous coals at high heating rates employing their own plastometer. They evaluated changes in viscosity which is reduced from the fluidity by applying the expression proposed by Frankel and Acrivos[18] for high solid-concentration suspensions:

$$\eta_r = 9/8[(\phi_S/\phi_m)^{1/3}/\{1-(\phi_S/\phi_m)^{1/3}\}]$$

where η_r, ϕ_S and ϕ_m respectively denote the relative viscosity of suspension, the volume fraction of solids and the maximum value of ϕ_S. Assuming that the metaplast itself has a constant viscosity with temperature, they introduced a critical value, ϕ_m , for ϕ_S based on the minimum fraction of metaplast physically required for the formation of suspension. Further,

Matsui *et al.*[19] explained the maximum fluidity for a blended coal by a model assuming that the molten coal is in the state of a suspension. The model is based on Mori's equation[20] to correlate the viscosity with the solid volume fraction, which is expressed as

$$\eta_r = 1 + \frac{3}{1/\phi_S - 1/0.52}$$

The equation was demonstrated to describe the minimum viscosity reduced from observed maximum fluidity using Morotomi's correlation.[21] They, however, calculated the minimum viscosity at a temperature range considerably different from that actually giving the minimum viscosity.

Recently, Solomon *et al.*[22] have proposed an empirical model based on their macromolecular network pyrolysis model[23] which lumps the product residue as a mixture of liquid and solid macromolecules. The solid macromolecules were assumed to be slurried with liquid molecules and a viscosity equation for slurry was applied to explain existing Gieseler fluidity data. The viscosity model is based on Mooney's equation[24] for slurry combined with Andrade's equation[25] for liquid given by

$$\eta_a = k_{V0} \exp\{E_V / (RT)\} \exp \frac{k_E \phi_S}{1 - \phi_S / \phi_C}$$

where η_a, k_{V0}, E_V, k_E, ϕ_S and ϕ_C respectively denote the bulk viscosity, the frequency factor and the activation energy for the viscosity, the Einstein coefficient, the volume fraction of solids and a critical value at which η_a goes to infinity (the gel point). The model contains the viscosity of liquid molecules given as a function of temperature, which has not been considered in the preceding models. By adjusting the equation to the data, they deduced the activation energies for the liquid viscosity which ranges from 210 to 420 kJ/mol depending on temperature. However, the product yields were not compared with those observed and, again, the activation energy was treated as one of the adjustable parameters. In summary, most of the above-mentioned models gave good fits to data because their model parameters were chosen to fit the

data for particular coals studied in a limited number of experiments at a narrow range of heating rate or holding temperature.

In the above-mentioned models the metaplast is considered to behave as a liquid and to be an intermediate responsible for softening. Nonetheless, the metaplast has so far remains as a fictitious species and left without being defined experimentally. This is mainly because of the difficulty to separate it from others in the simultaneous coal melting and softening processes. The metaplast is ambiguously defined as a group of species with low molecular mass which dissolves into the residual high-molecular mass components. Therefore, the metaplast in the models has been treated as a parameter to fit the models to experimental data. Thus, efforts have been focused on experimental quantification of the metaplast. Solvent extraction technique has one of the methods usually adopted to the quantification and there have been many investigations to derive relationship between the yield of solvent extracts from coal and the fluidity.[8,18,26-28] For example, Takanohashi *et al.*[27] found that CS_2-NMP extraction yield of the heat-treated coals is higher for coals having a higher fluidity. Further, Seki *et al.*[28] measured the fluidity of a coal and of its residues with different CS_2-NMP extraction yields and found that the fluidity of the residues are always lower than that of coal. They also found that the temperature range in which the fluidity varies is narrower for the residue with a higher extraction yield. Fong *et al.*[18] attributed coal softening to pyridine extract from their heat-treated coals without any reasonable examination. Similar attempts were carried out employing chloroform[29,31] as an extraction solvent to determine the amount of metaplast. The yields were compared with the fluidity and were suggested to have a certain relation to the softening characteristics.

Generally, coal extracts comprise a wide variety of compounds. Therefore, proper solvents have to be chosen to obtain the extracts to have a composition and property being invariable along with the progress of pyrolysis and carbonization. Hayashi *et al.*[35,36] reported that the yields of pyridine and chloroform extracts varied widely with pyrolysis but their average structure and molecular mass distribution exhibited little dependency on the yields. This findings seem to be interesting although obtained at heating rates much higher than those for the conventional cokemaking processes.

1.2.2 Gieseler Fluidity

In all previous models, apparent viscosity of coal has been evaluated in terms of the fluidity from the Gieseler plastometry. The plastometry employs a bed of coal particles and detects the torque mainly arisen from inter-particle forces which more or less depend on packing state of the bed. Morotomi *et al.*[22] reported that the Weissenberg effect is involved in measurements of the fluidity for caking coals with a Gieseler plastometer. Furthermore, Lloyd *et al.*[42] observed the fluidity for forty high-volatile bituminous coals and showed that the maximum fluidity ranges from 10^2 to 10^{12} ddpm depending on the coal nature. According to Soth and Russel,[43] fluidity of 1 ddpm is equivalent to a reciprocal viscosity of 10^{-6} $Pa^{-1} \cdot s^{-1}$. Thus, the viscosities reduced from maximum fluidity on the basis of their correlation ranged from 10^{-6} to 10^4 $Pa \cdot s$. Considering the viscosity much lower than that of water, their correlation seems fairly unreasonable.

In addition, the Gieseler plastometers are not applicable to evaluate the effect of the heating rate in a wide range. To meet measurements in a wide range of the heating rate, Deng *et al.*[44] adopted a needle penetration technique which is frequently applied to measure the viscosity of melts of polymers, pitches and asphalts. The needle penetration depth together with the volumetric dilation ratio was measured as a function of time upon heating for discs quarried from coal lump and for compressed pellets of pulverized coal particles having the same shape and size as the discs. They compared characteristics of dilation of a disc with those of the fluidity for Drummond coal, demonstrating that the whole temperature range for occurrence of the dilation roughly coincides with that for change in the fluidity. Further, they derived apparent viscosities of the specimens on the basis of an equation of motion.[45] Finding little difference between the apparent viscosities for the discs and pellets, they treated the viscosities derived for the latters as those for coal itself.

1.3 Objectives

This study aims to elucidate and model characteristics of coal softening and resolidification particularly at heating rates higher than those in the existing investigations as well as in the conventional cokemaking processes. Systematic measurements have been

conducted to quantity the dependence of the apparent coal viscosity on operating variables such as the heating rate, holding temperature and gas pressure. The needle penetration and the dilation characteristics have been measured with a novel needle penetrometer combined with dilatometer. The rates of volatiles release and pyridine extract formation have also been measured to evaluate the kinetics of pyrolysis and carbonization reactions. By organizing the results from the measurements, a model has been proposed for the coal viscosity and its applicability has been examined for the experimental results of the needle penetration characteristics. The model has been verified to explain reasonably well the observed effects of coal nature and heating rate on the needle penetration.

This thesis consists of six chapters which are summarized as follows:

General introduction is given in Chap.1 together with the background of the present study and the critical review of existing investigations relating to the study.

Chapter 2 describes characteristics of the needle penetration into coal pellet and the volumetric dilation of the pellet along with heating observed under various operating conditions for six kinds of coals. The net needle penetration depth obtained from the observed results are analyzed by the equation of needle motion to estimate the apparent coal viscosity. It is shown that for all cases the apparent viscosities upon heating vary with temperature in the range of 10^4 to 10^{12} Pa·s and that their activation energies estimated are larger than 400 kJ/mol which are too high as those for single species being chemically invariable upon heating.

Hence, in Chap. 3 is described results of experimental characterization of pyrolysis and carbonization reactions conducted under the same conditions as those in the needle penetration experiment. Based on the existing investigations and the results described in the previous chapter, coal softening is presumed to be accompanied by conversion of coal to semicoke *via* a plastic intermediate. Different methods such as a DSC, a ^{1}H NMR and solvent extraction are examined for experimental identification of the intermediate. Among them the yields of pyridine extracts are shown to vary having a close correspondence with the observed softening characteristics. From penetration experiments employing a pellet of the extract, it is confirmed that the extract behaves as a liquid with temperature dependency of the viscosity much less than parent coals. The extract is thus defined as the plastic intermediate.

In Chap.4, experimental results are described of characteristics of volatile release from the pellet which takes place upon heating in parallel to the pyrolysis and carbonization reactions. It is demonstrated that change of the mass loss of pellet with time occurs in a higher temperature range at higher heating rate while the ultimate mass loss is independent of the heating rate. A kinetic model is developed which assumes that coal consists of two components having different reactivities for pyrolysis; one converting to semicoke *via* the intermediate along with the volatiles release and the other converting to volatiles directly. The kinetic parameters involved in the model are analytically determined and the model is shown to comprehensively explain the mass loss characteristics for the different coals.

Chapter 5 organizes all the findings described in the preceding chapters as a mathematical model for prediction of the apparent coal viscosity. The model is based upon a pseudo-steady state equation of needle motion which was confirmed as described in Chap.2. The apparent viscosity in the equation is given by an existing slurry viscosity equation, assuming that the coal pellet is treated as a slurry composed of the plastic intermediate as liquid and of the other constituents, *i.e.*, the unreacted coal, semicoke and ash, as solid particles. The slurry composition is estimated from the kinetic reaction model described in the previous chapter. The predicted results are shown to explain reasonably well the observed effect of the heating rate on coal softening and the apparent coal viscosity.

Chapter 6 describes general conclusions of the present study and some comments on further works.

References

1) K. Nishioka: *Tetsu-to-Hagané*, **82** (1996), 353.

2) T. Nozaki: *Nenryokyokaishi*, **70** (1991), 883.

3) M. Sakawa: *Tetsu-to-Hagané*, **81** (1995), 261.

4) Y. Yoshida, J. Kumai, K. Yamaguchi, T. Kato, K. Miyasaka and M. Shiaraishi: *ibid.*, **45** (1966), 575.

5) Y. Yoshida, J. Kumai, K. Yamaguchi, Y, Toda, M. Shiaraishi and K. Maruyama:

ibid., **48** (1969), 738.

6) K. Miura, J. Hayashi, N. Noguchi, K. Hashimoto and H. Iwakiri: *Nenryokyokaishi*, **71** (1992), 1184.

7) K. Miura, J. Hayashi, N. Noguchi and K. Hashimoto: *ibid.*, **72** (1993), 883.

8) K. Miura, H. Nakagawa, D. Tsutsumi, T. Fujisawa and K. Niwa: *Tetsu-to-Hagané*, **82** (1996), 399.

9) J. Hayashi: Ph. D. Thesis, Kansai University, (1993)

10) K. Matsuoka, T. Kumagai and T. Chiba: *ISIJ International*, **36** (1996), 40.

11) D. W. van Krevelen; Coal, Elsevier, Amsterdam, (1961).

12) D. W. van Krevelen, F. J. Huntjens and H. N. M. Dormans: *Fuel*, **35** (1956), 462.

13) H. A. G. Chermin and D. W. van Krevelen: *ibid.*, **36** (1957), 85.

14) D. Fitzgelard: *ibid.*, **35** (1956), 178.

15) Idem: *Trans. Faraday Soc.*, **52** (1956), 362.

16) W. S. Fong, W. A. Peters and J. B. Howard: *Rev. Sci. Instrum.*, **56** (1985), 586.

17) W. S. Fong, Y. F. Khalil, W. A. Peters and J. B. Howard: *Fuel*, **65** (1986), 195.

18) N. A. Frankel and A. Acrivos, *Chem. Eng. Sci.*, **22** (1976), 847.

19) T. Matsui, K. Igawa and K. Sorimachi: Preprint of ISIJ , **8** (1995), 918.

20) Y. Mori and N. Ototake: *Kagakukogakuronbunsyu*, **20** (1956), 488.

21) H. Morotomi, N. Suzuki, T. Miyazu and M. Simura: *Nenryokyokaishi*, **53** (1974), 779.

22) P. R. Solomon, P. E. Best, Z. Z. Yu and S. Charpenay: *Energy and Fuels*, **6** (1992), 143.

23) P. R. Solomon, D. G. Hamblen, R. M. Carangelo, M. A. Serio and G. V. Deshpande, *Energy and Fuels*, **2** (1988), 405.

24) M. Mooney: *J. Colloid Sci.*, **6** (1951), 162.

25) T. Nakagawa: Rheology, 2nd ed., Iwanami Book Co., Tokyo, (1983), 108, 206.

26) K. Ouchi, K. Tanimoto, M. Makabe and H. Itoh: *Fuel*, **62** (1983), 1227.

27) T. Takanohashi, T. Yoshida, M. Iino, K. Katoh and K. Fukada: *Tetsu-to-Hagané*,

82 (1996), 366.

28) H. Seki, J. Kumagai, M. Matsuda, O. Itoh and M. Iino: *Fuel*, **68** (1989), 978.

29) H. R. Brown and P. L. Waters: *Fuel*, **45** (1966), 17.

30) Idem, *ibid*, **45** (1966), 41.

31) G. R. Oxley and G. J. Pitt: *ibid.*, **37** (1958), 19.

32) H. Jyo: *Nenryokyokaishi*, **63** (1984), 2.

33) M. Iino, Q. T. Li and M. Matsuda: *ibid.*, **64** (1985), 248.

34) Idem, *ibid.*, **65** (1986), 389.

35) J.-i. Hayashi, T. Maezono, M. Ando, K. Kusakabe and S. Morooka: *ibid.*, **69** (1990), 378.

36) J.-i. Hayashi, M. Ando, K. Kusakabe and S. Morooka: *ibid.*, **69** (1990), 446.

37) M. Kaiho and Y. Toda: *ibid.*, **58** (1979), 397.

38) P. L. Waters: *Fuel*, **41** (1962), 3.

39) M. R. Khan and R. G. Jenkins: *ibid.*, **65** (1986), 725.

40) Idem: *ibid.*, **63** (1984), 109.

41) M. R. Khan, C. W. Lee and R. G. Jenkins: *Fuel Proc. Tech.*, **17** (1987), 63.

42) W. G. Lloyd, J. W. Reasoner, J. C. Hower and L. P. Yates: *Fuel*, **69** (1990), 1257.

43) G. C. Soth and C. C. Russel: Proc. Am. Soc. Test. Mater., **43** (1943), 1176.

44) C.-R. Deng, Y. Sanada and T. Chiba: *Nenryokyokaishi*, **68** (1989), 728.

45) Soc. Polymer Sci. Japan: Rheology Sokuteihou, Kyoritu Pub. Co., Tokyo, (1965), 129.

Chapter 2
Apparent Viscosity Estimated from Needle Penetration into Coal Pellets

2.1 Introduction

Thermal plasticity is one of the fundamental properties that coal exhibits when heated above *ca.* 550 to 600 K. The thermal plasticity has long been mainly evaluated in terms of fluidity from the Gieseler plastometry[1,2] as mentioned in the previous chapter. The fluidity determined by the plastometry is one of the thermal properties not of coal itself but of the bed of coal particles. Deng *et al.*[3] developed a novel needle penetrometer to evaluate softening and resolidification properties of pelletized Drummond coal measuring needle penetration depth and volumetric dilation ratio. Examining effects of the heating rate, gas pressure and gas atmosphere, they showed that the needle penetration and dilation depended on all of these operating variables. Further, analysis of the observed needle penetration curves in a limited temperature range was carried out to estimate the coal viscosity based on an equation of motion which assumes that coal behaves as a Newtonian fluid with an apparent viscosity change with its temperature dependency given by Andrade's equation. The apparent activation energies for the viscosity varied from 418 to 1339 kJ/mol depending on the operating variables.

As is well known, the thermal plasticity depends not only on the operating variables above mentioned but also on original coal nature.[4-9] However, effect of coal nature has never been examined systematically. Hence, in this chapter the needle penetration and dilation characteristics are described, which were observed for six different kinds of coals ranging from 'caking' to 'weakly-caking' coals in a wide range of the heating rate, holding temperature and nitrogen gas pressure.[10] The observed needle penetration curves are also analyzed by an equation of motion in a full

experimental range of temperature and effect of the heating rate, nitrogen gas pressure and coal nature on the apparent viscosity is extensively discussed.

2.2 Experimental

2.2.1 Sample

Six kinds of coals were used as the sample. They had different elemental compositions, ash and volatile matter contents as listed in **Table 2.1**. Since little difference was found in the the needle penetration and dilation characteristics for a cylindrical disc quarried from coal lump and a pellet of pulverized coal[3], the latter was used here by pulverizing each coal sample into powders with a size range smaller than 100 mesh. 0.5 g of the particles was pelletized by applying 785 MPa mechanical pressure. The pellets were 10.0 mm in diameter but different in height, H_0, for different kinds of coals.

2.2.2 Apparatus and Procedure

Figure 2.1 shows a schematic diagram of the apparatus. The coal pellet was settled in a 10.6 mm i.d. steel cell which was fixed in a 50 cm^3 micro-autoclave. For measurement of the needle penetration a 2.0 mm o.d. cylindrical rod was used as a needle with a mass of 17 g and was placed on the center of the upper surface of the pellet while a 10.0 mm o.d. and 2.4 mm thick stainless steel disc was attached to the bottom tip of the rod for measurement of the volumetric dilation of the pellet. The vertical movement of the rod was detected by a linear-variable differential transformer.

The autoclave was heated in an infrared image furnace at a heating rate of 1 to 50 K/min from 298 K to a holding temperature between 698 and 823 K under N_2 gas pressures from 0.1 to 3.0 MPa. The needle penetration and dilation measurements were conducted separately for a pair of the pellets of the same coal. A preliminary experiment was carried out to correlate the observed temperature, T_a, at the bottom of the autoclave to the temperature, T, at the center of the pellet. In **Fig. 2.2** is shown an

Table 2.1 Relevant properties of coal samples so far used.

Coal	(Abbr.)	Ultimate Analysis [d.a.f.[b] wt%]					Proximate Analysis [m.f.[c] wt%]		Gieseler's Fluidity Parameters				Pellet	
		C	H	O[a]	S	N	Ash	Volatile	ST[d] [K]	MFT[e] [K]	FT[f] [K]	log(MF/ddpm) [-]	H_0 [mm]	ρ_0 [g/cm³]
Akabira	(AKA)	80.7	5.9	10.5	0.6	2.3	4.2	40.6	620	705	733	2.50	5.6	1.14
Cerrejon	(CER)	82.3	5.5	10.1	0.5	1.6	1.0	37.7	n.d.	n.d.	n.d.	n.d.	6.1	1.19
Black Water	(BLW)	86.8	4.9	5.8	0.4	2.1	7.7	26.4	687	725	752	2.51	5.4	1.20
Goonyella	(GOO)	87.4	4.9	5.2	0.6	2.0	7.6	26.4	681	735	769	3.25	5.2	1.05
Byron Creek	(BYC)	86.0	4.7	7.5	0.3	1.5	11.2	23.8	700	725	746	0.48	5.3	1.23
Peak Downs Highway	(PDH)	88.4	4.9	3.9	0.6	2.1	10.0	21.4	695	743	775	2.56	4.9	1.30

a; by difference, b; dry-ash-free basis, c; moisture-free basis, d; softening point temperature,
e; temperature given for maximum fluidity f; solidification point temperature

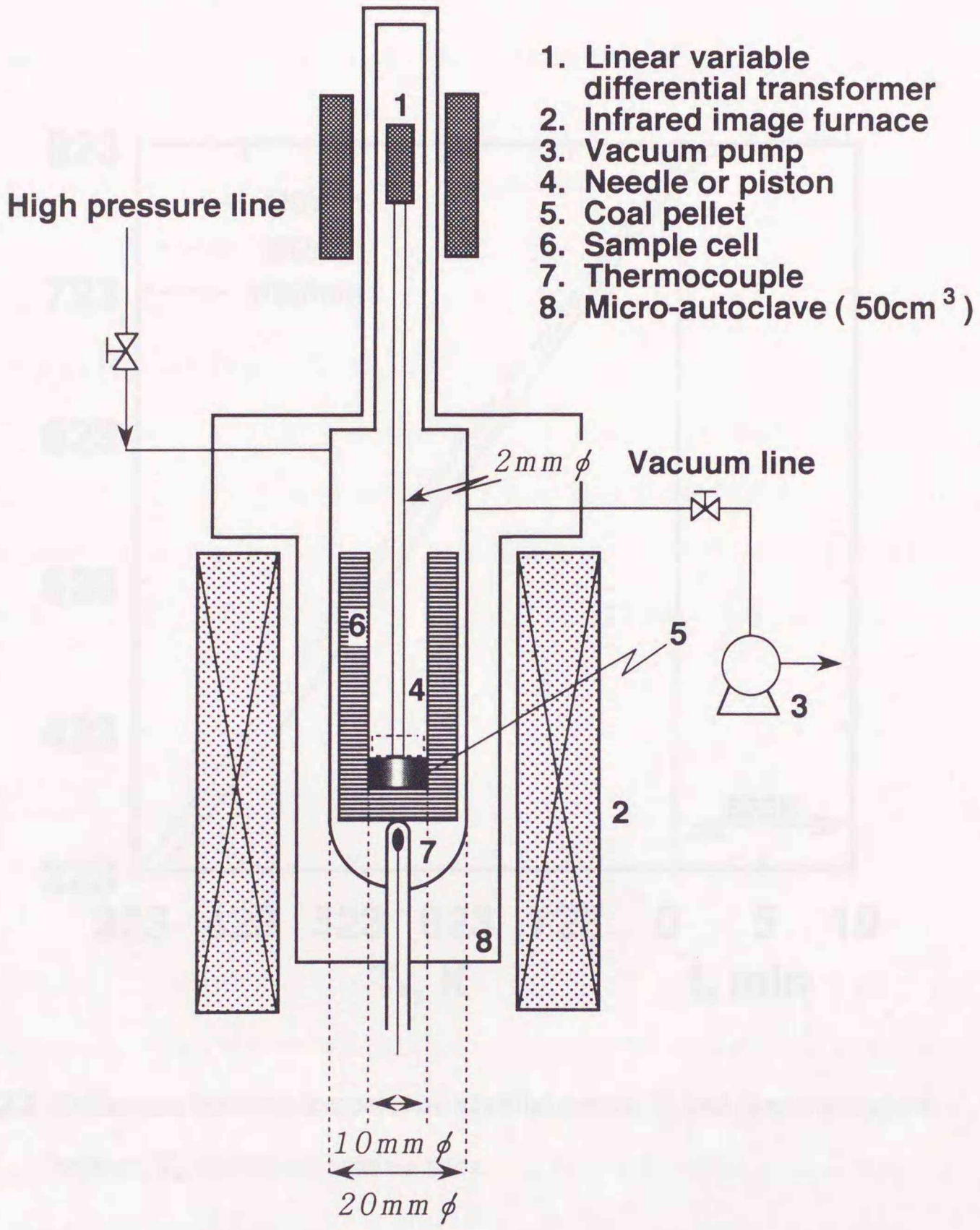

Fig. 2.1 Schematic diagram of needle penetrometer combined with dilatometer.

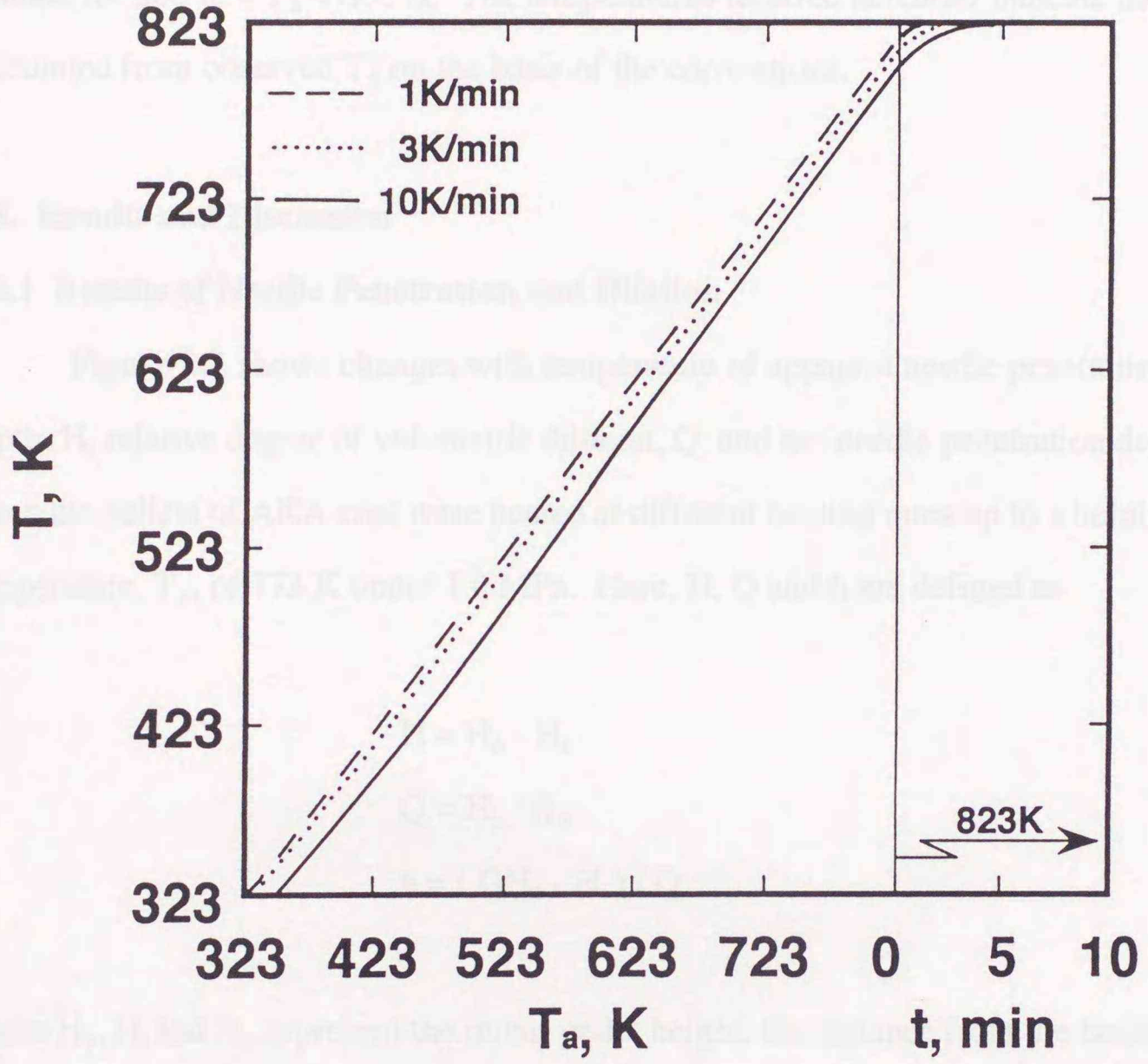

Fig. 2.2 Difference between temperature at pellet center, T, and that at autoclave bottom, T_a, at various heating rates.

example of the observed difference between T and T_a for AKA coal heated in nitrogen atmosphere of 0.1 MPa at different rates. The difference amounts 2 to 20 K and is seen to increase with the heating rate. At each heating rate a linear correlation between T and T_a was assumed as summarized in **Table 2.2** which was obtained by a least-square method for 500 K < T_a < 800 K. The temperatures referred hereafter indicate those calculated from observed T_a on the basis of the correlations.

2.3. Results and Discussion

2.3.1 Results of Needle Penetration and Dilation

Figure 2.3 shows changes with temperature of apparent needle penetration depth, H, relative degree of volumetric dilation, Q, and net needle penetration depth, h, when the pellets of AKA coal were heated at different heating rates up to a holding temperature, T_s, of 773 K under 1.0 MPa. Here, H, Q and h are defined as

$$H = H_0 - H_t$$

$$Q = H_p / H_0$$

$$h = (QH_0 - H_t) / Q$$

where H_0, H_t and H_p represent the initial pellet height, the distance from the bottom tip of the needle to the pellet bottom and the heated pellet height, respectively. It is seen from the figure that both needle penetration and dilation occur at the same temperature range from about 650 to 725 K. These changes shift to a higher temperature range for higher heating rates. For the heating rates of 2, 3 and 10 K/min, H and h are seen to fall off at about 5 mm suggesting termination of the penetration near the pellet bottom while at the slowest heating rate of 1 K/min the penetration terminates at h = *ca.* 3 mm before the needle reaches the bottom.

The above results were more or less similar for the other coals. In **Fig. 2.4** changes of the net penetration depth with temperature, *i.e.*, h vs. T plots, are compared

Table 2.2 Correlations between temperature at pellet center, T, and that at autoclave bottom, T_a, at various heating rates.

q_h[K/min]	Correlations
1	$T = 0.989 \times T_a + 2.567$
2	$T = 0.993 \times T_a - 2.350$
3	$T = 1.006 \times T_a - 16.054$
10	$T = 1.039 \times T_a - 53.249$

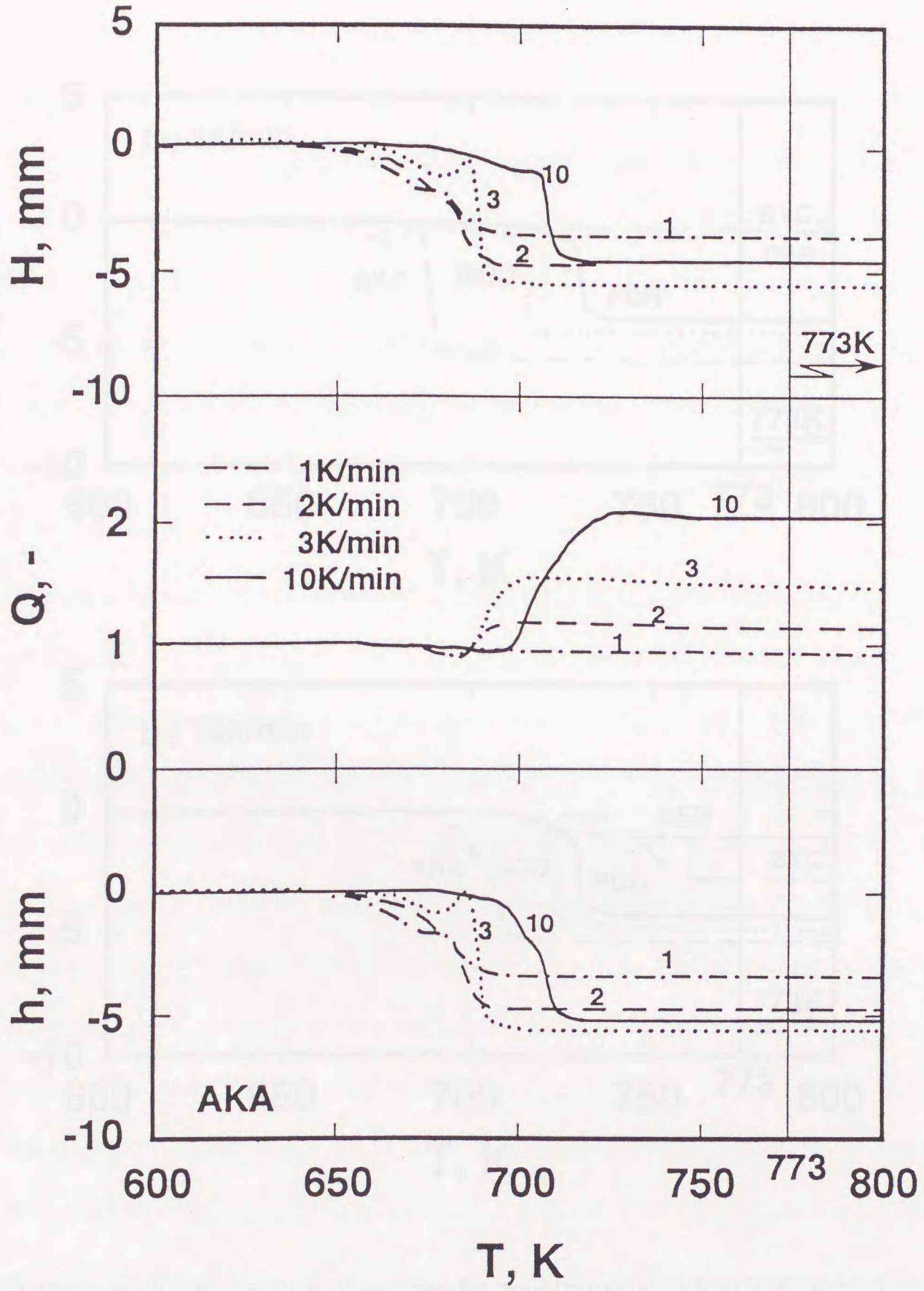

Fig. 2.3 Changes with temperature of apparent needle penetration depth, H, relative degree of volumetric dilation, Q, and net needle penetration depth, h, at different heating rates up to 773 K for AKA coal under 1.0 MPa.

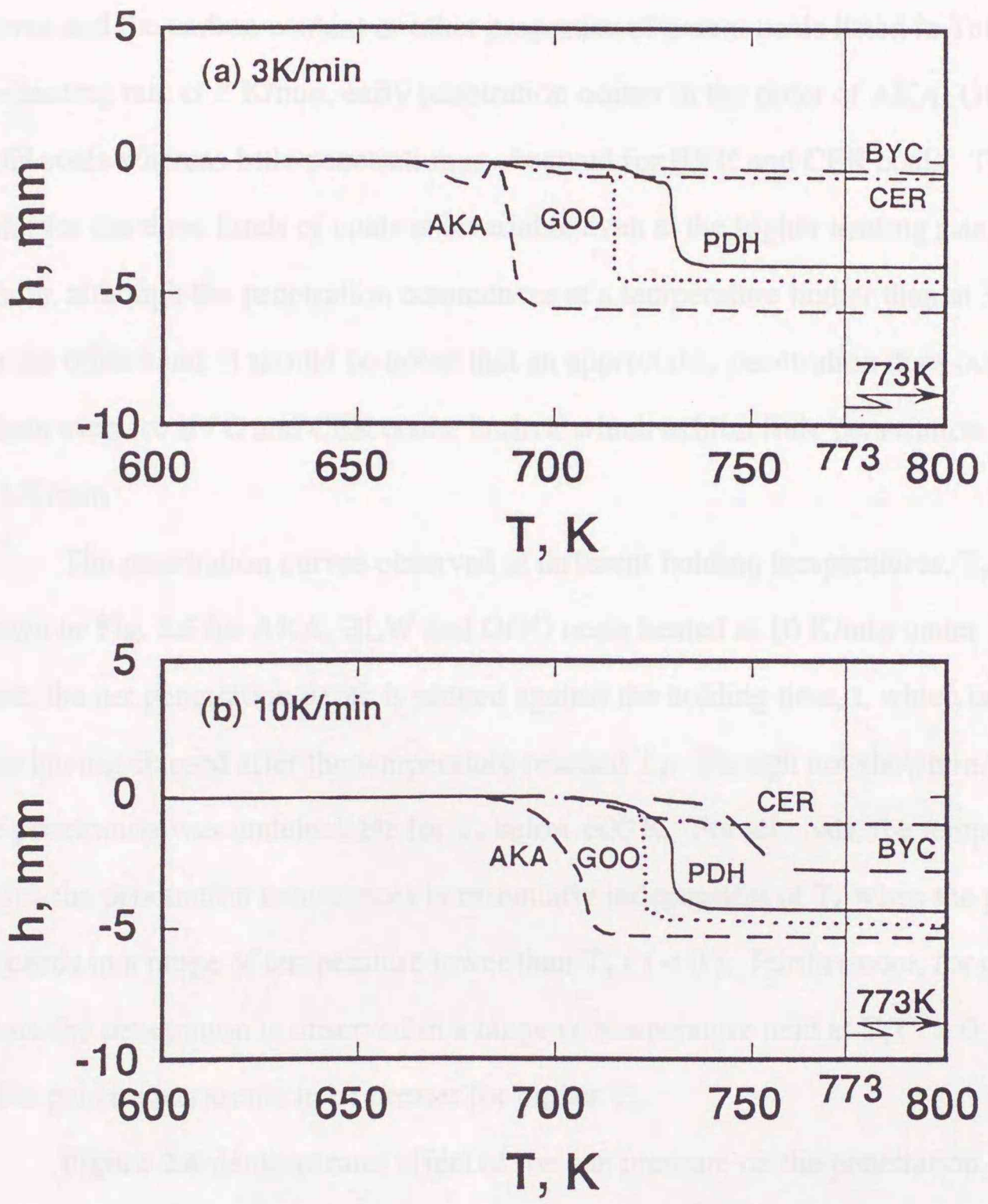

Fig. 2.4 Changes with temperature of net needle penetration depth at 3 K/min(a) and 10 K/min(b) up to 773 K for different coals under 1.0 MPa.

for five kinds of coals heated at 3 K/min (a) and 10 K/min (b) up to 773 K under 1.0 MPa. From the figure the temperature range for occurrence of the penetration is seen to depend on the coals as has been indicated that the thermal plasticity in general depends on coal rank.[11] However, no regular relationship is found between the penetration curves and the carbon content or other properties of parent coals listed in Table 2.1. At the heating rate of 3 K/min, early penetration occurs in the order of AKA, GOO and PDH coals whereas little penetration is observed for BYC and CER coals. The above order for the three kinds of coals is invariable even at the higher heating rate, *i.e.*, 10 K/min, although the penetration commences at a temperature higher than at 3 K/min. On the other hand, it should be noted that an appreciable penetration does occur at 10 K/min even for BYC and CER coals, both of which exhibit little penetration propensity at 3 K/min.

The penetration curves observed at different holding temperatures, T_s, are shown in **Fig. 2.5** for AKA, BLW and GOO coals heated at 10 K/min under 1.0 MPa. Here, the net penetration depth is plotted against the holding time, t, which is defined as time having elapsed after the temperature reached T_s. Though not shown in the figure, the penetration was undetectable for T_s below 600 K. For all coals, the temperature at which the penetration commences is essentially independent of T_s when the penetration proceeds in a range of temperature lower than T_s ($t < 0$). Furthermore, for cases where the penetration is observed in a range of temperature held at T_s ($t > 0$), the rate of the penetration seems to be greater for higher T_s.

Figure 2.6 demonstrates effect of the gas pressure on the penetration curves for CER, BLW and PDH coals at 20 K/min up to 823 K. For PDH coal which has the lowest volatile matter content among the coals no appreciable effect can be seen, while for the other two coals having volatile matter contents higher than PDH coal the penetration is promoted as the gas pressure increases. These results imply that a larger portion of light pyrolysis products is confined within the pellet at higher gas pressure resulting in a high softening property of the pellet.

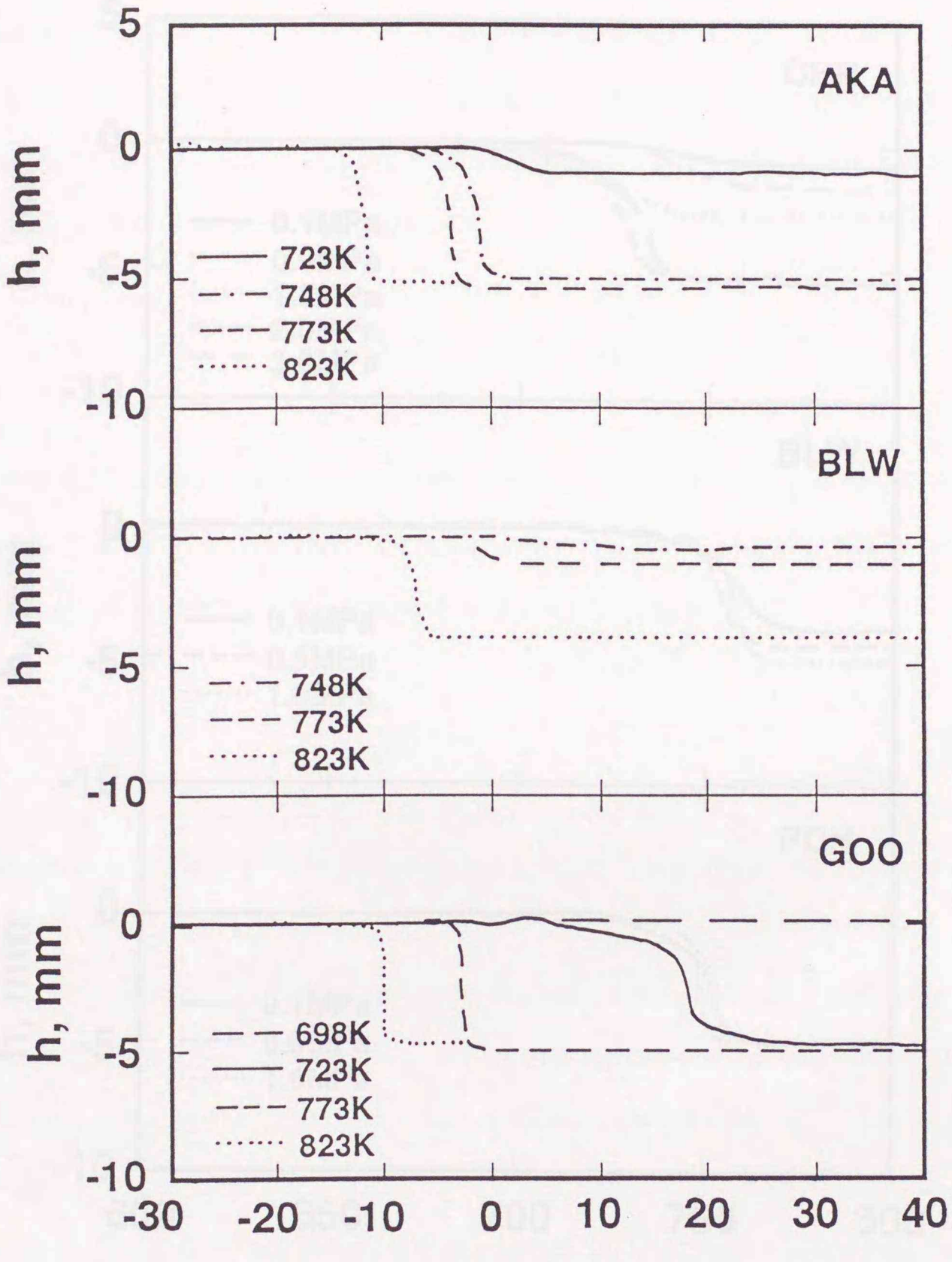

Fig. 2.5 Changes with holding time of net needle penetration depth at 10 K/min up to different holding temperatures for AKA, BLW and GOO coals under 1.0 MPa.

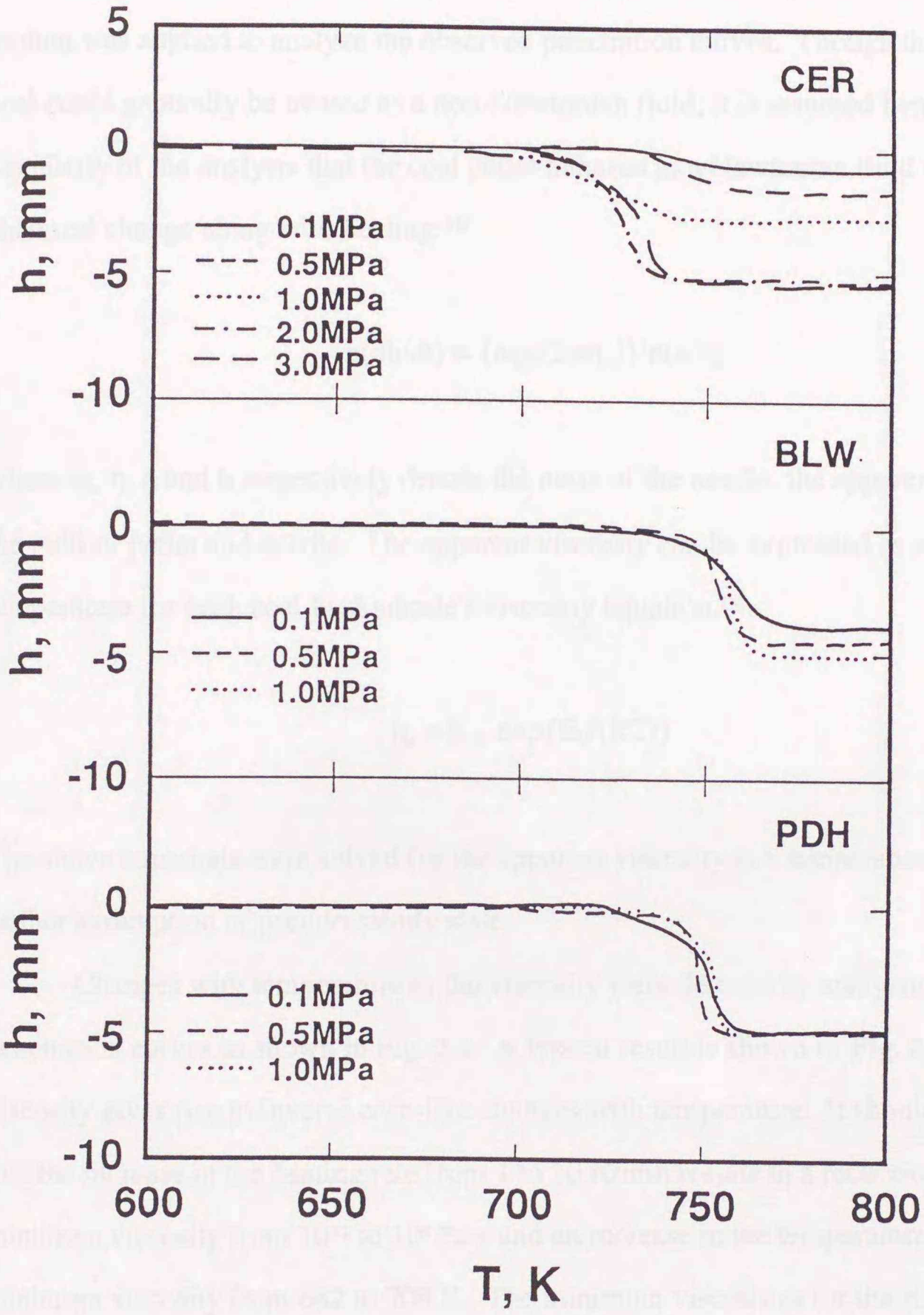

Fig. 2.6 Changes with temperature of net needle penetration depth at 20 K/min up to 823 K for CER, BLW and PDH coals under 1.0 MPa.

2.3.2 Estimation of Coal Viscosity

In an effort to estimate the apparent viscosity of softening coals, an equation of motion was applied to analyze the observed penetration curves. Though the softening coal could generally be treated as a non-Newtonian fluid, it is assumed here for simplicity of the analysis that the coal pellet behaves as a Newtonian fluid without any chemical change along with heating:[12)]

$$h(dh/dt) = \{mg/(2\pi\eta_a)\}\ln(a/b)$$

where m, η, a and b respectively denote the mass of the needle, the apparent viscosity, the radii of pellet and needle. The apparent viscosity can be expressed as a function of temperature for each coal by Andrade's viscosity equation.[13)]

$$\eta_a = k_{V0} \exp\{E_V/(RT)\}$$

The above equations were solved for the apparent viscosity at a temperature with a further assumption of pseudo-steady state.

Changes with temperature in the viscosity were derived by analyzing the penetration curves as shown in Fig. 2.3. A typical result is shown in **Fig. 2.7**. The viscosity gives rise to inverse corn-like changes with temperature. It should be noted that the increase in the heating rate from 1 to 10 K/min results in a reduction of the minimum viscosity from 10^{12} to 10^{4} Pa·s and an increase in the temperature for the minimum viscosity from 682 to 708 K. The minimum viscosities for the six coals are plotted against the heating rate in **Fig. 2.8**. For all the coals the minimum viscosities remarkably decrease with the heating rate and, in particular, for GOO and PDH coals they decrease by four to five orders of magnitude when the heating rate is increased from 1 to 10 K/min. The minimum viscosities depend upon not only heating rate but

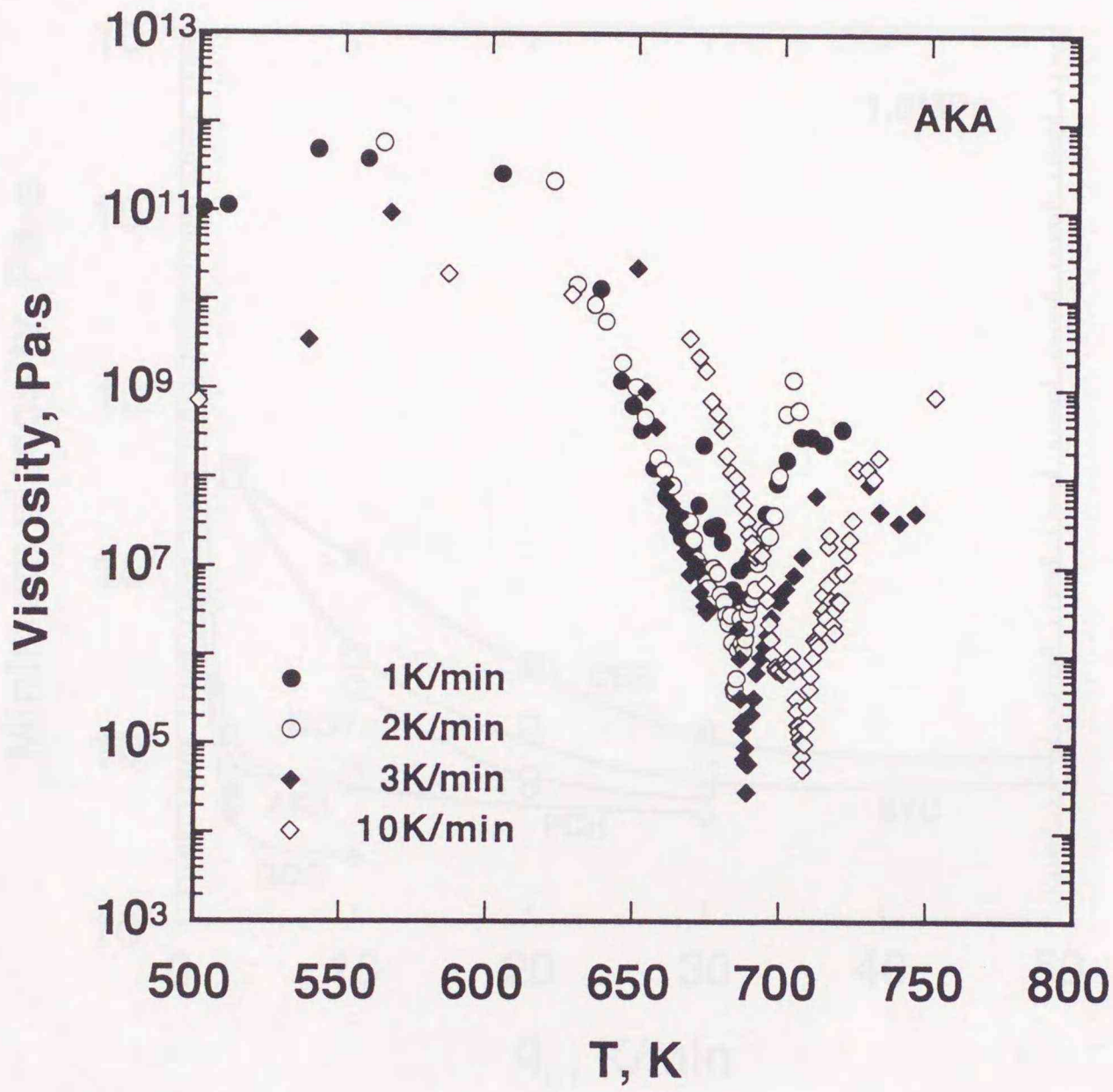

Fig. 2.7 Changes of apparent viscosity with temperature for AKA coal heated at different heating rates under 1.0 MPa.

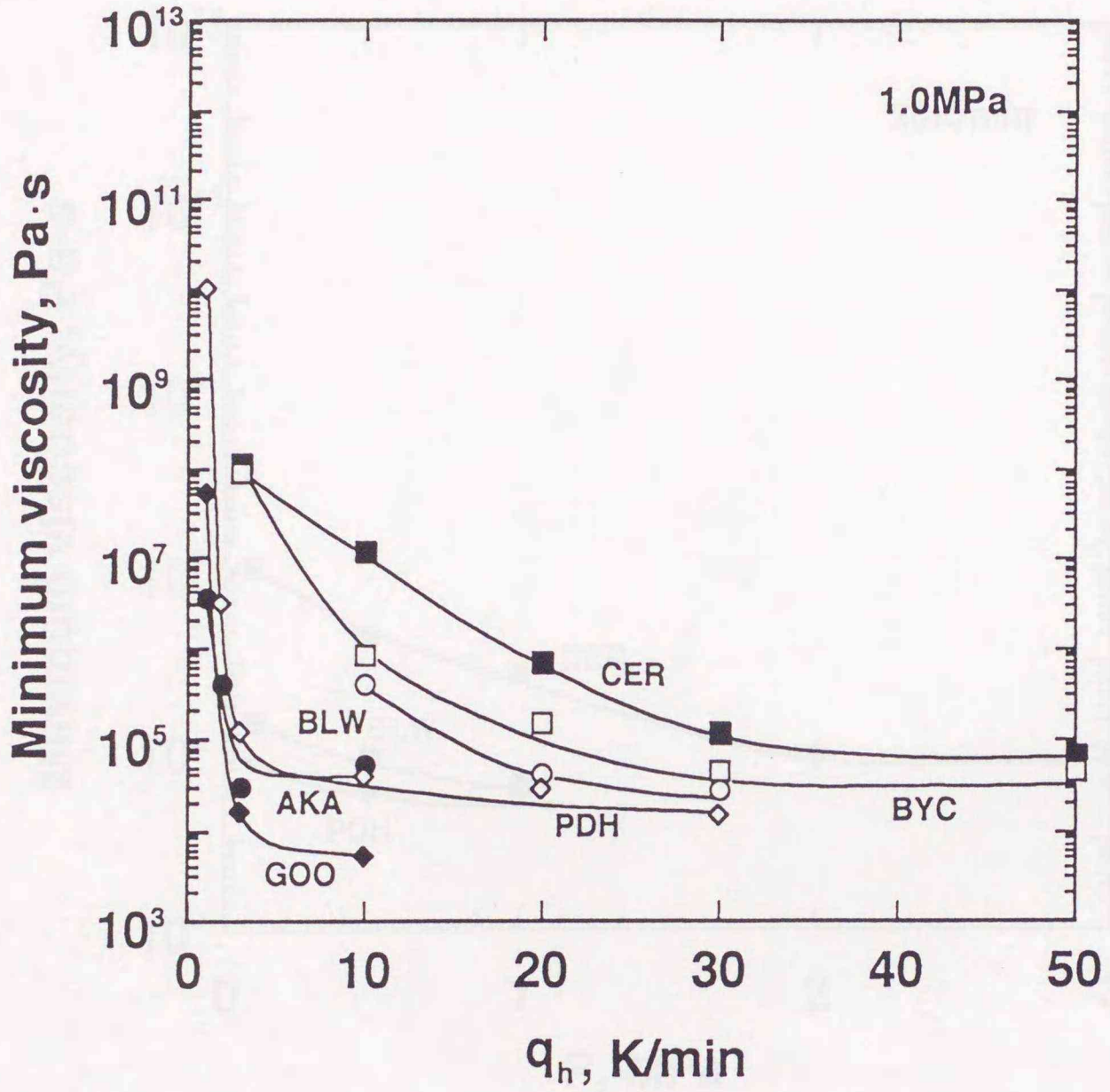

Fig. 2.8 Effect of heating rate on minimum viscosity for different coals heated under 1.0 MPa.

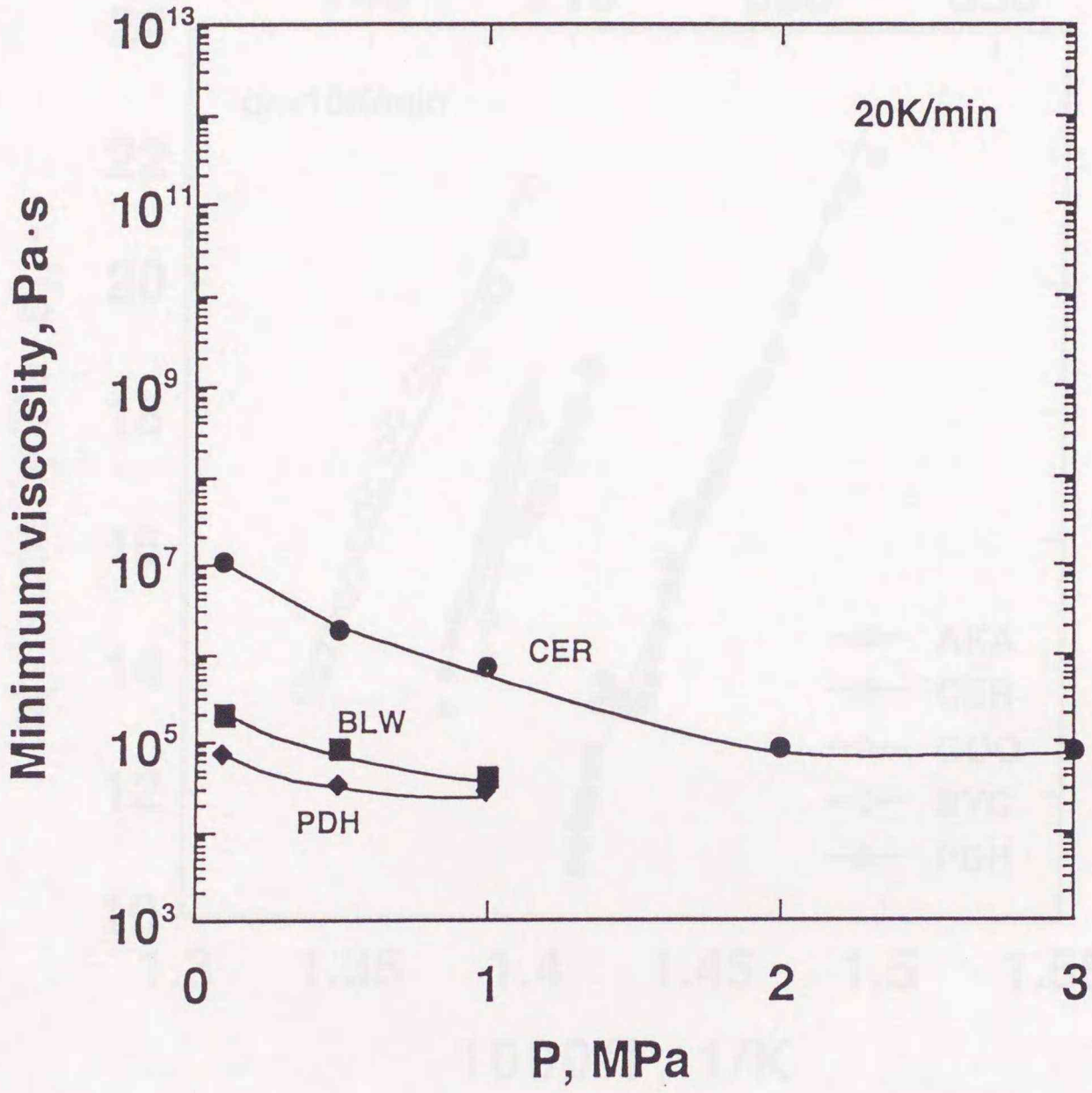

Fig. 2.9 Effect of nitrogen gas pressure on minimum viscosity for different coals heated at 20 K/min.

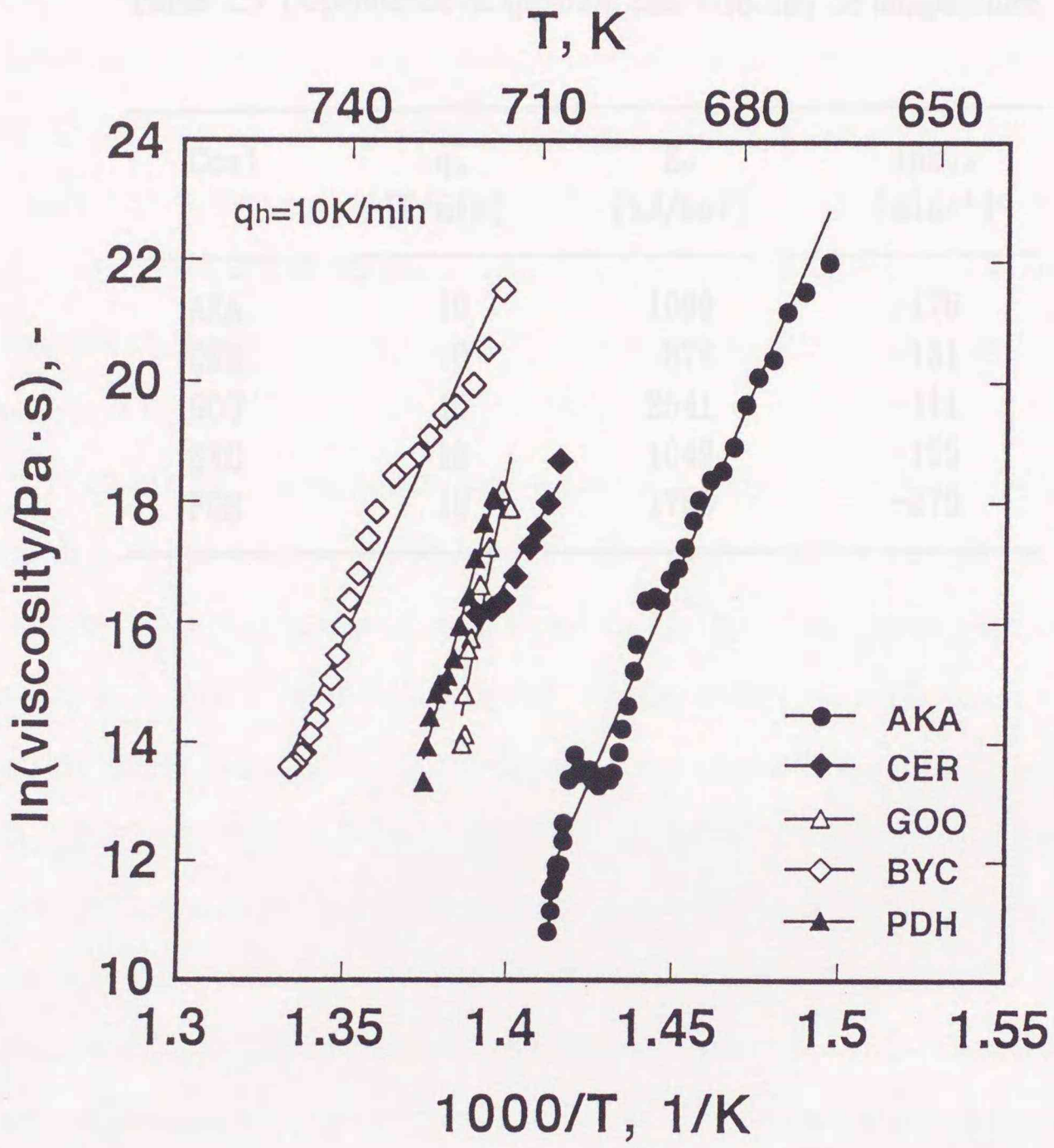

Fig. 2.10 Plots based on Andrade's equation for apparent viscosity of different coals within a low temperature range.

Table 2.3 Dependence of apparent coal viscosity on temperature.

Coal	q_h [K/min]	E_v [kJ/mol]	$\ln k_{v0}$ [min^{-1}]
AKA	10	1099	-176
CER	10	874	-131
GOO	10	2541	-411
BYC	10	1049	-155
PDH	10	1760	-278

also gas pressure. The effect of the nitrogen gas pressure on the minimum viscosities for different three coals heated at 20 K/min was examined. The result is shown in **Fig. 2.9**. The minimum viscosities decrease as the gas pressure increases. The minimum viscosity for CER coal, having more volatile matters, depends on the pressure significantly than the two coals with less volatile matter content from proximate analysis. The result suggests that tar of low-molecular weight, which does not contribute to softening under atmospheric pressure but under high pressure stay in pyrolyzing coal to influence softening. Though not shown in the figure, the temperature for the minimum viscosity was independent of the pressure for any heating rates tested.

When the Andrade equation is applied for analysis of the viscosity decrease within a narrow range of temperature just after the needle penetration commenced, the viscosity varies with temperature as shown in **Fig. 2.10** for different coals at the heating rate of 10 K/min. If the relationship between $\ln\eta$ and 1/T for each coal is approximated as depicted as a straight line in the figure, the apparent activation energies for viscosity, E_v, range from 874 to 2541 kJ/mol, as listed in **Table 2.3**. These values are in the same order of magnitude as those obtained for a coal heated at different gas pressures and gas atmospheres.[3] However, as indicated by Waters,[14] they would be unreasonably high if molecular rearrangement along with heating is responsible for the viscosity change of the coal consisting of very large molecules. For the temperatures higher than 600 K, pyrolysis of the coal would inevitably occur producing the plastic intermediate with lower molecular weight as well as thermal fragments with higher molecular weight which is followed by semicoke formation by condensation of the molecules. The details of these chemical change are extensively described in the next chapter.

2.4 Conclusions

The thermal plasticity of coal was quantitatively investigated in terms of observed needle penetration into a cylindrical pellet of pulverized coal particles and

dilation of the pellet for six kinds of caking or weakly-caking coals. Measurements were carried out under nitrogen gas atmosphere in a range of the heating rate from 1 to 50 K/min, the holding temperature up to 823 K and the gas pressure from 0.1 to 3.0 MPa. The observed results showed that the needle penetration and dilation for the pellets occur simultaneously and depend on the coal nature and the heating rate. In particular, the coals with little softening propensity at low heating rates exhibited an appreciable softening property at high heating rates.

The apparent viscosity of the coal pellet was estimated by analyzing the net descent of the needle through the pellet on the basis of the equation of motion and Andrade's equation. However, the Andrade equation was found impossible to be applied for the observed result in the whole range of temperature. In addition, even if the application was confined to the results in a lower temperature range the estimated viscosity showed unreasonably high temperature dependency, suggesting a necessity for the analysis to consider not only physical but chemical change of coal with temperature.

References

1) D. W. van Krevelen, F. J. Huntjens and H. N. M. Dormans: *Fuel*, **35** (1956), 462.

2) D. Fitzgelard: *ibid.*, **35** (1956), 178.

3) C.-R. Deng, Y. Sanada and T. Chiba: *Nenryokyokaishi,* **68** (1989), 728.

4) M. Kaiho and Y. Toda: *Fuel*, **58** (1979), 397.

5) M. R. Khan and R. G.Jenkins: *ibid.* **65** (1986), 725.

6) Idem: *ibid.*, **63** (1984), 109.

7) M. R. Khan, C. W. Lee and R. G. Jenkins: *Fuel Proc. Tech.*, **17** (1987), 63.

8) T. Chiba, K. Matsuoka, S. Ikeda and Y. Sanada: Proc. of The First Int. Cong. on Sci. and Technol. of Ironmaking, ISIJ, Sendai, (1994), 314.

9) W. S. Fong, Y. F. Khalil, W. A. Peters and J. B. Howard: *Fuel*, **65** (1986), 195.

10) K. Matsuoka, T. Kumagai and T. Chiba: *ISIJ International*, **36** (1996), 40.

11) H. Kimura and S. Fujii: Sekitankagaku-to-Kogyo, Sankyo Pub. Co., Tokyo, (1979), 265.

12) Soc. Polymer Sci. Japan: Rheology Sokuteihou, Kyoritu Pub. Co., Tokyo, (1965), 129.

13) T. Nakagawa: Rheology, 2nd ed., Iwanami Book Co., Tokyo, (1983), 206.

14) P. L. Waters: *Fuel*, **41** (1962), 3.

Chapter 3
Quantification of Metaplast Formed during Carbonization

3.1 Introduction

In the existing investigations, the softening and resolidification characteristics of coal upon heating have been studied by using different analytical techniques. For example, differential scanning calorimetry (DSC) was utilized to estimate phase transitions of coal upon heating.[1-5] Janikowski and Stenberg[3] analyzed ten different coals by a DSC and found two temperature regions, *i.e.*, one of which is attributed to water loss while the other of which reflects an increase of chemical reactivity. However, the results from DSC analysis are always qualitative so that the increasing rate of the reactivity can not be evaluated quantitatively. Furthermore, it is impossible to separate the contribution to the reactivity increase by physical phase change of coal from solid to liquid from that by chemical reactions like metaplast formation. On the other hand, proton nuclear magnetic resonance (^{1}H-NMR) techniques have often been applied to evaluation of softening characteristics of coal.[6,7] Sakurovs *et al.*[7] measured the relative concentration of mobile hydrogen by a novel ^{1}H-NMR thermal-analysis technique and related it to softening characteristics. However, though the technique can detect the average mobility of hydrogen, it is impossible for the technique not only to identify hydrogen being responsible for the mobility change upon heating but also to detect the contribution by other molecular species to the mobility change.

From the above shortcomings in the existing analytical techniques, it would be reasonable to describe the chemical change based on chemical characterization. Solvent extraction techniques have long been applied for the characterization. Thus, the extracts from heated coal with chloroform, THF, pyridine, quinoline and CS_2-NMP have been defined as the metaplast and related to the fluidity of the coals.[8-15] However, the coal extracts generally comprise a wide variety of compounds. Therefore, proper solvents have to be chosen to obtain the extracts to have a composition and property being invariable along with the progress of pyrolysis and carbonization. Hayashi *et al.*[16,17] reported that the yields of pyridine and chloroform extracts

widely varied with the progress of pyrolysis but their average structure and molecular mass distribution exhibited little dependency of the yields.

In this chapter, the heat flux by a DSC, the yield of mobile hydrogen by a ^{1}H-NMR and the yield of pyridine extract in heated coal were measured to evaluate the rate of formation and disappearance of the metaplast during carbonization.

3.2 Experimental

3.2.1 Sample

Six kinds of the coals listed in Table 2.1 were used as the sample. About 5 mg and 100 mg of coal pulverized to sizes smaller than 100 mesh were respectively subjected to the DSC and ^{1}H NMR analyses. On the other hand, the pellet heat-treated under the same conditions as the penetration experiments was pulverized and was then subjected to pyridine extraction.

3.2.2 Apparatus and Procedure

In the DSC measurement the sample was loaded into an aluminum cell and was heated at 10 K/min up to 823 K. Nitrogen gas was flowed at a rate of 80 ml/min to sweep volatiles released by pyrolysis reaction. After heating, the sample was cooled down to a room temperature and was heated again at 10 K/min up to 823 K. The heat flux of the coal (first heating) and the residue (second heating) was measured consecutively.

In ^{1}H NMR analysis the sample was heated in a NMR probe at 4 K/min up to 823 K under a flow of nitrogen gas to inhibit oxidation and sweep the volatiles from the sample. Solid echo measurements of the ^{1}H NMR transverse relaxation signals were made on the specimens at regular intervals during pyrolysis. The signals were characterized by their initial amplitude and the nature of their time decay or relaxation rate.

Measurements were also conducted on the mass fraction of pyridine extract contained in the pellet. When the coal pellet was heated in the needle penetrometer shown in Fig. 2.1, it was cooled by blowing air after the prescribed heating. However, it is considered that pyrolysis and carbonization reactions can proceed during the cooling. Therefore, they must be quenched after heating. **Figure 3.1** shows a schematic diagram of the apparatus to quench the pellets. Two

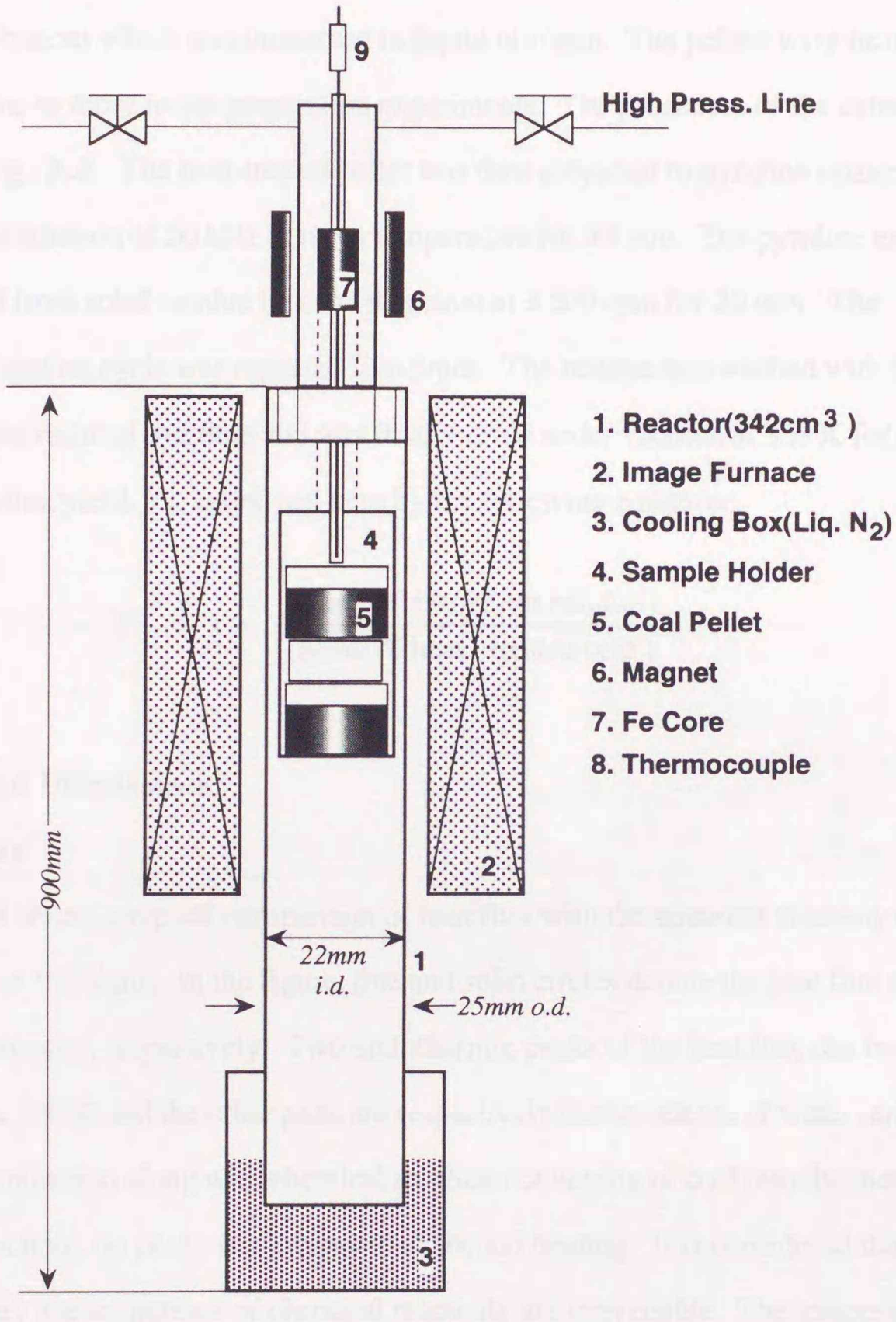

Fig. 3.1 Schematic diagram of experimental apparatus to quench pellets.

different kinds of coal pellets were put into the holder settled into the stainless steel tube reactor whose volume is 342 cm^3. The holder was hanged by the magnet and was frozen by dropping it into the reactor bottom which was immersed in liquid nitrogen. The pellets were heated under the same conditions as those in the penetration experiments. The procedure of the extraction is summarized in **Fig. 3.2**. The heat-treated pellet was then subjected to pyridine extraction under ultrasonic irradiation of 50 kHz at room temperature for 30 min. The pyridine extract, PS, was separated from solid residue by centrifugation at 3,500 rpm for 20 min. The extraction-centrifugation cycle was repeated five times. The residue was washed with 50 ml methanol to remove residual pyridine and was finally dried under vacuum at 353 K for eight hours. The extraction yield, Y_P, is defined here by the following equation;

$$Y_P = 1 - \frac{(\text{Mass of extraction residue})}{(\text{Mass of heat - treated coal})}$$

3.3 Results and Discussion

3.3.1 Heat Flux

Figure 3.3 shows a typical comparison of heat flux with the apparent viscosity for AKA coal heated at 10 K/min. In the figure, line and solid circles denote the heat flux of first heating and the viscosity, respectively. Two endothermic peaks of the heat flux can be seen. The first peak near 350 K and the other peak are respectively due to release of water remaining in coal and phase transition along with chemical reaction converting of coal into the metaplast. Though not shown here, no peaks was observed at second heating. It is considered that changes of heat flux due to increase of chemical reactivity are irreversible. The temperature for the second endothermic peak roughly coincides with that for the minimum viscosity. The result suggests that softening characteristics are related to the change of the heat flux due to chemical reactivity change. Though the temperature given for the maximum yield of the metaplast can be measured by DSC technique, the concentration of the intermediate cannot be measured.

3.3.2 Mobile Hydrogen

The nuclei of hydrogen atoms, which are distributed throughout the molecular units of

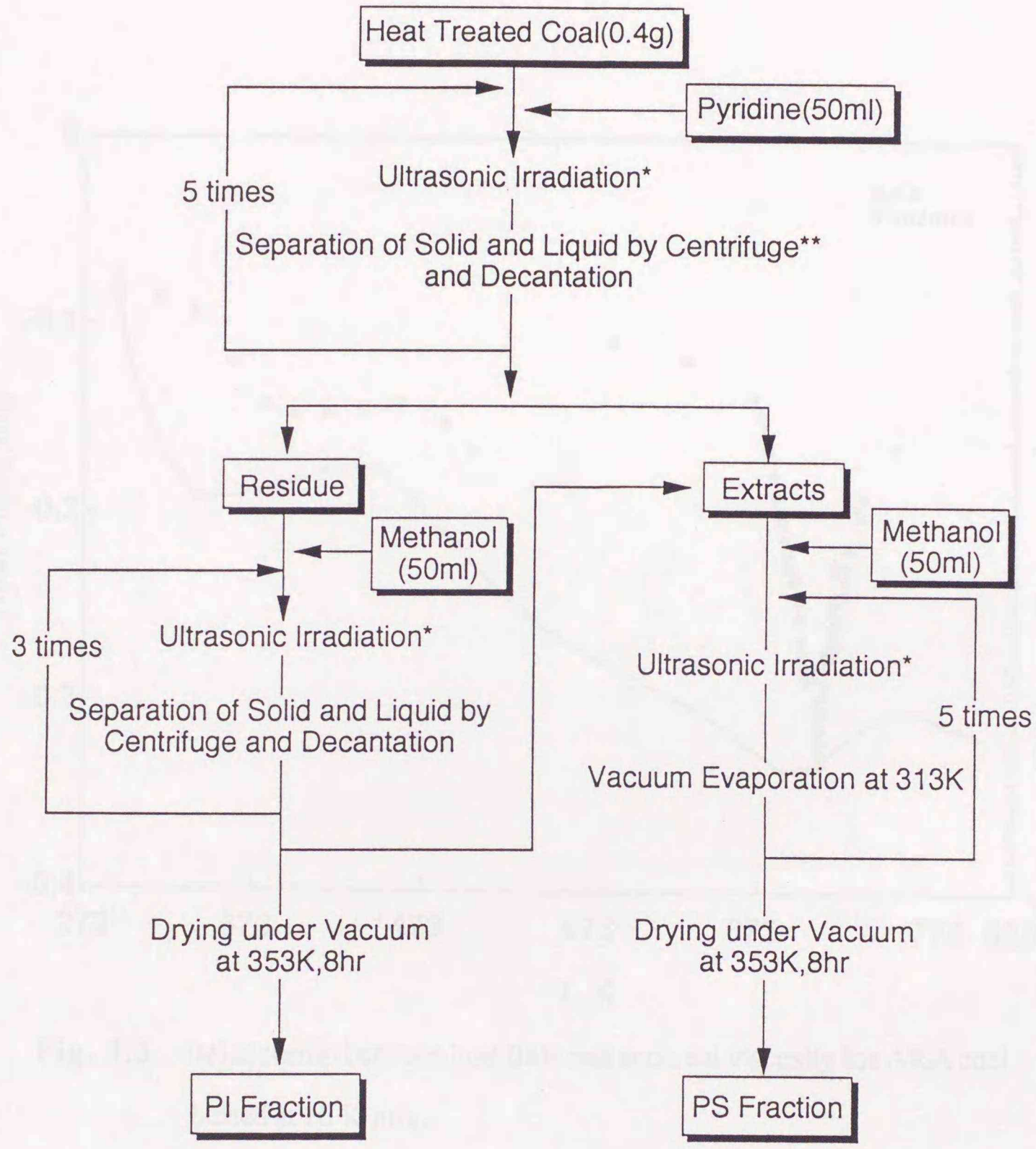

* Ultrasonic Irradiation; 50kHz for 30min

** Separation by Centrifuge; at 3,500rpm for 20min

Fig. 3.2 Procedure of extraction of coal with pyridine under ultrasonic irradiation.

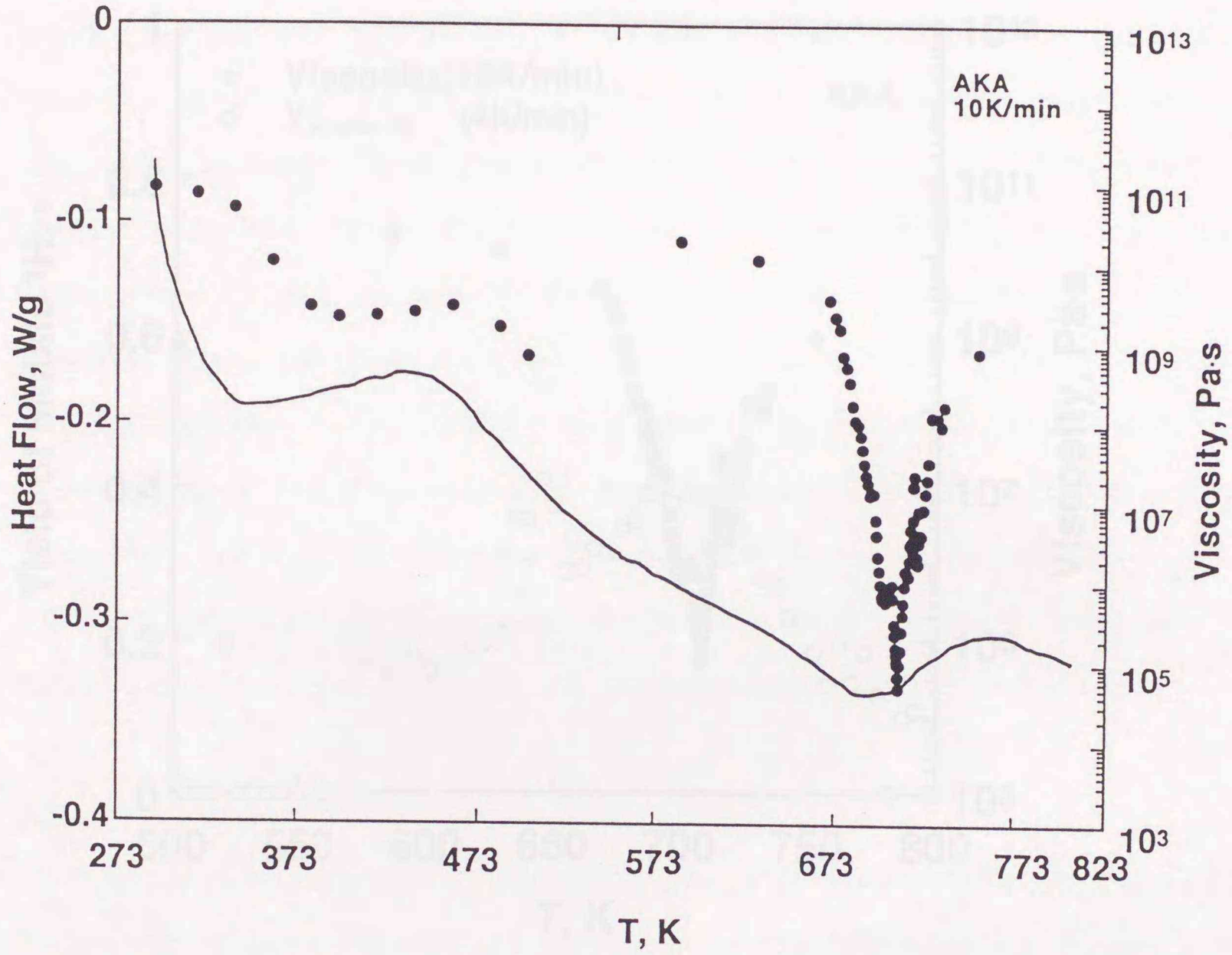

Fig. 3.3 Relationship between heat flow and apparent viscosity for AKA coal heated at 10 K/min.

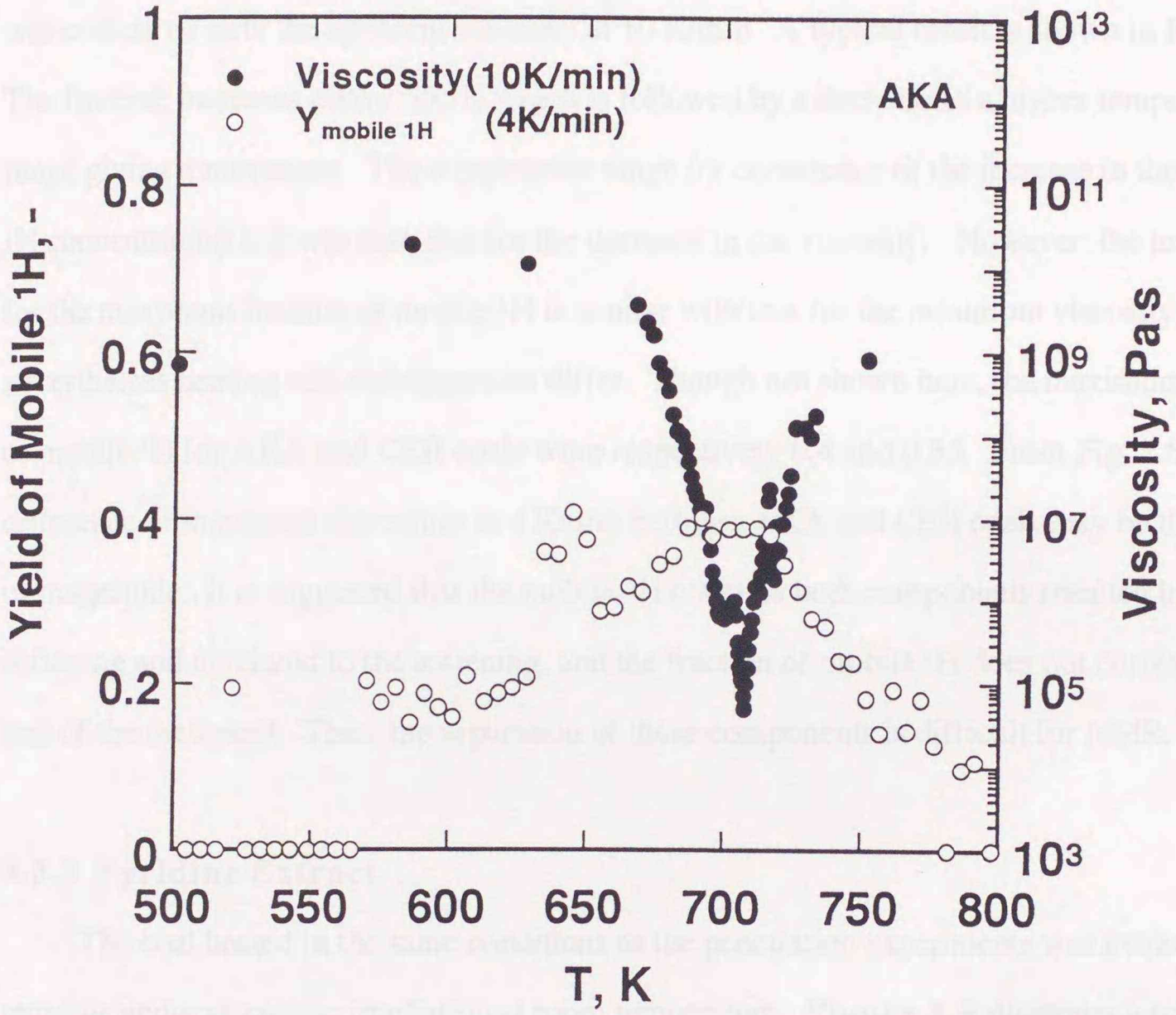

Fig. 3.4 Relationship between yield of mobile hydrogen and apparent viscosity for AKA coal.

organic materials behave as minuscule bar magnets. Since the protons are embedded in the molecular lattice, these movements are those of the molecular units. By solving the ^1H NMR signals into a slowly relaxing exponential or "mobile" components and rapidly relaxing Gaussian or "rigid" components, the yield of hydrogen that is mobile in the coal specimen at any temperature can be estimated. The yield of mobile ^1H for coal heated at a rate of 4 K/min was compared with the apparent viscosity at 10 K/min. A typical result is shown in **Fig. 3.4.** The fraction increases above 550 K which is followed by a decrease in a higher temperature range giving a maximum. The temperature range for occurrence of the increase in the mobile ^1H concentration is lower than that for the decrease in the viscosity. However, the temperature for the maximum fraction of mobile ^1H is similar with that for the minimum viscosity, nevertheless heating rate and apparatus differ. Though not shown here, the maximum fractions of mobile ^1H for AKA and CER coals were respectively 0.4 and 0.35. From Fig. 2.8 the difference of minimum viscosities at 4 K/min between AKA and CER coals may be three orders of magnitude. It is suggested that the mobile ^1H contains both components resulted in softening and unrelated to the softening, and the fraction of mobile ^1H does not correspond to that of the metaplast. Thus, the separation of these components is difficult for NMR.

3.3.3 Pyridine Extract

The coal heated in the same conditions as the penetration experiments was extracted with pyridine under ultrasonic irradiation at room temperature. **Figure 3.5** illustrates a typical effect of the heating rate on pyridine extraction yield, Y_P, for GOO coal. It is seen that change of Y_P significantly depends on the heating rate. Y_P increases above 650 K, which is followed by a rapid decrease in a higher temperature range giving a maximum for each heating rate. The maximum Y_P appears with a larger value at higher temperature range. **Figure 3.6** presents changes of Y_P with temperature for three different coals heated at 10 K/min. Y_P is higher for the coal having lower minimum viscosity as shown in Fig. 2.8.

In **Fig. 3.7** is shown relationship between the temperature for the minimum viscosity and those for the endothermic peak, yield of the maximum mobile ^1H and the maximum Y_P. These temperatures are similar, nevertheless experimental condition and apparatus differ. It is

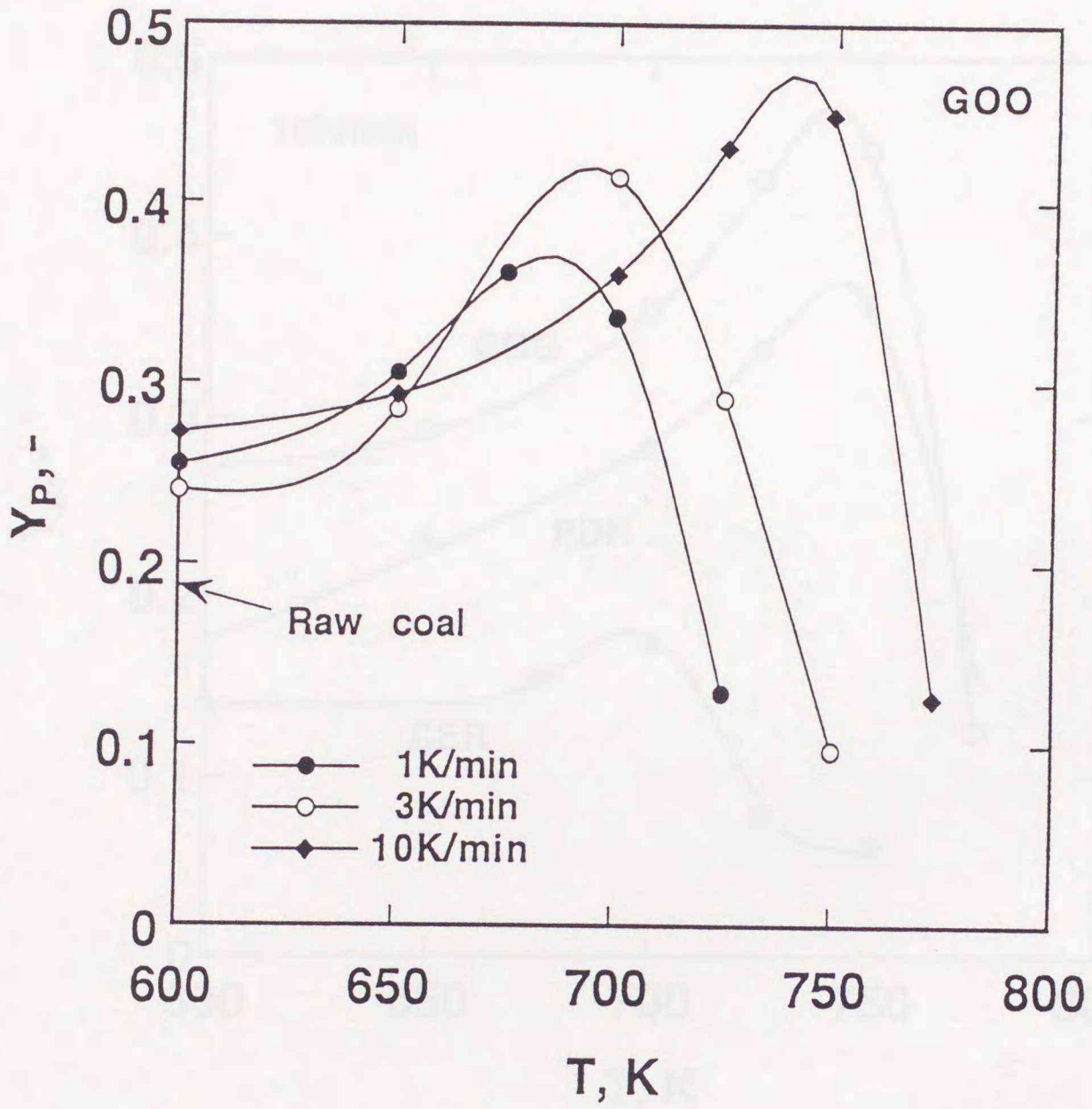

Fig. 3.5 Effect of heating rate on Y_P for GOO coal heated under 1.0 MPa.

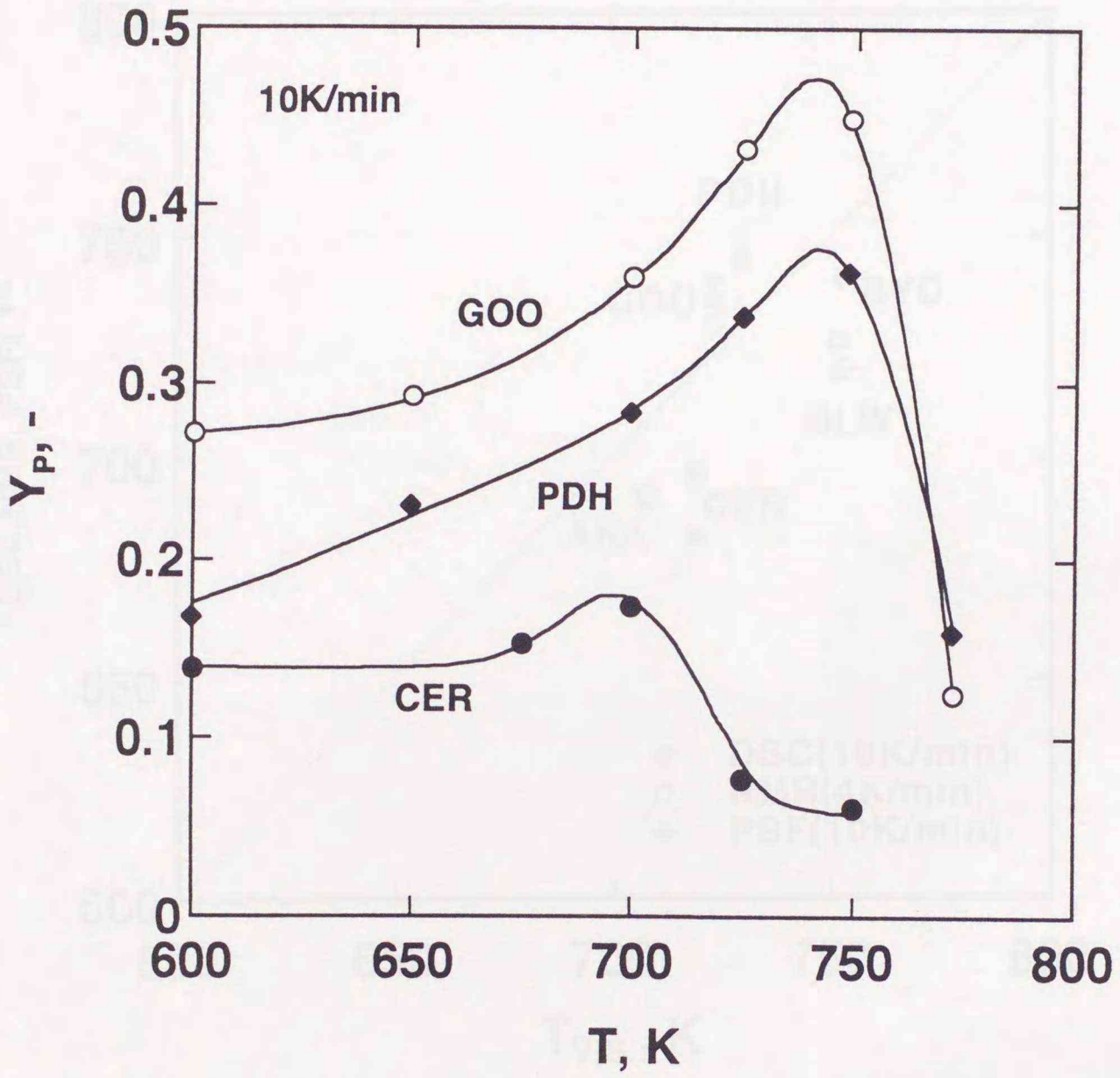

Fig. 3.6 Changes of Y_P with temperature for different coals heated at 10 K/min under 1.0 MPa.

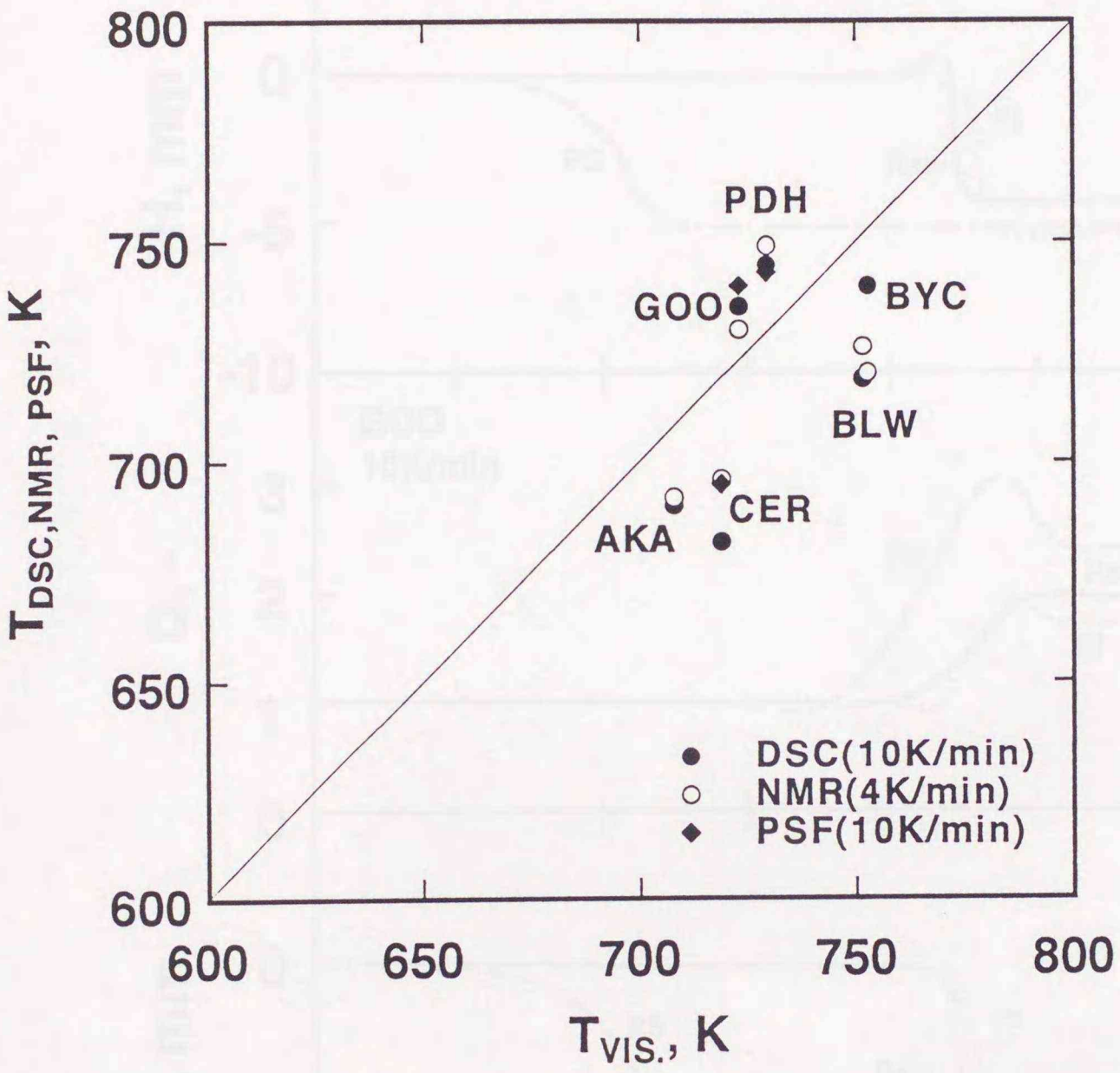

Fig. 3.7 Relationship between temperature for minimum viscosity and that for endothermic peak, maximum yield of mobile hydrogen, and maximum Y_P.

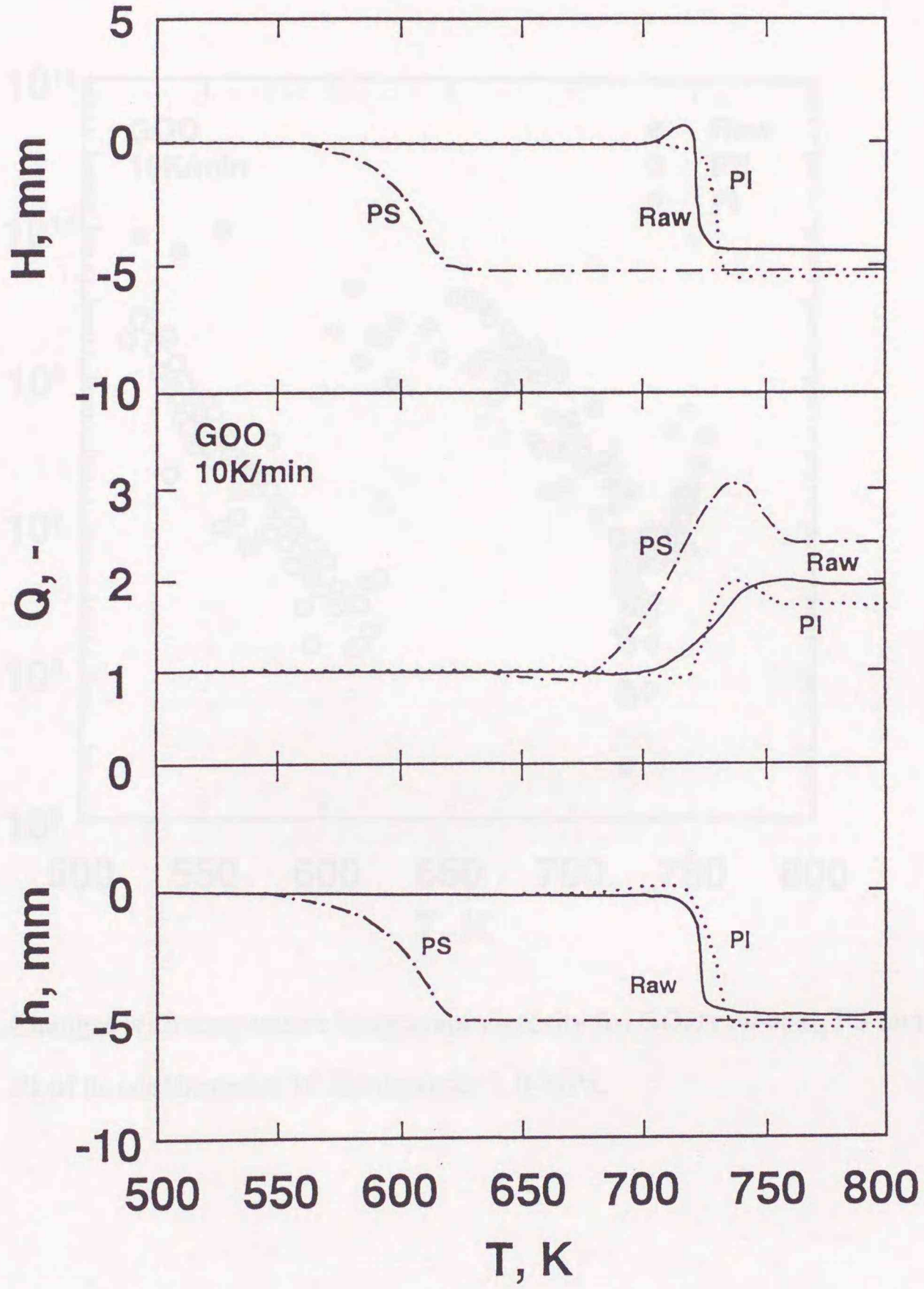

Fig. 3.8 Changes with temperature of apparent needle penetration depth, H, relative degree of volumetric dilation, Q, and net needle penetration depth, h, for GOO coal heated at 10 K/min under 1.0 MPa.

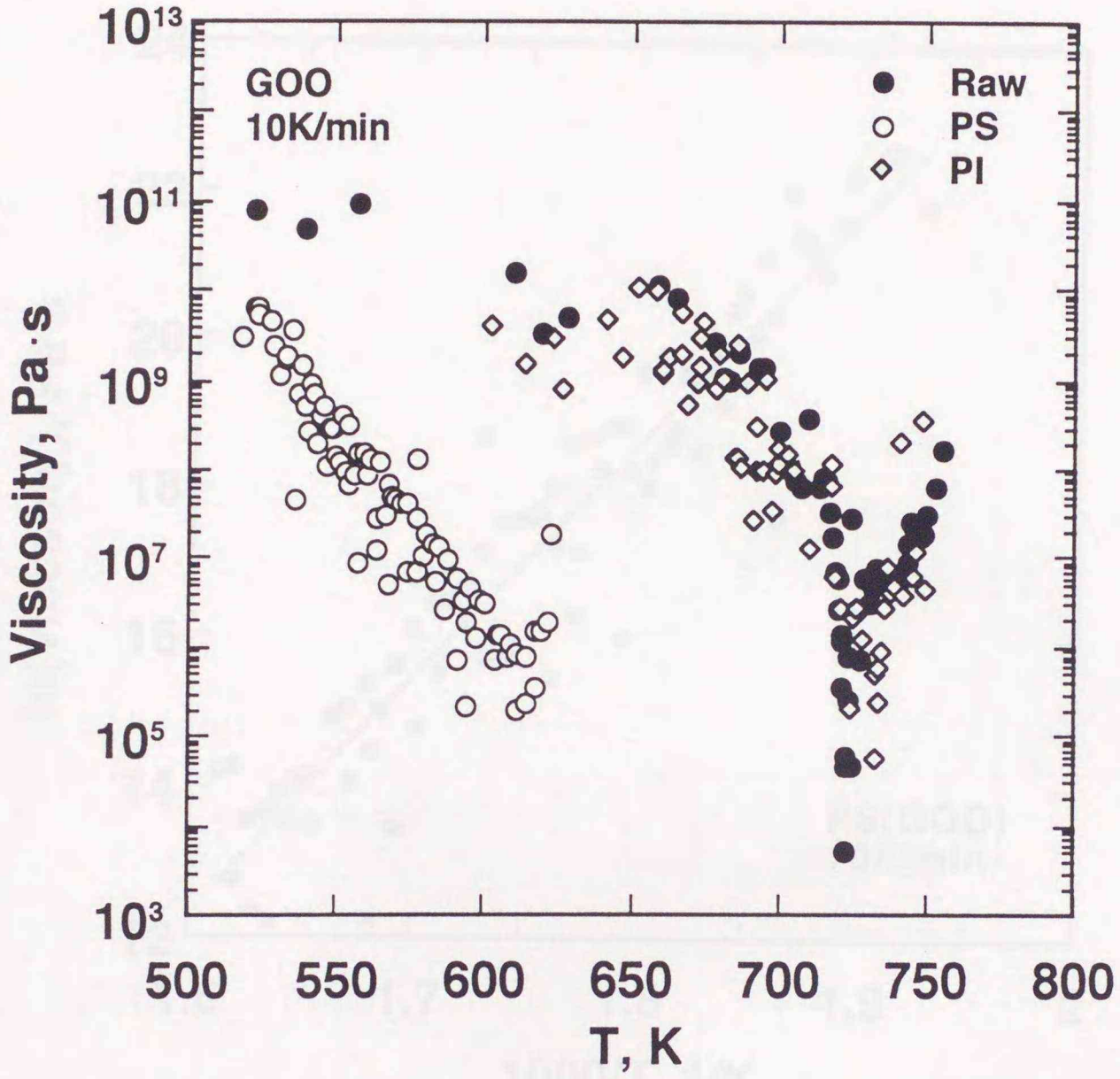

Fig. 3.9 Changes with temperature in apparent viscosity for GOO raw coal, PS and PI of its coal heated at 10 K/min under 1.0 MPa.

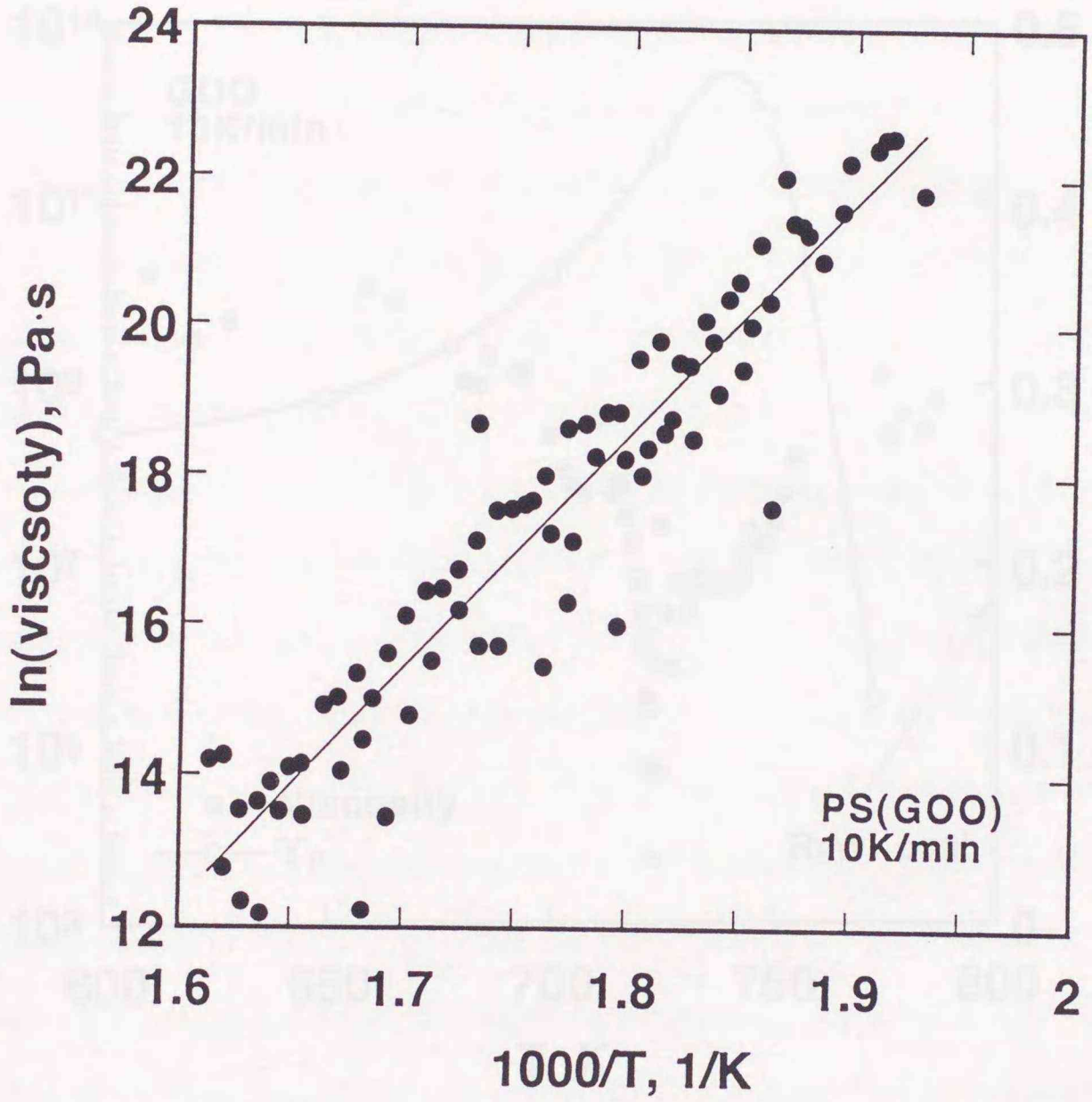

Fig. 3.10 Plots based on Andrade's equation for apparent viscosity of PS for GOO coal.

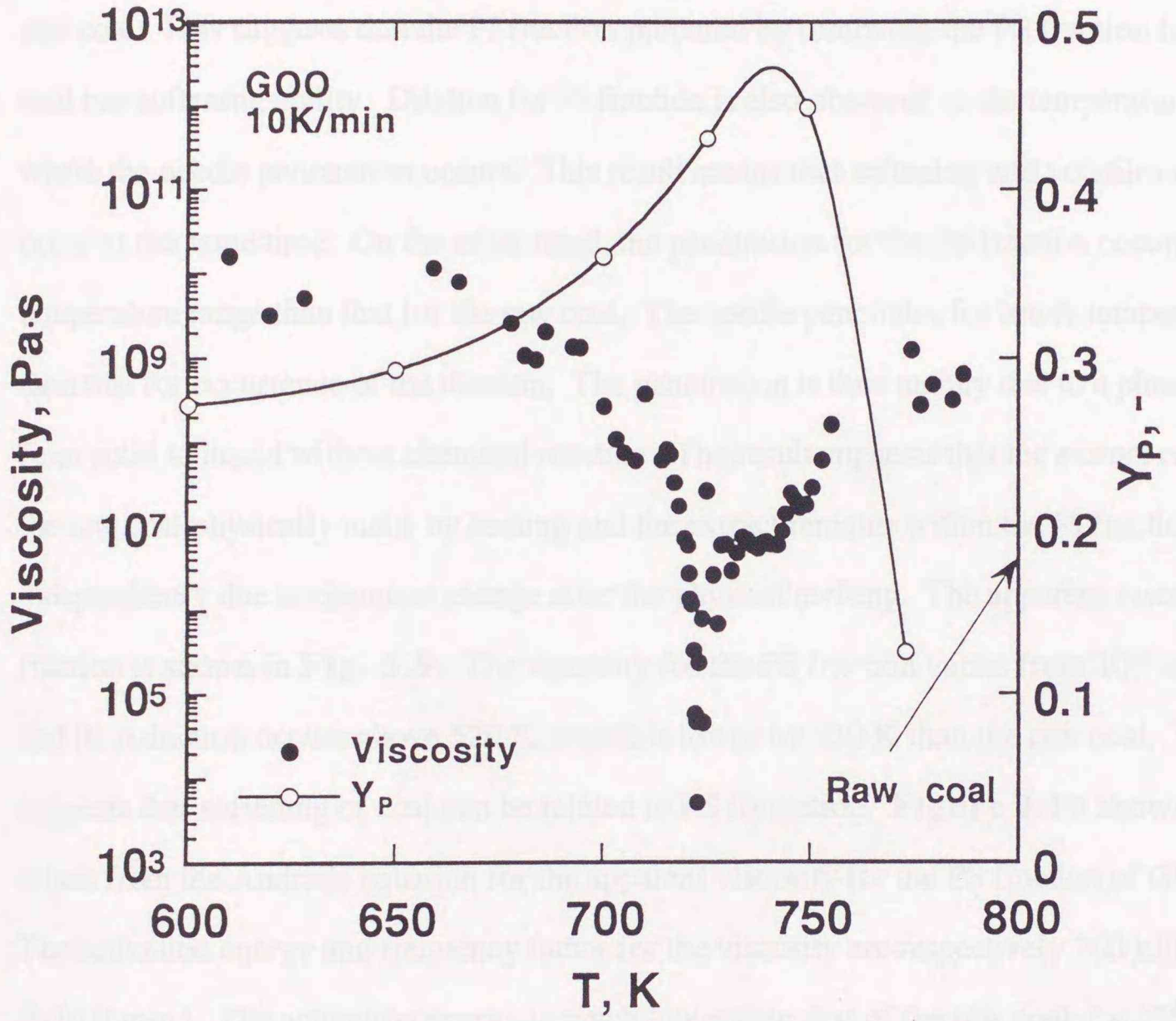

Fig. 3.11 Relationship between apparent viscosity and Y_P for GOO coal heated at 10 K/min under 1.0 MPa.

suggested that softening occurs at the temperature region where molecular mobility is high.

Figure 3.8 represents changes with temperature in apparent needle penetration depth, H, relative degree of volumetric dilation, Q, and net needle penetration depth, h, for the pellets made of GOO raw coal, its PS and PI fraction heated at 10 K/min under 1.0 MPa. The temperature range for occurrence of the penetration of the PI fraction is higher than that of the raw coal. This suggests that the PI fraction prepared by removing the PS fraction from the raw coal has softening ability. Dilation for PI fraction is also observed in the temperature range where the needle penetration occurs. This result means that softening and volatiles release occur at the same time. On the other hand, the penetration for the PS fraction occurs in a lower temperature range than that for the raw coal. The needle penetrates for lower temperature range than that for occurrence of the dilation. The penetration is thus mainly due to a phase transition from solid to liquid without chemical reaction. The result suggests that the extract contained in the raw coal physically melts by heating and the extract remains within the PI fraction forms independently due to chemical change after the physical melting. The apparent viscosity of each fraction is shown in **Fig. 3.9**. The viscosity for the PS fraction varies from 10^{10} to 10^{5} Pa.s and its reduction occurs above 520 K, which is lower by 130 K than the raw coal. This suggests that softening of coal can be related to PS formation. **Figure 3.10** shows plots arisen from the Andrade equation for the apparent viscosity for the PS fraction of GOO coal. The activation energy and frequency factor for the viscosity are respectively 260 kJ/mol and $5x10^{-17}$ min^{-1}. The activation energy is much lower than that of the raw coal, *i.e.*, 2540 kJ/mol as listed in Table 2.3 and roughly coincides with that of pitch *i.e.*, 226 kJ/mol.[18] From the above results, the PS fraction can be reasonably assumed to behave as a liquid upon heating.

In **Fig. 3.11** relationship between the viscosity and Y_P for GOO coal heated at 10 K/min under 1.0 MPa is shown. The temperature for the minimum viscosity is in disagreement with that for the maximum Y_P. However, the temperature range for occurrence of viscosity change coincides with that for change of Y_P. It is seen that increase of Y_P is related to decrease of the viscosity.

3.4 Conclusions

In this chapter the heat flux, fraction of mobile ^1H and yield of pyridine extract were measured for quantification of the metaplast formation in a wide range of operating variables. The following conclusions are to be made.

The temperature giving for the minimum viscosity was similar to those for the endothermic peak, the maximum yield of mobile ^1H and maximum yield of pyridine extract. Softening characteristics seem to have a certain relation to the mobility of molecules. The DSC and ^1H NMR are difficult to be applied to quantification of the metaplast. On the other hand, the solvent extraction method is applicable for quantification of the metaplast. The increase in the extraction yield is related to the softening characteristics. The pyridine extract can behave as a liquid in molten coal upon heating.

References

1) Y. Yun and E. M. Suuberg, *Fuel*, **72** (1993), 1245.

2) Y. Yürüm, A. K. Karabakan and N. Altuntas: *Energy and Fuels*, **5** (1991), 701.

3) S. K. Janikowski and V. I. Stenberg: *Fuel*, **68** (1989), 95.

4) J. P. Elder and M. B. Harris: *ibid.*, **63** (1984), 262.

5) O. P. Mahajan, A. Tomita, J. R. Nelson and P. L. Walker Jr.: *ibid.*, **56** (1977), 33.

6) L. J. Lynch, D. S. Webster, R. Sakurovs, W. A. Barton and T. P. Maher: *ibid.*, **67** (1988), 579.

7) R. Sakurovs, L. J. Lynch, T. P. Maher and R. N. Banerjee: *Energy and Fuels*, **1** (1987), 167.

8) H. R. Brown and P. L. Waters: *Fuel*, **45** (1966), 17.

9) K. Miura, H. Nakagawa, D. Tsutsumi, T, Fujisawa and K. Niwa: *Tetsu-to-Hagané*, **82** (1996), 399.

10) M. Iino, Q. T. Li and M. Matsuda: *Nenryokyokaishi*, **64** (1985), 248.

11) Idem, *ibid.*, **65**, (1986) 389.

12) K. Ouchi, K. Tanimoto, M. Makabe and H. Itoh: *Fuel*, **62** (1983), 1227.

13) T. Takanohashi, T. Yoshida, M. Iino, K. Katoh and K. Fukada: *Tetsu-to-Hagané*, **82** (1996), 366.

14) H. Seki, J. Kumagai, M. Matsuda, O. Itoh and M. Iino: *Fuel*, **68** (1989), 978.

15) G. R. Oxley and G. J. Pitt: *ibid.*, **37** (1958), 19.

16) J.-i. Hayashi, T. Maezono, M. Ando, K. Kusakabe and S. Morooka: *Nenryokyokaishi*, **69** (1990), 378.

17) J.-i. Hayashi, M. Ando, K. Kusakabe and S. Morooka: *ibid.*, **69** (1990), 446.

18) T. Nakagawa: Rheology, 2nd ed., Iwanami Book Co., Tokyo (1983), 108.

Chapter 4
Estimation of Devolatilization Characteristics by A Simple Model

4.1 Introduction

In Chap. 2 changes with time in the needle penetration depth and volumetric dilation ratio were measured for coal pellets in a wide range of operating variables.[1] The observed effect of heating rate and coal nature on penetration curves are explained by a simple model[2] based on an equation of motion in which coal is assumed to behave as a Newtonian fluid. However, the model contains ten unknown model parameters and the determination is arbitrary.

Release of volatiles occurs during softening and resolidification processes. Thus, mass fraction for the pellet and pulverized particles due to volatiles release was respectively measured as a function of time by using a thermobalance and a micro-autoclave under the same conditions as the penetration experiment. In this chapter, the mass fraction curves were evaluated by a simple reaction model[3] and the kinetic parameters for pyrolysis and carbonization reactions included in the needle penetration model were estimated.

4.2 Experimental

4.2.1 Sample

Six kinds of the coals having different elemental compositions and volatile matter contents as listed in Table 2.1 were pulverized to sizes smaller than 100 mesh. The pulverized coals were pelletized as described in Chap. 2. The pellet and particles of 100 mg were used respectively in the micro-autoclave experiment and in the thermogravimetric analysis, TGA.

4.2.2 Apparatus and Procedure

In TGA experiment the sample was heated at 7 K/min from room temperature up to 426 K under nitrogen gas atmosphere and was kept for 20 min to remove the water remaining in coal. It was then heated at 50 K/min up to prescribed holding temperatures and was further heated for 60 min. On the other hand, a stainless steel 60 cm^3 micro-autoclave was used in the micro-autoclave experiment. The schematic diagram of apparatus is shown in **Fig. 4.1**. The apparatus was quite similar with that for the penetration experiment as shown in Fig. 2.1. Each of two different kinds of coal pellets was put into a steel cell of 10.6 mm *i.d.* placed in the autoclave and then heated. It was confirmed that in the preliminary experiments that changes in the mass fraction for each pellet were not affected by the adsorption of volatiles from the other pellet. The experiment was carried out for the range of the heating rate from 1 to 50 K/min, the holding temperature from 673 to 823 K and the nitrogen gas pressure of 0.1 and 1.0 MPa. After prescribed time elapsed, the pellets were cooled at about 100 K/min by blowing air. After cooling, solid residues were weighed and the mass fraction was calculated on the basis of initial mass.

4.3 Results and Discussion

4.3.1 Release of Volatiles from Pulverized Particles and Pellets

Figure 4.2 shows a typical comparison between TGA and the micro-autoclave results for changes in the mass fraction with holding time for CER coal particles and pellets heated at 50 K/min and 0.1 MPa up to various holding temperatures. In the figure the mass fraction, W/W_0, plots against holding time, t, which is defined as time having elapsed after the temperature reached the holding one. Lines and symbols respectively denote the data from TGA and the micro-autoclave experiments. It is seen that yields of volatiles released from the pellet are larger than those from the pulverized particles below the holding temperature of 723 K. On the other hand, the yields are similar above 773 K. The devolatilization characteristics seem to depend on sample type. Similar results were obtained for different kinds of coals. Differences in the

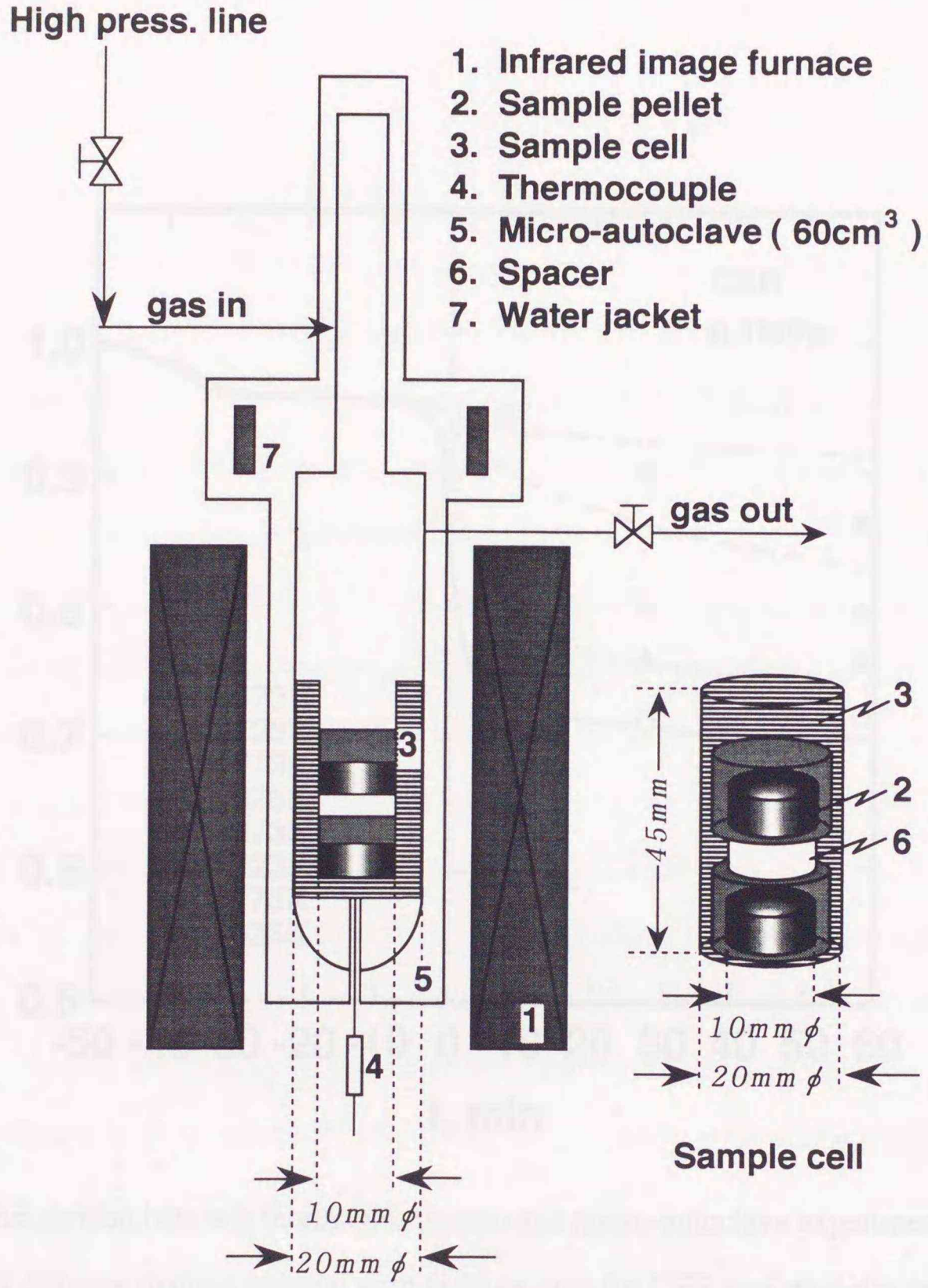

Fig. 4.1 Schematic diagram of experimental apparatus.

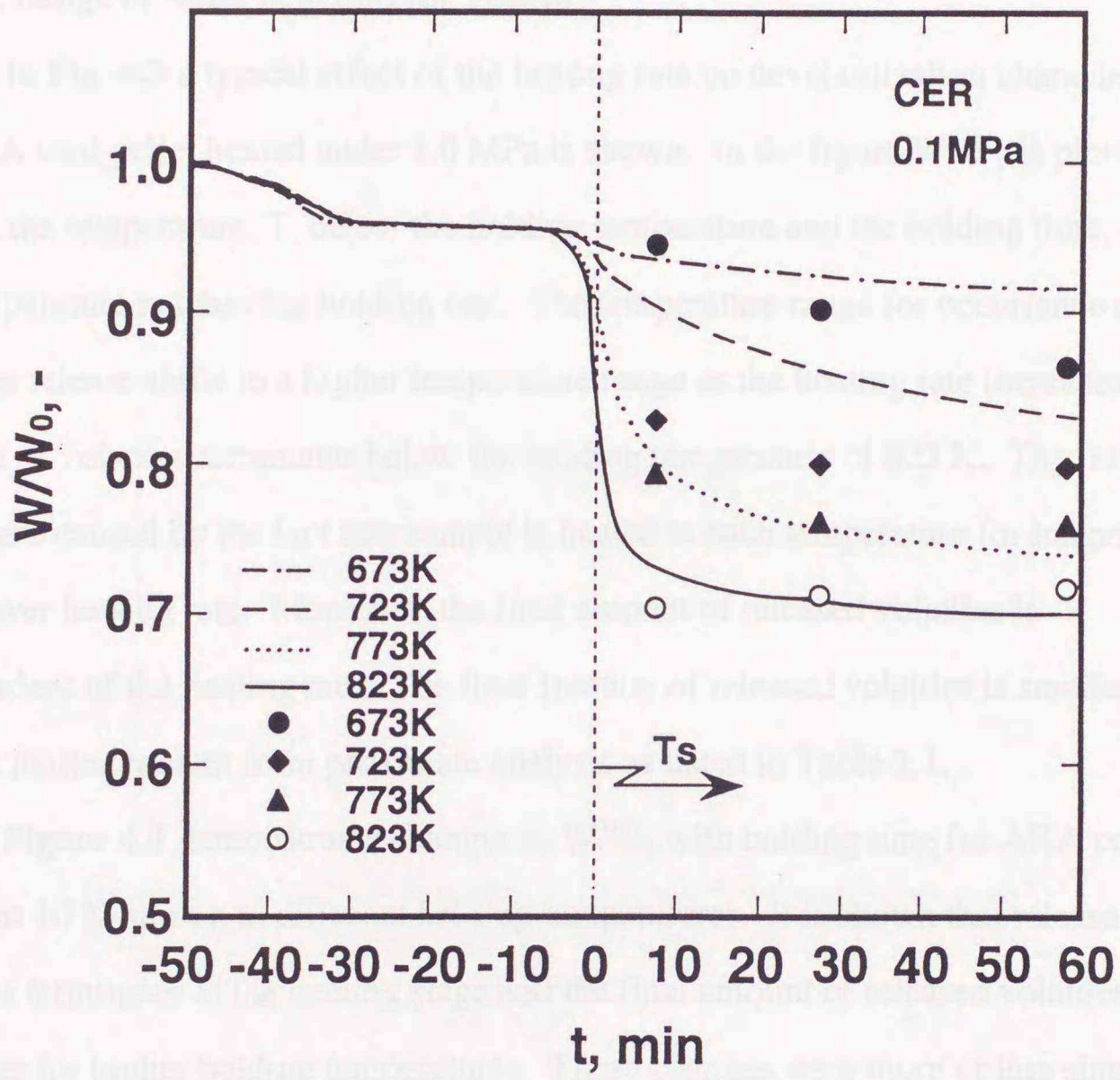

Fig. 4.2 Comparison between thermogravimetric and micro-autoclave experiments for changes in mass fraction with holding time for CER coal particles and pellets heated at 50 K/min and 0.1 MPa up to various holding temperatures.

reactor dimension, specific surface areas of the sample, and cooling rate may cause difference in the mass fraction. However, the details are unknown. Therefore, effects of the operating variables on devolatilization characteristics were investigated using the pellet.

4.3.2 Change of Mass Fraction for Pellets

In **Fig. 4.3** a typical effect of the heating rate on devolatilization characteristics for AKA coal pellet heated under 1.0 MPa is shown. In the figure W/W_0 is plotted against the temperature, T, below the holding temperature and the holding time, t, after the temperature reaches the holding one. The temperature range for occurrence of volatiles release shifts to a higher temperature range as the heating rate increases. Release of volatiles terminates below the holding temperature of 823 K. The former results are caused by the fact that sample is heated at each temperature for longer time with lower heating rate. Moreover, the final amount of released volatiles is independent of the heating rate. The final fraction of released volatiles is smaller than volatile matter content from proximate analysis as listed in Table 2.1.

Figure 4.4 demonstrates changes in W/W_0 with holding time for AKA coal heated at 10 K/min up to different holding temperatures. It is shown that release of volatiles terminates at the heating stage and the final amount of released volatiles increases for higher holding temperatures. These changes were more or less similar for different kinds of coals as mentioned below.

Figure 4.5 shows the effect of coal nature on devolatilization characteristics. Profiles of W/W_0 curves are similar for different coals. The release of volatiles terminates at the heating stage and W/W_0 at the holding stage is constant depending on the coal nature. The final fraction of coal having higher volatile matter contents is higher.

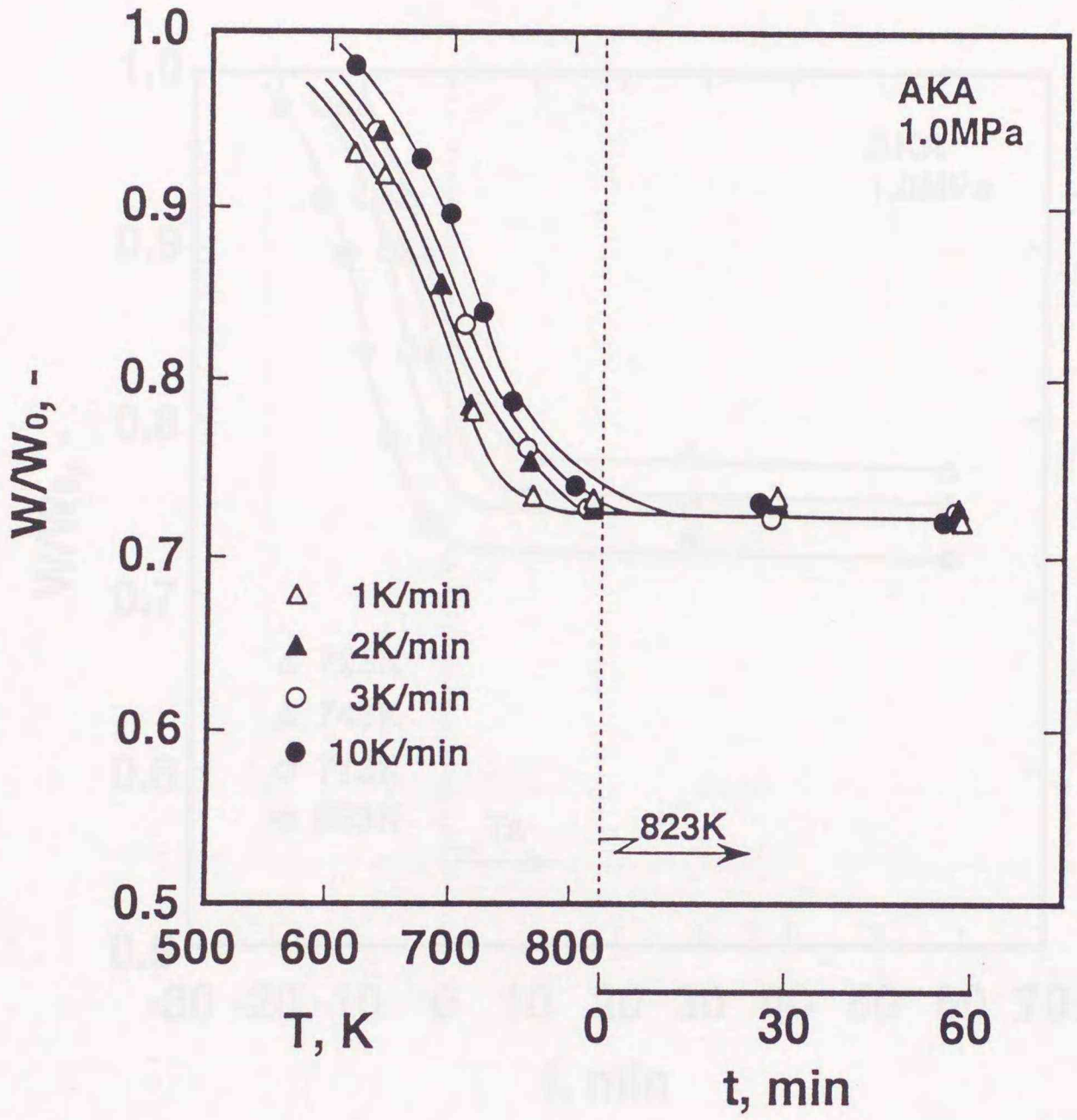

Fig. 4.3 Effect of heating rate on mass fraction for AKA coal pellet heated at 1.0 MPa with holding temperature of 823 K.

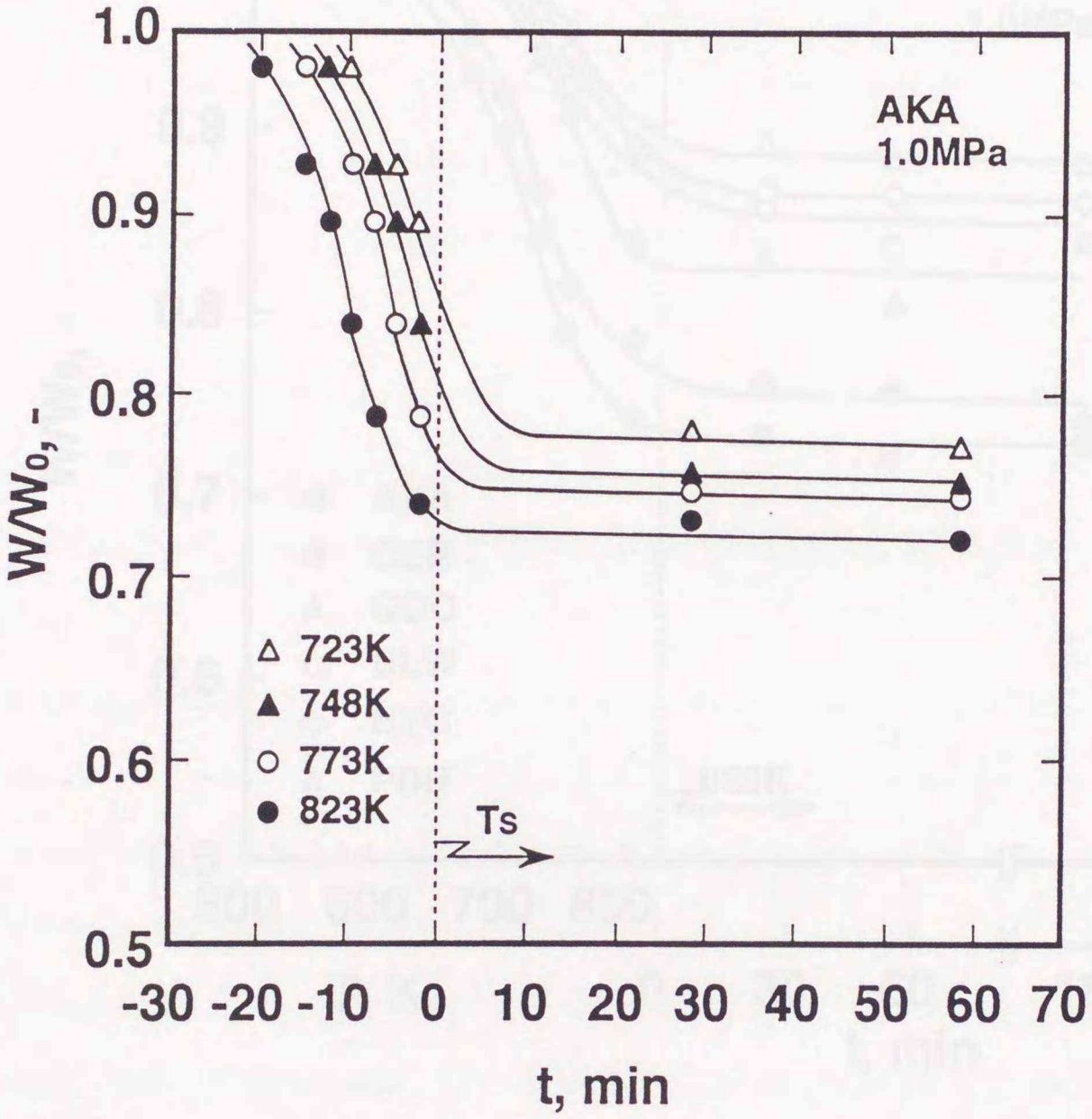

Fig. 4.4 Effect of holding temperature on mass fraction for AKA coal pellet heated at 10 K/min under 1.0 MPa.

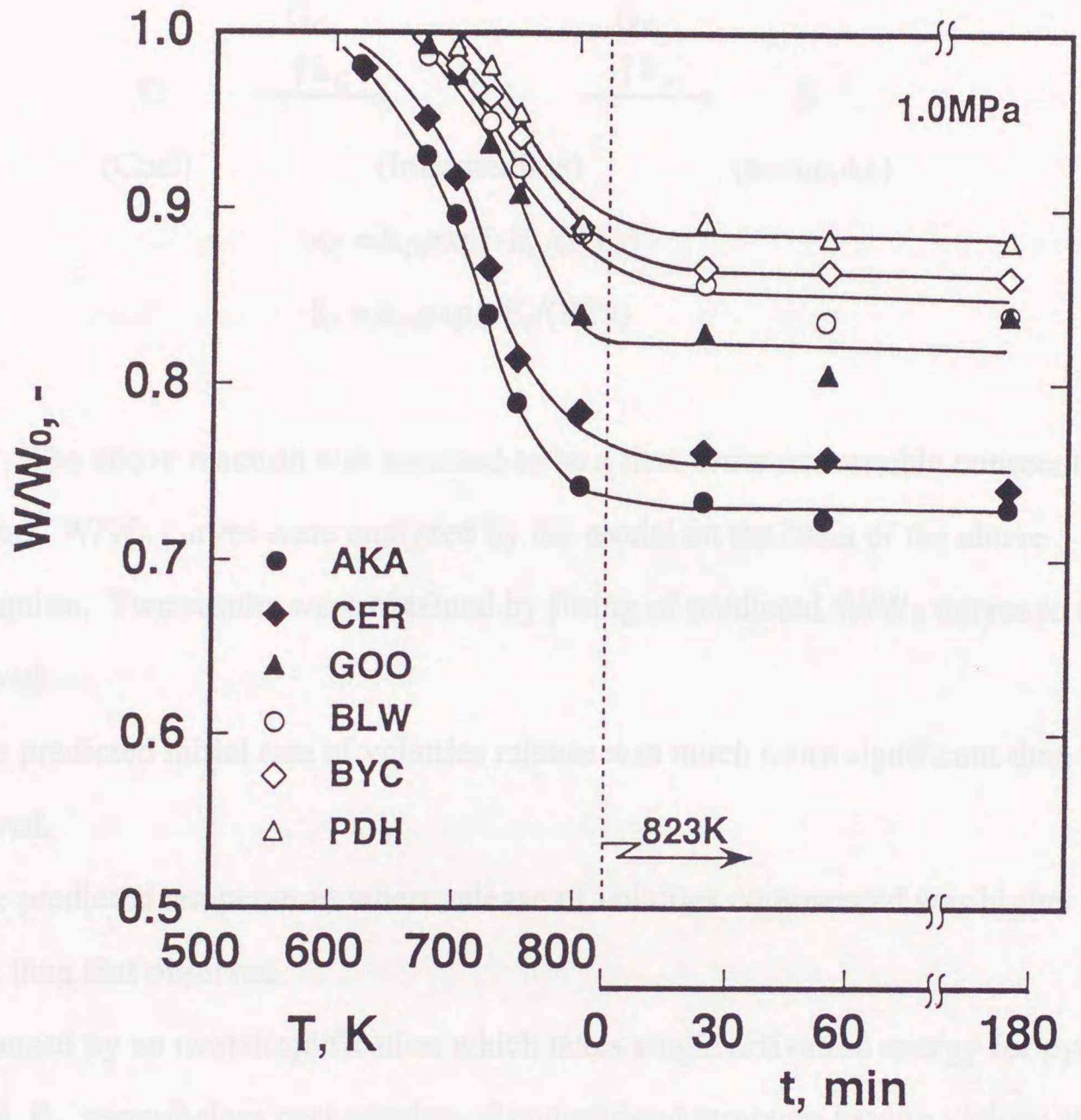

Fig. 4.5 Devolatilization characteristics for different coal pellets heated at 10 K/min under 1.0 MPa up to 823K.

4.3.3 Estimation by A Simple Reaction Model

The above results were explained by a simple model[4] assuming that coal, C, upon heating converts into semicoke, S, *via* an intermediate, P, along with release of the volatiles, G_C and G_P.

$$\mathrm{C} \xrightarrow[\uparrow k_C]{G_C} \mathrm{P} \xrightarrow[\uparrow k_P]{G_P} \mathrm{S}$$

(Coal) (Intermediate) (semicoke)

$$k_C = k_{C0}\exp\{-E_C/(RT)\}$$

$$k_P = k_{P0}\exp\{-E_P/(RT)\}$$

The above reaction was assumed to be a first-order irreversible consecutive reaction. W/W_0 curves were analyzed by the model on the basis of the above assumption. Two results were obtained by fitting of predicted W/W_0 curves to those observed:

1) The predicted initial rate of volatiles release was much more significant than that observed.

2) The predicted temperature where release of volatiles commenced was higher by *ca.* 100 K than that observed.

It is caused by an oversimplification which takes single activation energy for pyrolysis of coal, E_C, nevertheless coal consists of complicated structure having various chemical linkages to be broken,[5,6] and species of volatiles depend on temperature.[7]

Thus, a developed model is proposed here. In this model hypotheses such as coal liquefaction and gasification[8,9] are set up as follows. Coal consists of two components, C_C and C_G, having different reactivities for pyrolysis; one producing volatiles along with formation of semicoke *via* the intermediate and the other converting to gas directly:

$$C_C \xrightarrow[\uparrow k_C]{G_C} P \xrightarrow[\uparrow k_p]{G_P} S \qquad \text{-(I)}$$

(Coal) (Intermediate) (semicoke)

$$C_G \xrightarrow{k_G} G_G \qquad \text{-(II)}$$

(Coal) (Gas)

In this developed model, the initial sample mass, W_0, is assumed to be equal to sum of the initial mass of components of C_C and C_G and is given by

$$W_0 = W_{CC0} + W_{CG0}. \qquad \text{-(4.1)}$$

C_C consists of two component converting to the volatiles, G_C, and P. Therefore, the initial mass of C_C is written as

$$W_{CC0} = W_{GC0} + W_{CP0} \qquad \text{-(4.2)}$$

where $W_{GC0} = W_{CC0}VM_C$, $W_{CP0} = W_{CC0}(1\text{-}VM_C)$.

Moreover, P consists of two components converting to G_P and S, and represents as follows.

$$W_P = W_{GP} + W_{PS} \qquad \text{-(4.3)}$$

Here, W_{GP} and W_{PS} respectively denote as

$$W_{GP} = W_P VM_P$$

$$W_{PS} = W_P(1\text{-}VM_P).$$

When temperature is constant, total amount of volatiles released from 0 to t is given by,

$$W_G = W_{GC} + W_{GP} + W_{GG}. \qquad -(4.4)$$

W_{GC}, W_{GP} and W_{GG} respectively denote

$$W_{GC} = W_{CC0} VM_C\{1-\exp(-k_C t)\} \qquad -(4.5)$$

$$W_{GP} = W_{CC0}(1-VM_C)VM_P/(k_P-k_C) \times$$
$$[k_P\{1-\exp(-k_C t)-k_C\{1-\exp(-k_P t)\}] \qquad -(4.6)$$

$$W_{GG} = W_{CG0}\{1-\exp(-k_G t)\}. \qquad -(4.7)$$

Therefore, the mass fraction of solid residue, $W/W_0(=(W_0- W_G)/W_0)$, is represented as follows by the following equation,

$$W/W_0 = 1 - VM\times W_{CC0}/W_0[\{f_C + k(1 - f_C) \times$$
$$\{1 - \exp(-k_C t)\}-(k -1)(1 - f_C)\{1 - \exp(-k_P t)\}]$$
$$- W_{CG0}/W_0\{1 - \exp(-k_G t)\}, \qquad -(4.8)$$

where $k = k_P/(k_P - k_C)$, $f_C = VM_C/VM$.

The observed mass fraction is explained by that calculated using Eq. 4.8 based on the following assumptions.

i) Rate constant, k_i, in Eq. 4.8 is expressed by the Arrhenius law,

$$k_i = k_{i0}\exp\{-E_i/(RT)\}. \qquad -(4.9)$$

ii) The final mass fraction due to release of the volatiles from the reaction (I) is equal to VM.

$$VM = VM_C + VM_P(1 - VM_C) \qquad -(4.10)$$

iii) Temperature distribution within the pellet is negligible.

iV) Temperature, T, and rate constant, k_i, are steady for very short time upon heating (instantaneous steady state).

The model contains six parameters (k_{C0}, k_{P0}, k_{G0}, E_C, E_p and E_G) and the parameters were determined as follows. k_{G0} and E_G were given roughly on the basis of the assumption which volatiles release due to the reaction (II) commences for lower temperature range. It is considered that the reaction (I) occurs in a higher temperature range near the holding temperature. The data at the temperature range where volatiles release would drastically occurs were analyzed to determine k_C and E_C . k_{P0}, E_P and VM were determined by the final fraction at the holding temperature. f_C was determined by fitting the predicted curves to the experimental results for the whole temperature range. Furthermore, the model parameters were adjusted to fit the prediction to the observed changes in W/W_0 for the same coal heated at different heating rates. The initial mass fraction of C_G was considered to depend on the coal nature. As the details were unknown, it was fixed to be 0.10 for all conditions. Temperature width in the consecutive calculation upon heating was 1 K for all the prediction, because no difference was shown if the width was less than 3 K in the preliminary calculation.

Figure 4.6 shows a typical comparison of predicted W/W_0 with those observed for AKA coal heated at different rates. It is seen that the observed effect of the heating rate on W/W_0 is explained by the model. The results were similar for the other coals. **Figure 4.7** shows adjustment of predicted curves to the experimental results for

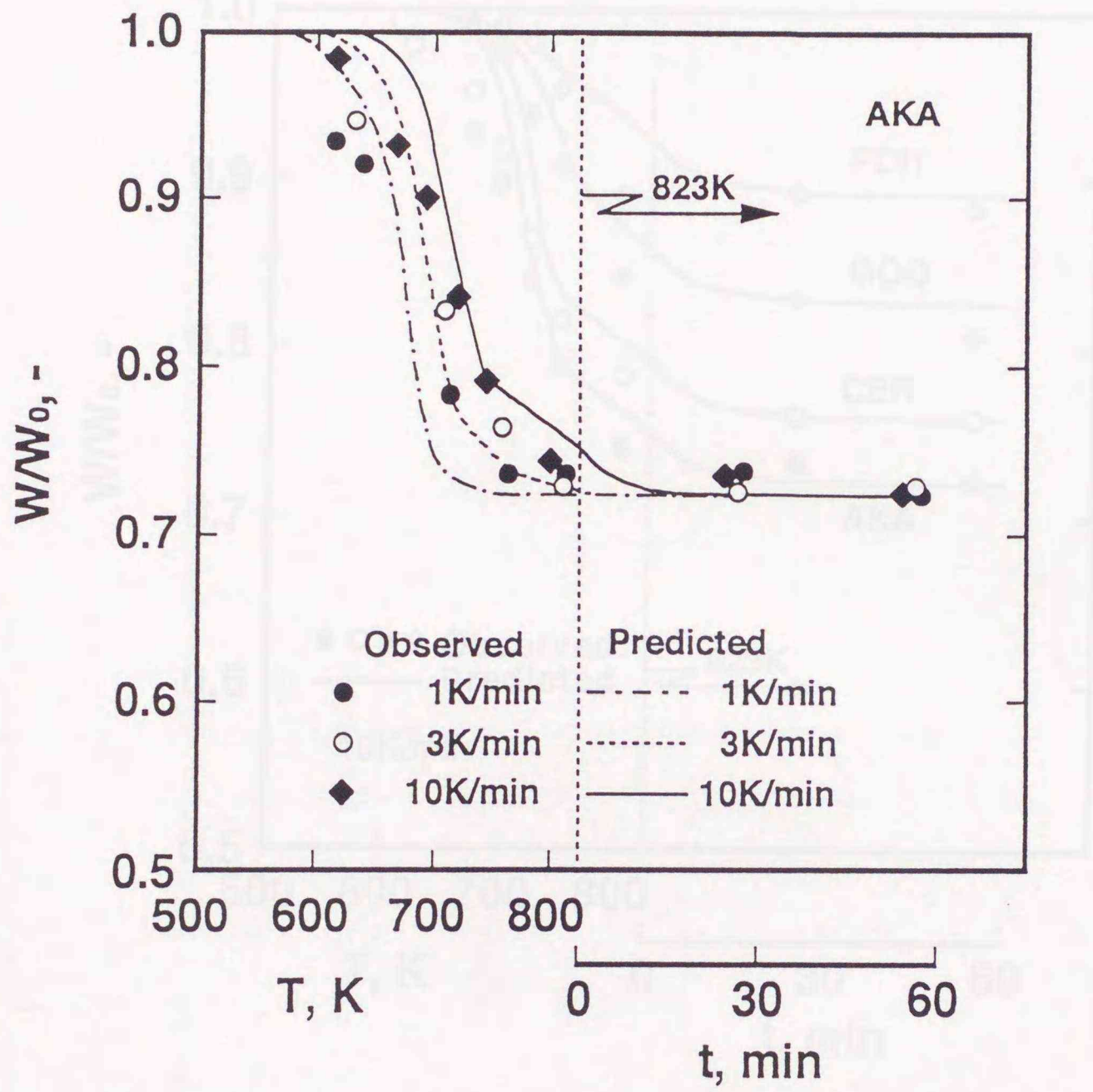

Fig. 4.6 Comparison of observed and predicted mass fractions with those predicted for AKA coal heated at different rates.

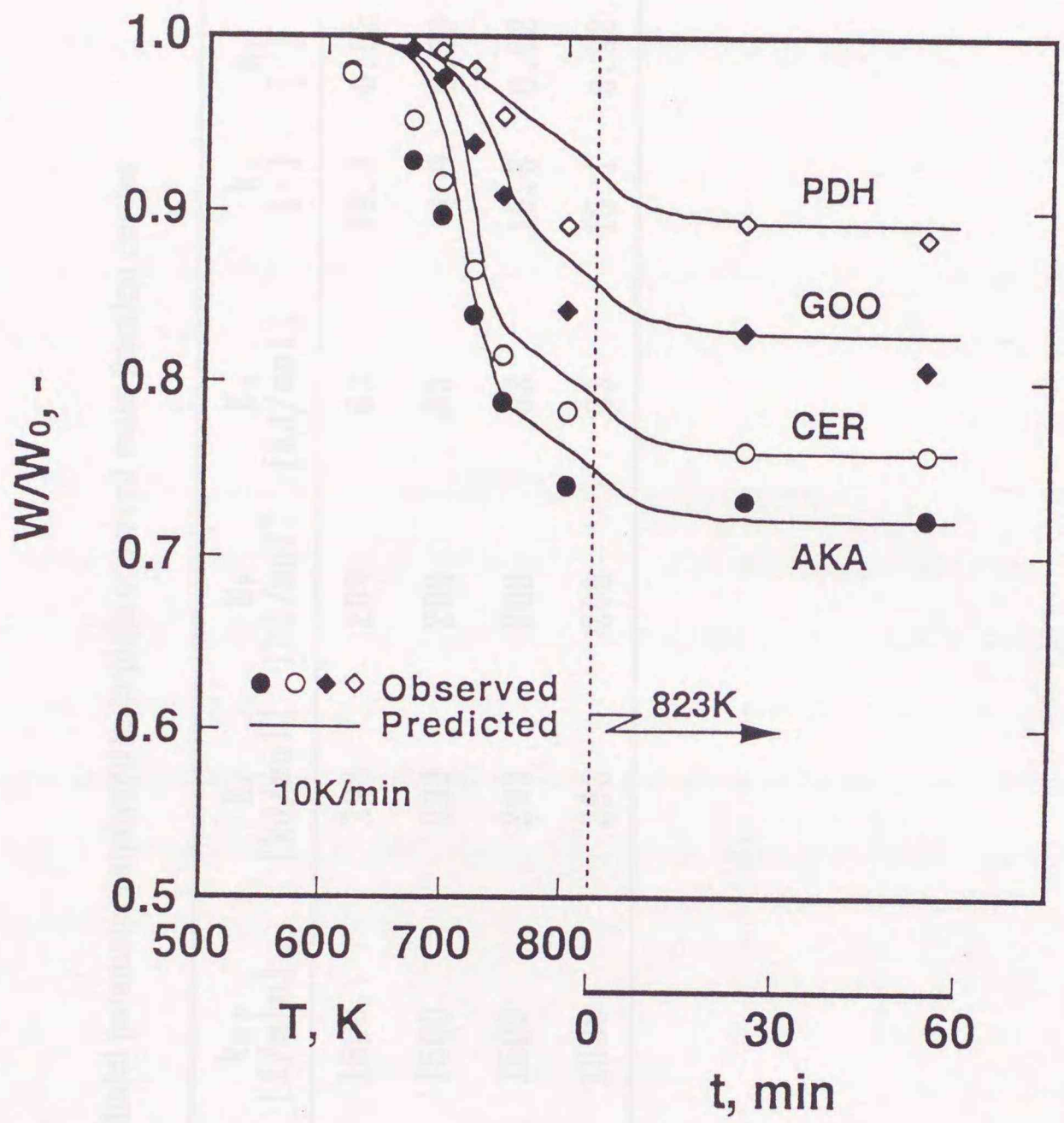

Fig. 4.7 Comparison of observed and predicted mass fractions with those predicted for different coals heated at 10 K/min.

Table 4.1 Model parameters analyzed to explain observed mass fraction curves.

Coal	k_{C0} [1/min]	k_{P0} [1/min]	k_{G0} [1/min]	E_C [kJ/mol]	E_P [kJ/mol]	E_G [kJ/mol]	k_1 [-]	k_2 [-]	VM [-]	f_C [-]
AKA	5.0×10^{21}	7.0×10^{14}	1500	293	209	63	19.1	0.92	0.22	0.4
CER	1.0×10^{21}	1.8×10^{15}	1500	293	209	63	4.9	0.85	0.17	0.4
GOO	8.0×10^{20}	2.1×10^{14}	1500	293	209	63	19.5	0.92	0.09	0.4
PDH	5.0×10^{20}	2.8×10^{14}	1500	293	209	63	15.1	0.92	0.01	0.4

different coals heated at 10 K/min up to 823 K. It is clear that the developed model assuming only two coal components can describe the effects of coal nature and heating rate on changes in W/W_0. Here, the model parameters given for the calculation are listed in **Table 4.1**. The activation energies, E_C, E_P and E_G, and frequency factor, k_{G0}, are respectively 293, 209 and 63 kJ/mol and 1500 min^{-1} for any coals. On the other hand, VM and frequency factors, k_{C0} and k_{P0}, depend on the coal nature.

4.4 Conclusions

Devolatilization characteristics of coal upon heating were investigated for six kinds of coals by using the thermobalance and the micro-autoclave under various conditions. W/W_0 curves shifted to a higher temperature range with increasing the heating rate. Total amount of released volatiles was independent of the heating rate and increased with the holding temperature. A simple reaction model was proposed for the explanation of devolatilization characteristics assuming that coal consists of two components having different reactivities for pyrolysis; one producing the volatiles along with formation of semicoke *via* an intermediate and the other converting to gas directly. The model was verified to well explain the observed effects of the heating rate as well as the coal nature on mass fraction.

References

1) K. Matsuoka, T. Kumagai and T. Chiba : *ISIJ International*, **36** (1996), 40.

2) K. Matsuoka, J.-i. Hayashi and T. Chiba : submitted to *ISIJ International*

3) K. Matsuoka, H. Kawai, T. Kumagai and T. Chiba : *Tetsu-to-Hagané*, **82** (1996), 383.

4) K. Matsuoka, H. Kawai, T. Kumagai and T. Chiba : Preprint of Soc. of Chem. Eng. Japan, Niigata, (1995), 322.

5) M. A. Serio, D. G. Hamblen, J. R. Markham and P. R. Solomon : *Energy and Fuels*, **1** (1987), 138.

6) Energy Sougoukogaku-kenkyujo-Sekitankenkyukai, Sekitangijyutusouran, (1993), p.116 [Denryokusinpousya].

7) K. H. van Heek and W. Hodek : *Fuel*, **73** (1994), 886.

8) H. Nagaishi, H. Moritomi, Y. Sanada and T. Chiba : *Energy and Fuels*, **2** (1988), 522.

9) S. Takeda, M. Ikegami, K. Kitano, N. Takezawa and T. Chiba : *Nenryokyokaishi*, **70** (1991), 424.

Chapter 5
A Simple Model for Softening and Resoldification

5.1 Introduction

When heated beyond *ca.* 600 K, coal undergoes pyrolysis and carbonization reactions. For caking coals the former reaction extensively promotes softening of the bulk of coal while the latter resolidification, accompanying volatiles release. The softening and resolidification processes have been evaluated on the basis of fluidity defined by the Gieseler plastometry. Fitzgelard[1,2] analyzed the fluidity using a model which describes the conversion of coal to semicoke by the following consecutive reaction proposed by van Krevelen *et al.*;[3]

$$\text{coal} \rightarrow \text{metaplast} \rightarrow \text{semicoke}$$

In the model, the fluidity was related to formation of the metaplast which was assumed to behave as a liquid and was expressed by a polynomial equation of the metaplast concentration. Fong *et al.*[4,5] developed a plastometer with which the fluidity was measured for caking coals at high heating rates. They evaluated changes of the viscosity transformed from the fluidity, applying the equation proposed by Frankel and Acrivos[6] for high solid-concentration suspensions. Assuming further that the metaplast has a viscosity being constant with temperature, they introduced a minimum fraction of the metaplast required for the formation of suspension.

The metaplast in the above-mentioned models has been functionally defined as an intermediate to be responsible for softening and, in particular, its fraction has been treated as a parameter to fit the models to experimental data. Thus, efforts have been focused on experimental quantification of the metaplast and derivation of some relationships between the yield of solvent extracts from coal and the fluidity.[4,7-9] Generally, since the extracts comprise a wide variety of compounds, proper solvents have to be chosen for the extracts to have a composition and property being invariable along with the progress of pyrolysis

and carbonization. Hayashi *et al.*[10,11] reported that the yields of pyridine and chloroform extracts varied widely with pyrolysis but their average chemical structure and molecular mass distribution exhibited little dependency on the yields. Solomon *et al.*[12] recently proposed an empirical viscosity model based on their macromolecular network pyrolysis model[13] which lumps the product residue as liquid and solid macromolecules. The latter component was assumed to be slurried with liquid molecules and a viscosity equation for slurry was applied to explain existing Gieseler fluidity data. By adjusting the equation to the data they deduced the activation energies of the liquid viscosity which ranges from 210 to 420 kJ/mol depending on temperature. However, the product yields were not compared with those observed and, again, the activation energy was treated as one of the adjustable parameters.

In this study as described in the preceding chapters, the needle penetration and the dilation characteristics were measured by the needle penetrometry and the rates of volatiles release and pyridine extract formation were measured to evaluate the yield of the metaplast. Furthermore, the needle penetration depth into the pellet made of the pyridine extract was measured to develop its viscosity equation in chapter 3. By organizing the results from these measurements, a model is proposed for the coal viscosity and its applicability is tested for the experimental results. The model is verified to explain reasonably well the observed effects of coal nature and heating rate on the needle penetration.

5.2 Prediction by Model

5.2.1 Mathematical Model

In order to explain the above experimental findings, a mathematical model is developed. As summarized in **Fig. 5.1**, the model describes the needle penetration based on an equation of motion for the needle, ;

$$h(dh/dt) = mg/(2\pi\eta_a)\ln(a/b) \qquad -(5.1)$$

Pseudo-steady state equation of motion

$$h(dh/dt) = mg/(2\pi\eta_a)\ln(a/b) \qquad -(5.1)$$

$$h = \sqrt{mg/(\pi\eta_a)\ln(a/b)t + h_0^2} \qquad -(5.2)$$

Apparent viscosity for slurry andliquid

Slurry (Vand's equation)

$$\ln(\eta_a/\eta_P) = k_1(1-f_P)/\{1-k_2(1-f_P)\} \qquad -(5.3)$$

Liquid (Andrade's equation)

$$\eta_P = k_{V0}\exp\{E_V/(RT)\} \qquad -(5.4)$$

Pyrolysis and carbonization reactions and yields

$$C_C \xrightarrow{k_C} P \xrightarrow{k_P} S \qquad -(I)$$

$$C_G \xrightarrow{k_G} G_G$$

$$Y_{CC} = \exp(-k_C t) \qquad -(5.5)$$

$$Y_P = \{k_C/(k_C-k_P)\}\{\exp(-k_C t)-\exp(-k_P t)\}+Y_P\exp(-k_P t) \qquad -(5.6)$$

$$Y_S = Y_{CC0}+Y_{P0}-Y_{CC}-Y_P-Y_{GC}-Y_{GP} \qquad -(5.7)$$

$$Y_{CG} = \exp(-k_G t) \qquad -(5.8)$$

Fig. 5.1 Basic equations for model.

where m, η_a, a and b respectively denote the mass of the needle, the apparent viscosity of coal and the radii of the pellet and the needle. The above equation assumes that softening coal behaves as a Newtonian fluid and has successfully been applied for simplification of the analysis in Chap. 2.[14] Hence, knowing η_a at a given temperature, h can be calculated as

$$h = \sqrt{mg/(\pi\eta_a)\ln(a/b)t + h_0^2} \qquad -(5.2)$$

Based on the results obtained in Chap. 3, the model further assumes that PS fraction behaves as a lubricant or liquid vehicle for solid PI and ash. Thus, the softening coal is treated as a slurry and its viscosity is simulated by Vand's equation; [16]

$$\ln(\eta_a/\eta_P) = k_1(1-f_P)/\{1-k_2(1-f_P)\} \qquad -(5.3)$$

which is applicable for a wide range of the shape factor and concentration of solid particles. In the above equation, k_1, k_2 and f_P represent the Einstein shape factor, the hydrodynamic interaction coefficient and volume fraction of liquid, respectively. Further, the liquid viscosity, η_P, is expressed by Andrade's equation for PS fraction as indicated in Fig. 3.13; [17]

$$\eta_P = k_{V0}\exp\{E_V/(RT)\} \qquad -(5.4)$$

On the other hand, the volume fraction of PS, f_P, can be related to the yield of PS, Y_P, according to a pyrolysis model developed in Chap. 4.[15] Extending the existing pyrolysis models,[1-3] our model assumes that coal consists of two reactive components, C_C and C_G, which convert to semicoke (S) *via* an intermediate (P) and directly to volatiles (G_G), respectively. Here, further volatiles formation is assumed to take place along with the conversions of C_C to P (G_C) and P to S (G_P). Thus, the pseudo-elemental reactions are written as

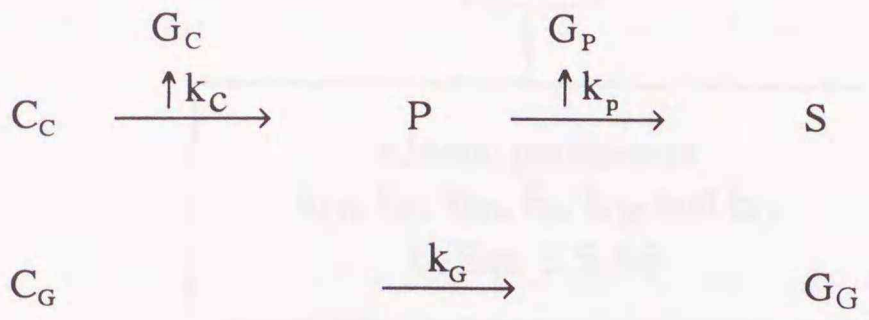

and the yields of C_C, C_G, P and S are respectively given by the following equations:

$$Y_{CC} = \exp(-k_C t) \qquad -(5.5)$$

$$Y_P = \{k_C/(k_C-k_P)\}\{\exp(-k_C t)-\exp(-k_P t)\}+Y_P\exp(-k_P t) \qquad -(5.6)$$

$$Y_S = Y_{CC0}+Y_{P0}-Y_{CC}-Y_P-Y_{GC}-Y_{GP} \qquad -(5.7)$$

$$Y_{CG} = \exp(-k_G t) \qquad -(5.8)$$

Eqs. 5.5 to 5.8 have been verified to give a good fit to the observed characteristics of volatiles release from the heated pellet using the Arrhenius equations;

$$k_i = k_{i0}\exp\{-E_i/(RT)\}$$

for reaction rate constants.[17)]

The applicability of the present model for prediction of the needle penetration was tested, estimating the kinetic parameters independently from the experiment on solvent extraction (Chap. 3) and volatiles release(Chap. 4)[17)]. The procedure of determination of the model parameters are summarized in **Fig. 5.2**. Parameters in the Andrade equation were determined from semi-logarithmic plots of η_P against the reciprocal temperature (Fig. 3.13). The other unknown model parameters were given after examining the

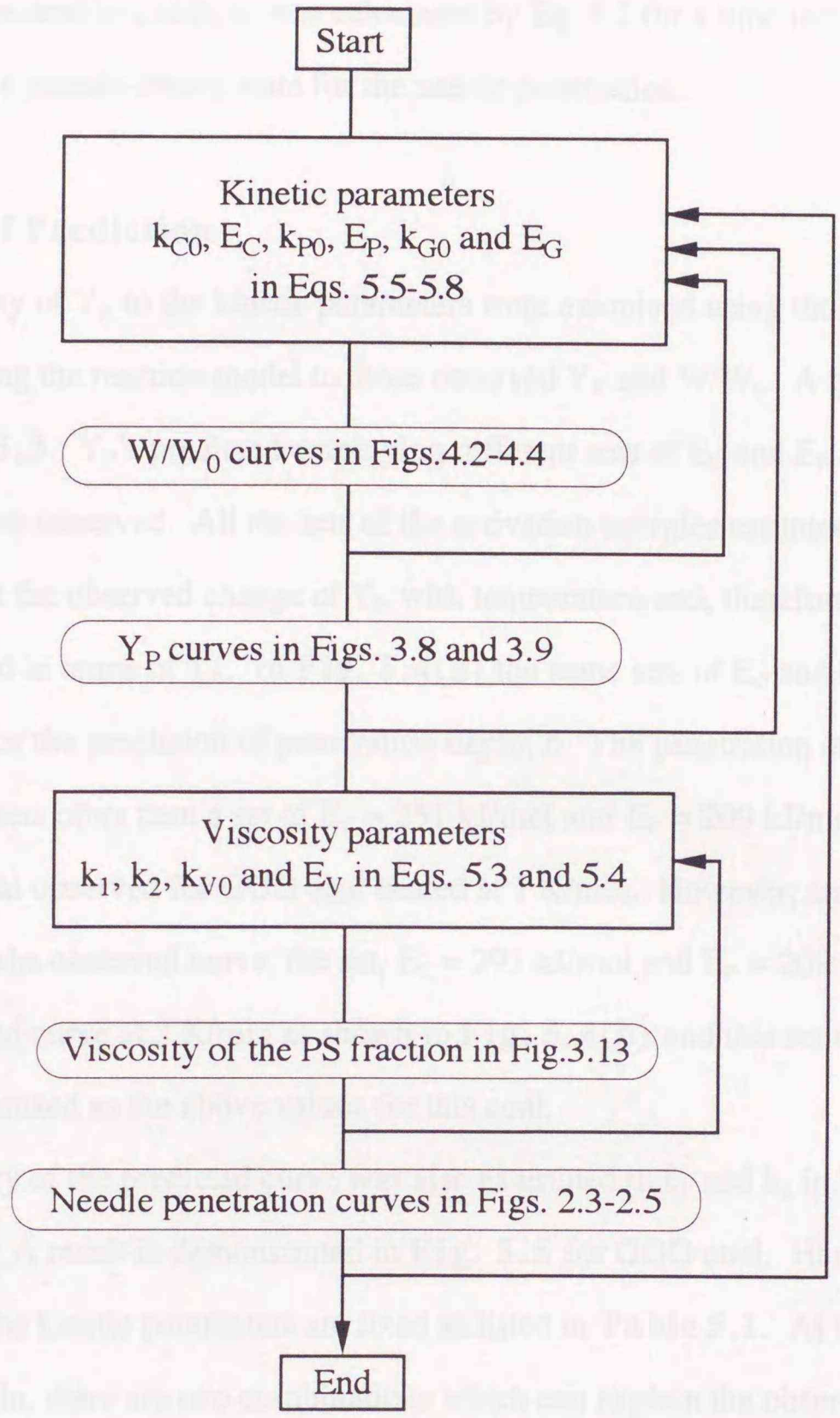

Fig. 5.2 Procedure of determination of model parameters.

sensitivity of the predicted penetration curve to them. For a given set of the model parameters, the penetration depth, h, was calculated by Eq. 5.2 for a time interval short enough to assume a pseudo-steady state for the needle penetration.

5.2.2 Results of Prediction

The sensitivity of Y_P to the kinetic parameters were examined using those determined by fitting the reaction model to those observed Y_P and W/W_0. A typical result is shown in **Fig. 5.3**. Y_P's predicted employing different sets of E_C and E_P are compared with those observed. All the sets of the activation energies assumed here seem to similarly explain the observed change of Y_P with temperature and, therefore, these cannot be optimized in terms of Y_P. In **Fig. 5.4(a)** the same sets of E_C and E_P were further examined for the prediction of penetration depth, h. The penetration curves predicted with the sets other than a set of E_C = 251 kJ/mol and E_P = 209 kJ/mol reasonably fit to that observed for GOO coal heated at 1 K/min. However, among those which can explain the observed curve, the set, E_C = 293 kJ/mol and E_P = 209 kJ/mol, can explain the observed curve at 3 K/min as shown in **Fig. 5.4(b)** and this set of E_C and E_P was finally optimized as the above values for this coal.

The sensitivity of the predicted curve was also examined to k_1 and k_2 in Vand's equation (Eq. 5.3). A result is demonstrated in **Fig. 5.5** for GOO coal. Here, values of k_{V0} and E_V and the kinetic parameters are fixed as listed in **Table 5.1**. At the lower heating rate, 1 K/min, there are two combinations which can explain the observed curve equally well, however, at the higher heating rate, 3 K/min, the set of k_1 = 19.5 and k_2 = 0.92 gives a better fit.

Table 5.1 summarizes all the model parameters assumed for the individual coals. The same sets of the parameters of all the activation energies and the frequency factor, k_{G0}, can be employed for all the coals whereas the frequency factors, k_{C0}, k_{P0} and k_{V0}, and viscosity parameters, k_1 and k_2, must be varied depending on the coal nature. In addition, k_1 and k_2 are also given as functions of the coal nature.

In **Figs. 5.6 (a) and (b)** are shown comparison of the predicted mass fraction

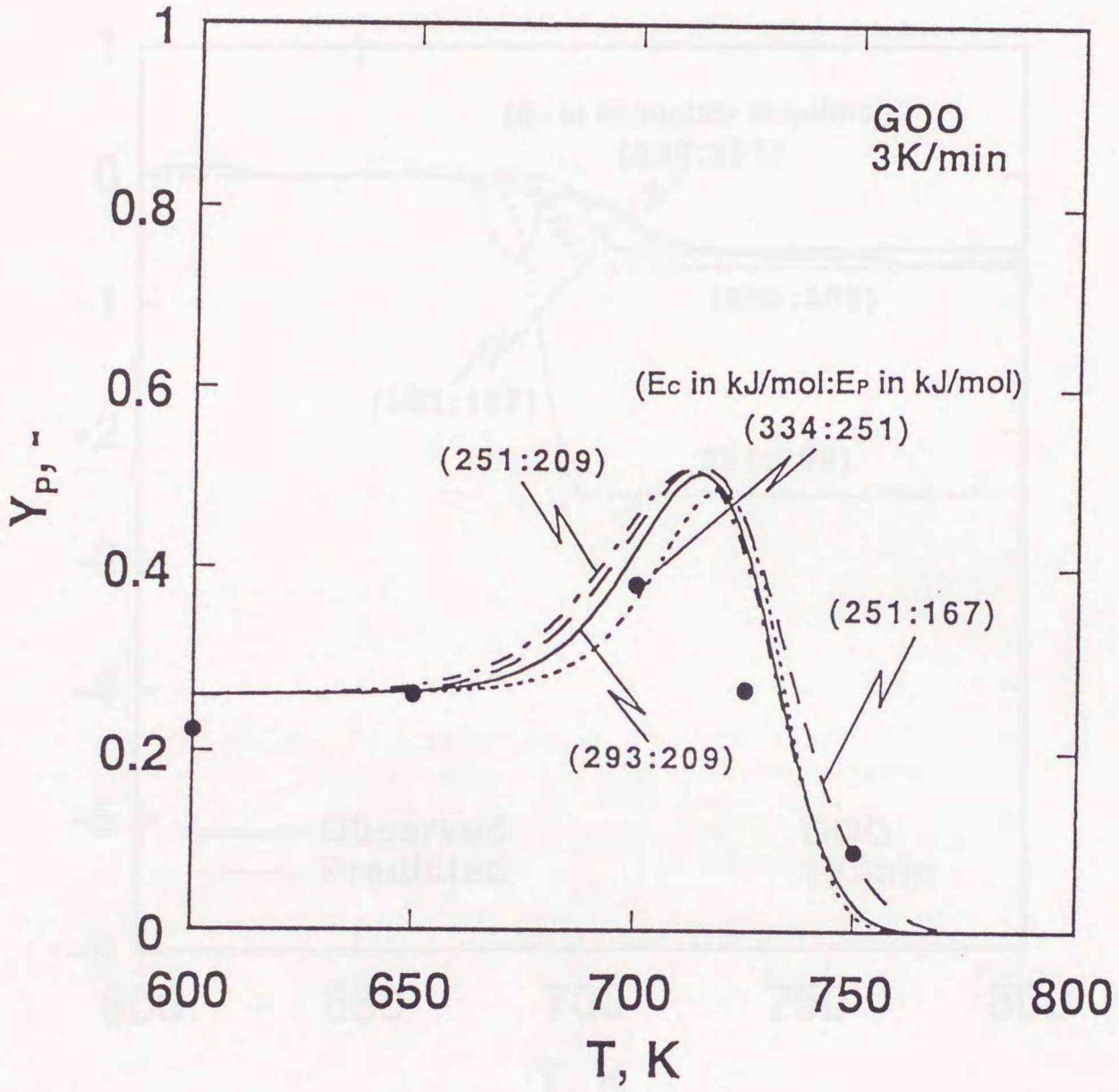

Fig. 5.3 Predicted effect of E_C and E_P on Y_P versus T for GOO coal heated at 3 K/min.

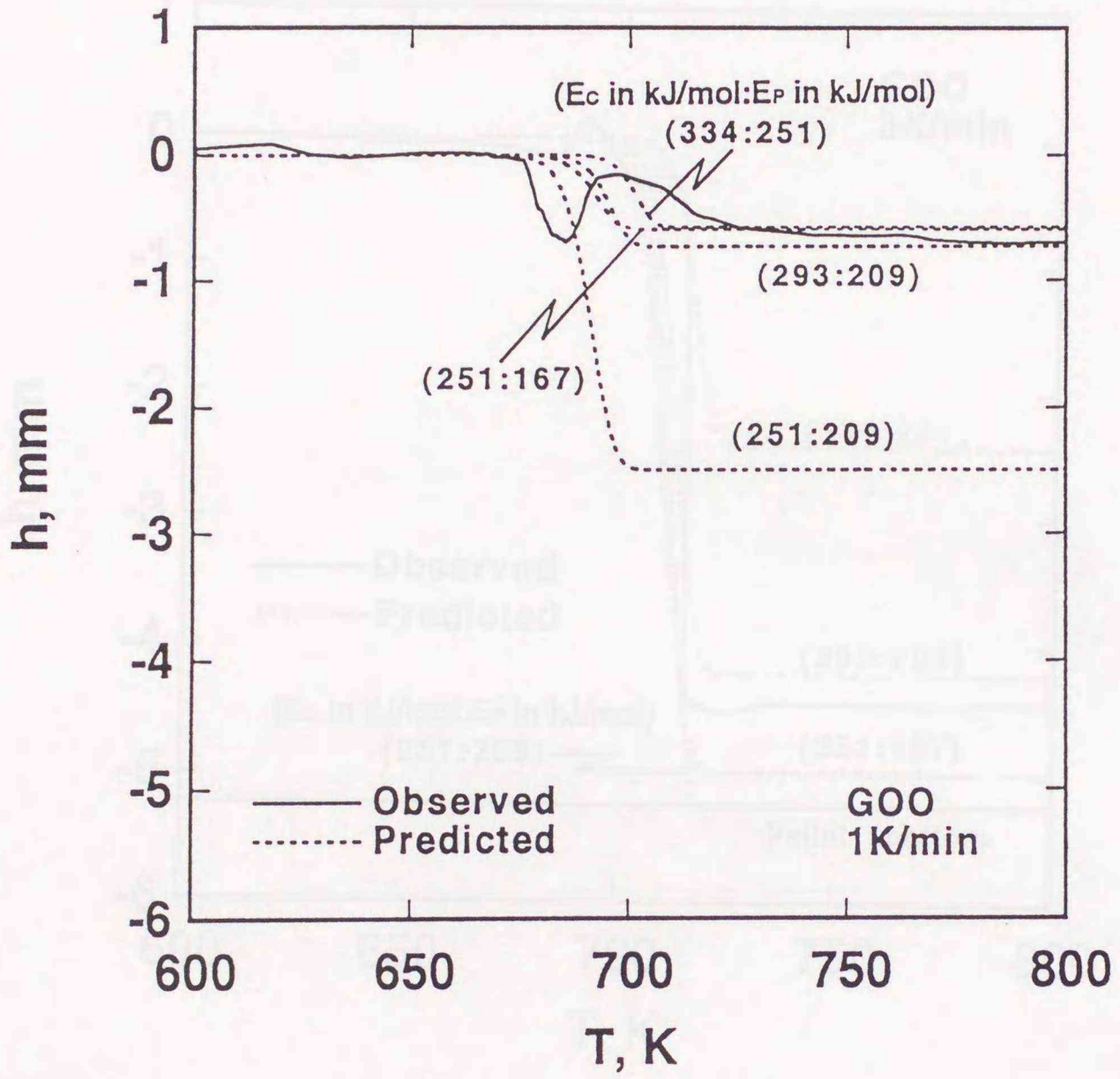

Fig. 5.4 (a) Predicted effect of E_c and E_p on penetration depth versus T for GOO coal heated at 1 K/min.

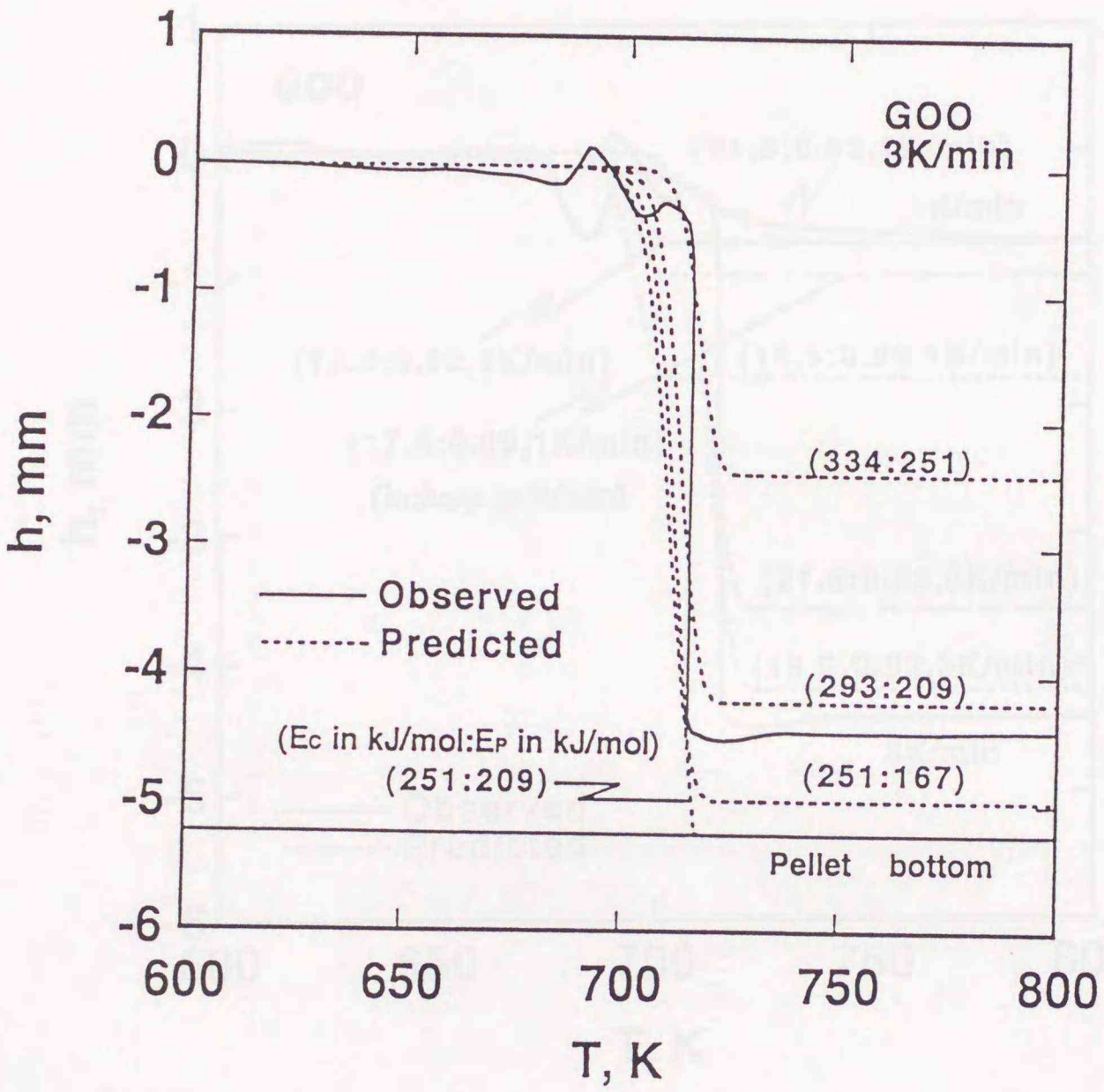

Fig. 5.4 (b) Predicted effect of E_C and E_P on penetration depth versus T for GOO coal heated at 3 K/min.

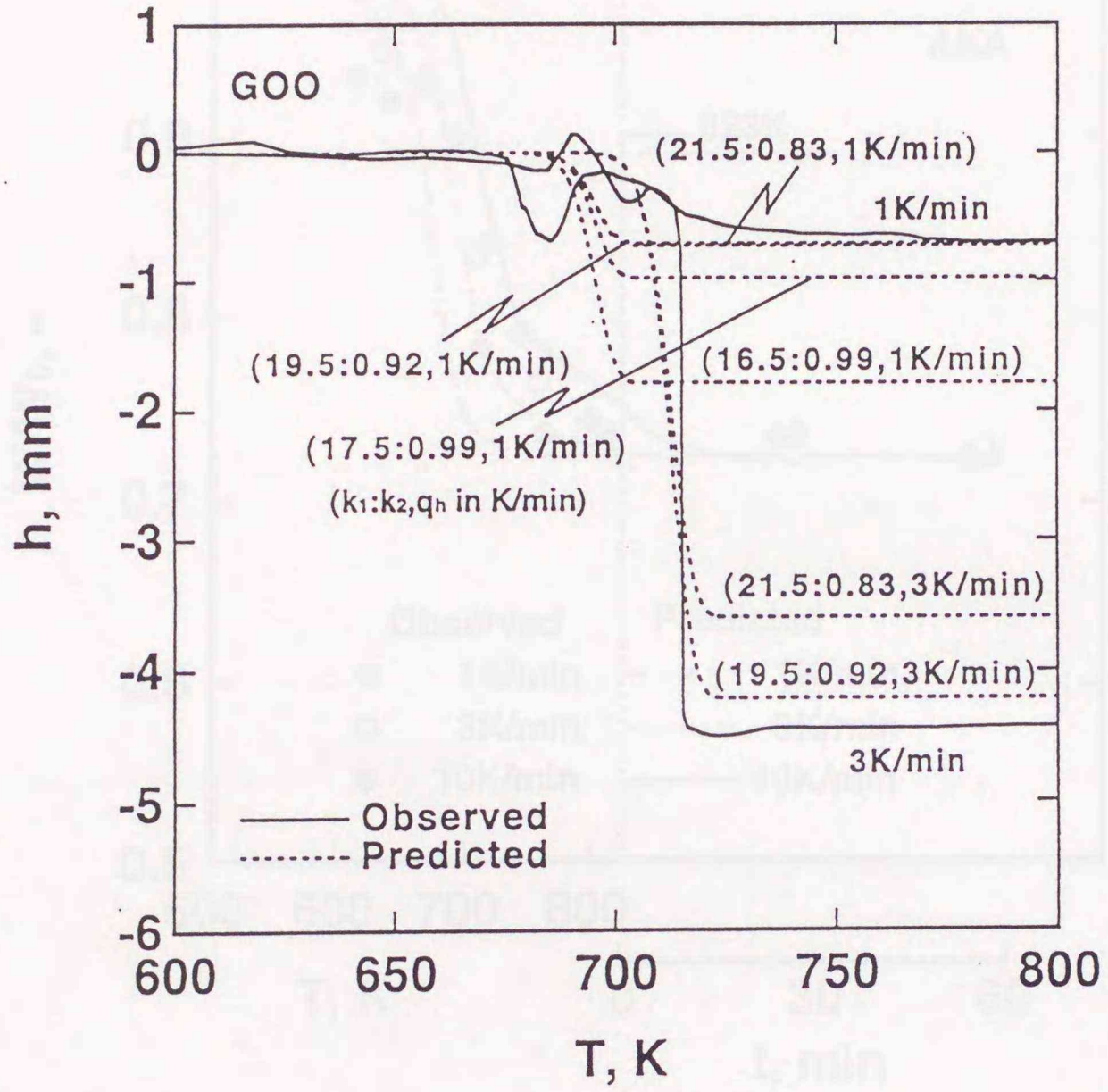

Fig. 5.5 Predicted effect of k_1 and k_2 on penetration depth versus T for GOO coal heated at 1 and 3 K/min.

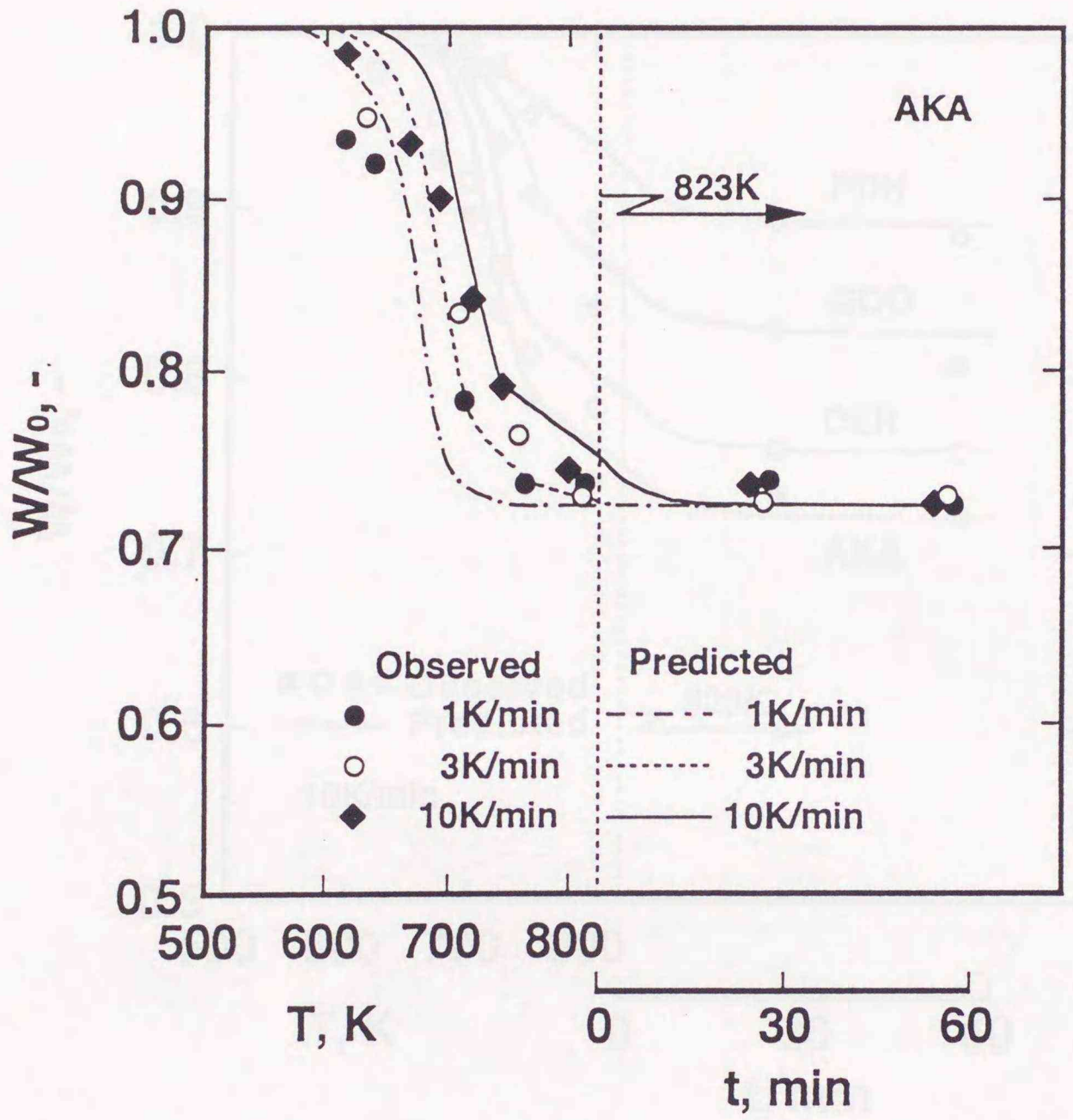

Fig. 5.6 (a) Comparison of observed mass loss curves with those predicted for GOO coal heated at different rates.

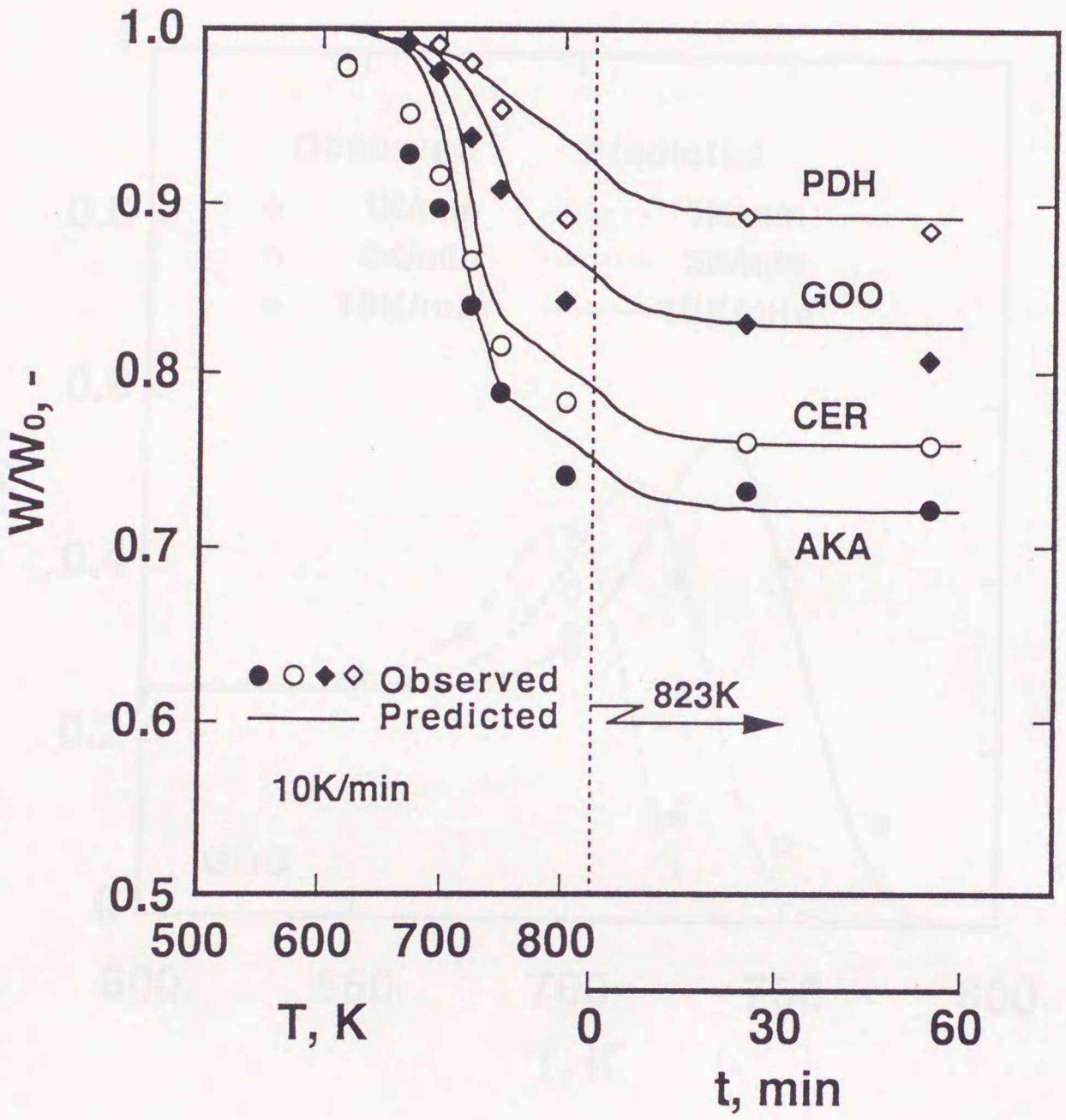

Fig. 5.6 (b) Comparison of observed mass loss curves with those predicted for different coals heated at 10 K/min.

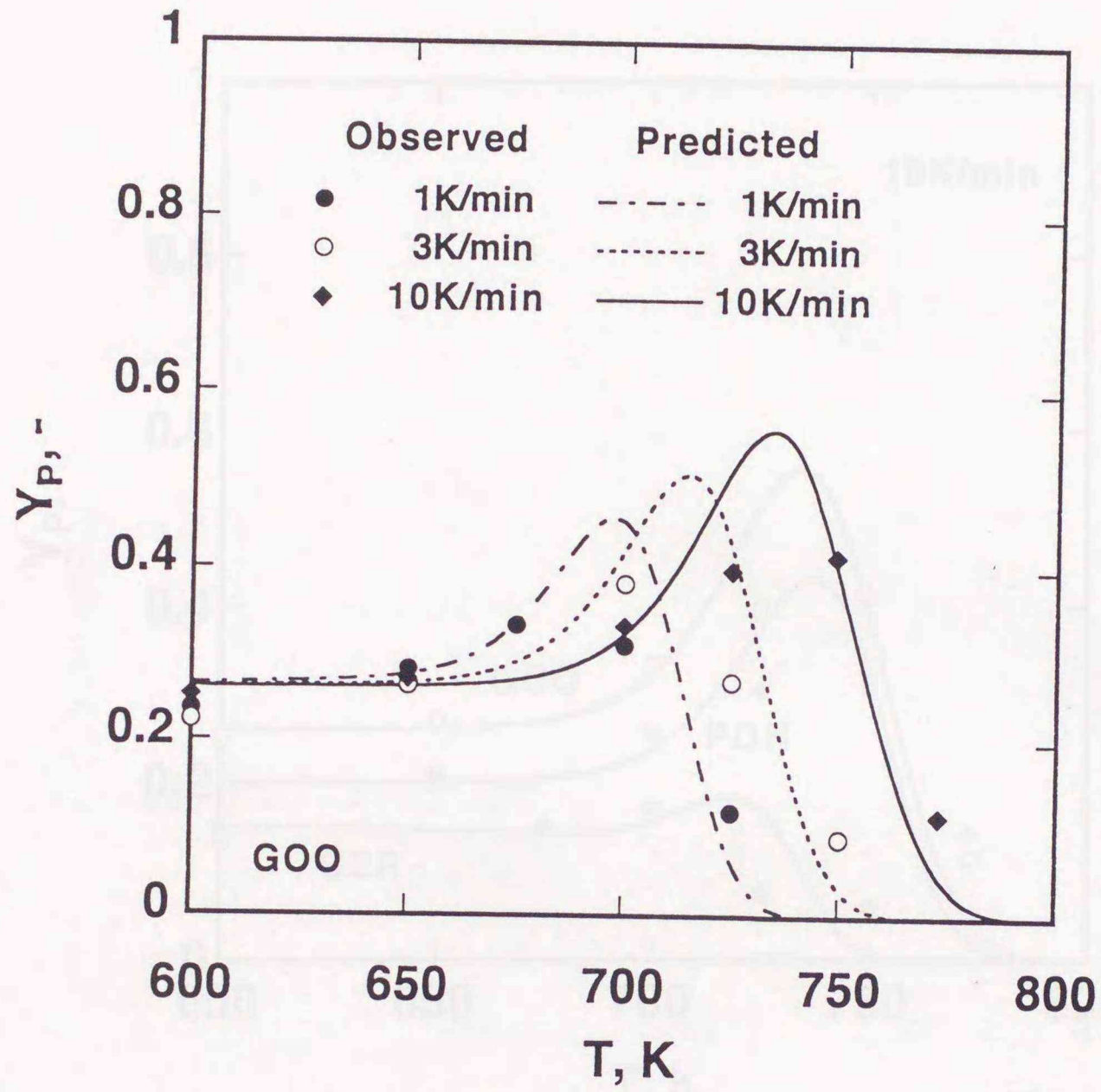

Fig. 5.7 (a) Comparison of observed Y_P with those of predicted for GOO coal heated at different rates.

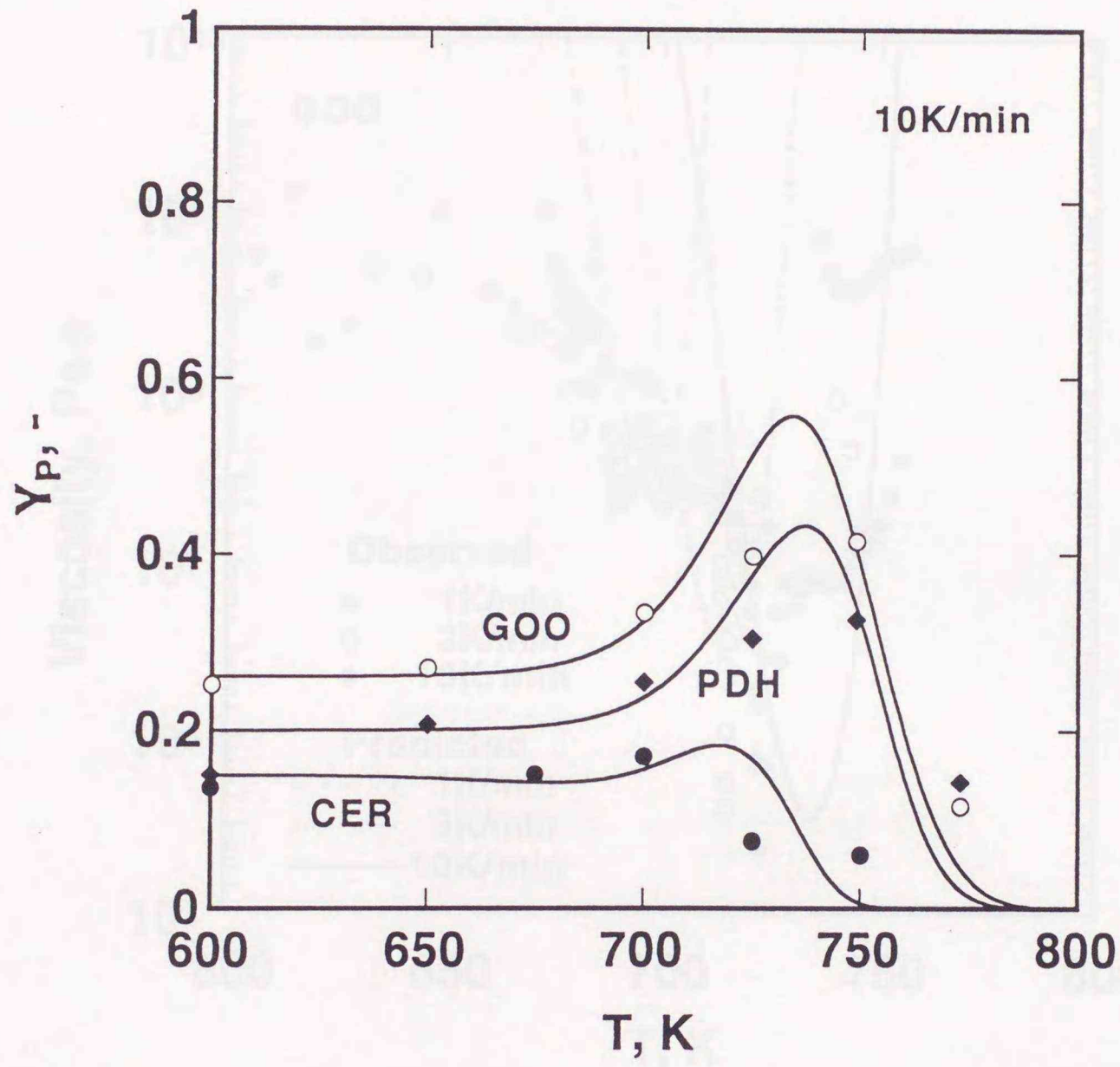

Fig. 5.7 (b) Comparison of observed Y_P with those of predicted for different coals heated at 10 K/min.

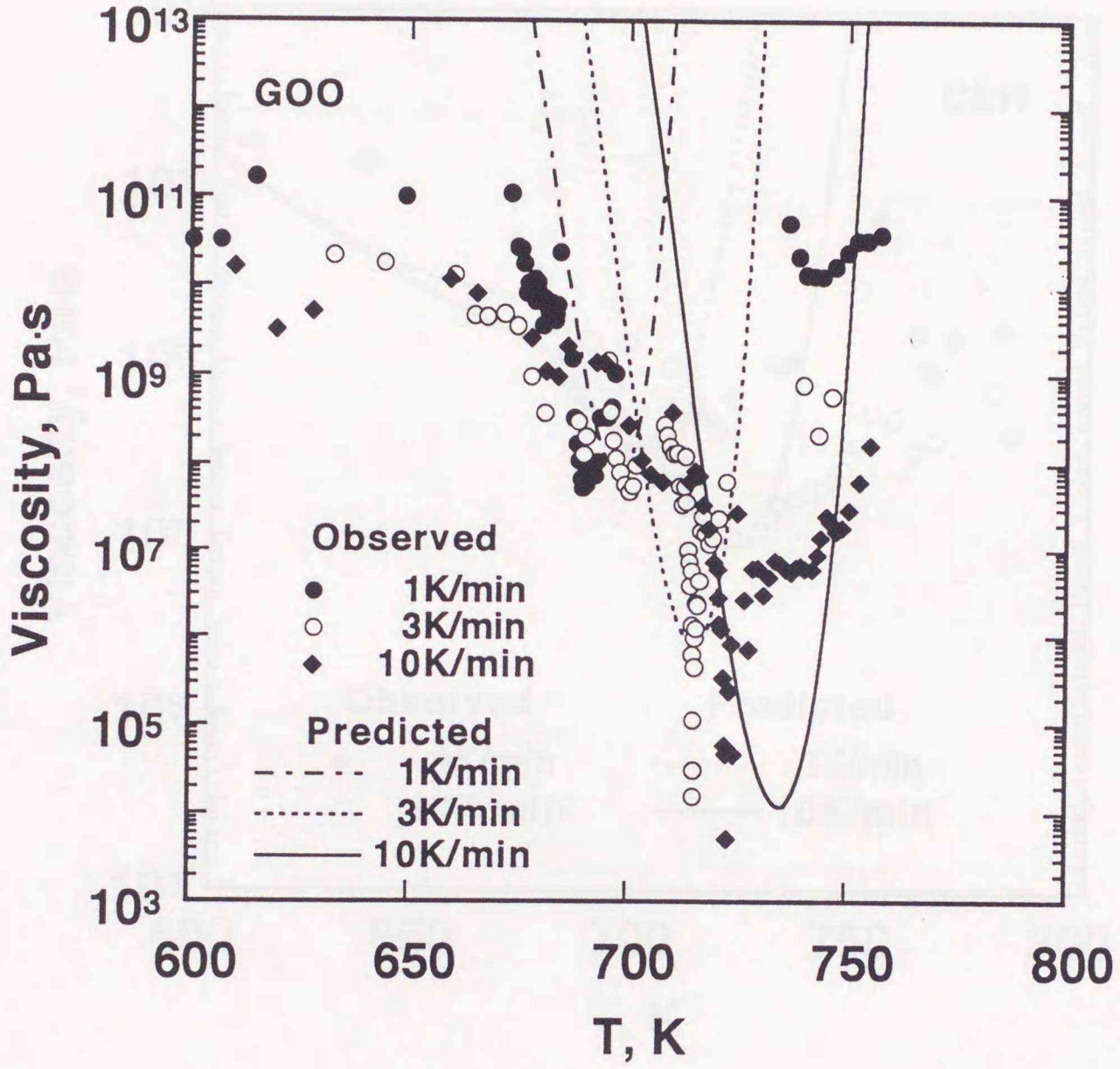

Fig. 5.8 (a) Comparison of observed viscosity with those predicted for GOO coal heated at different rates.

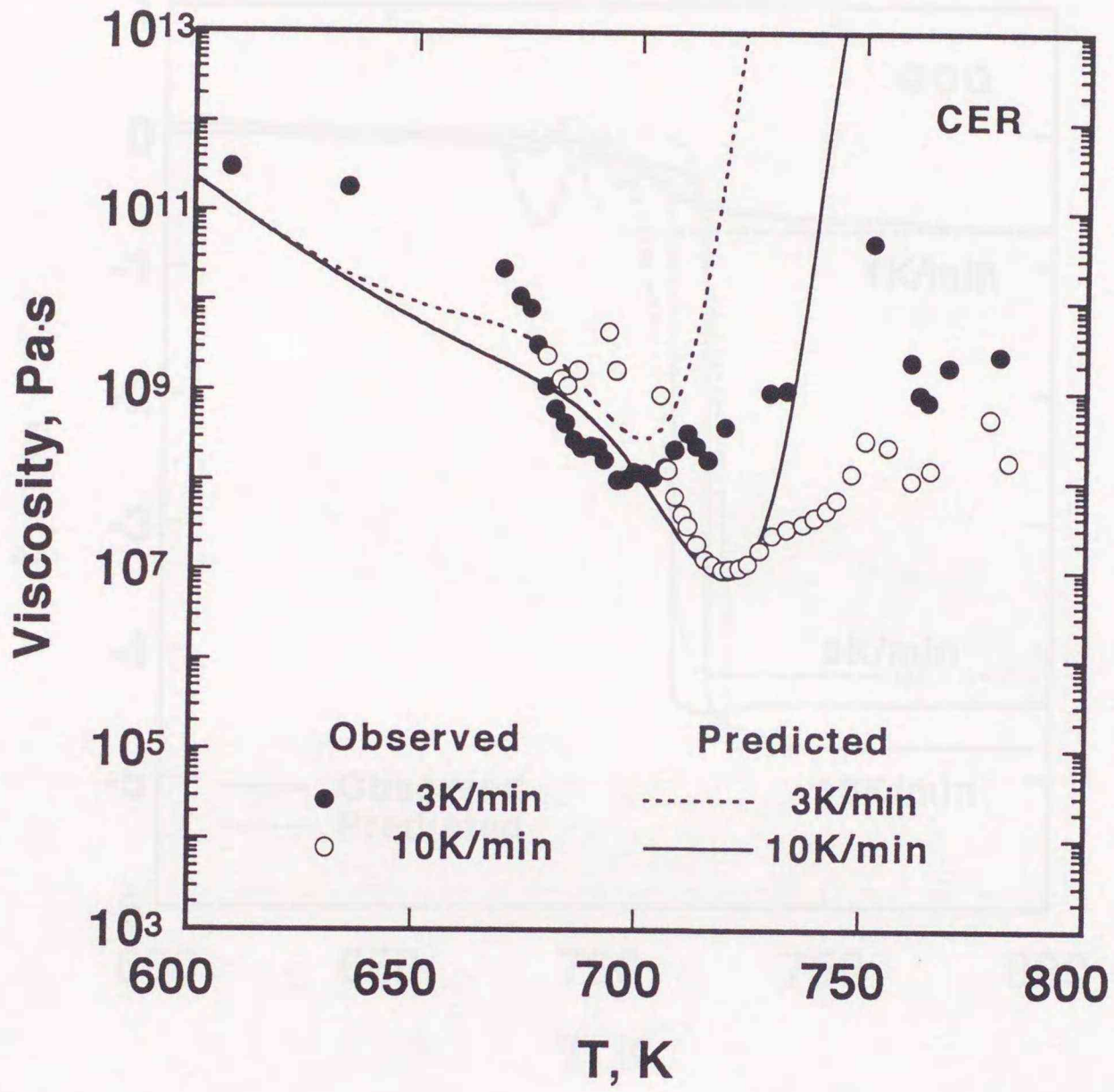

Fig. 5.8 (b) Comparison of observed viscosity with those predicted for CER coal heated at different rates.

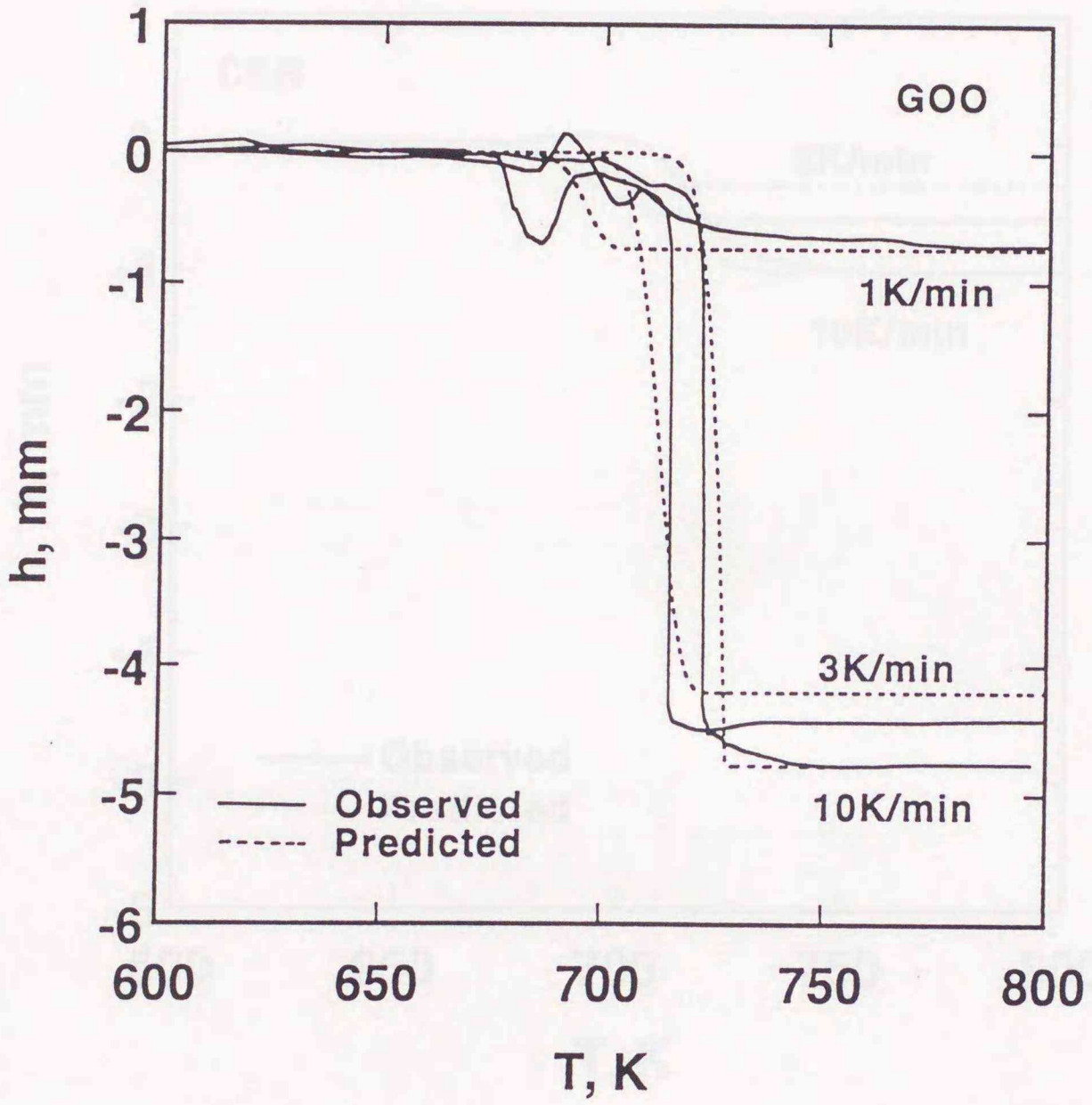

Fig. 5.9 (a) Comparison of observed needle penetration depths with those predicted for GOO coal heated at different rates.

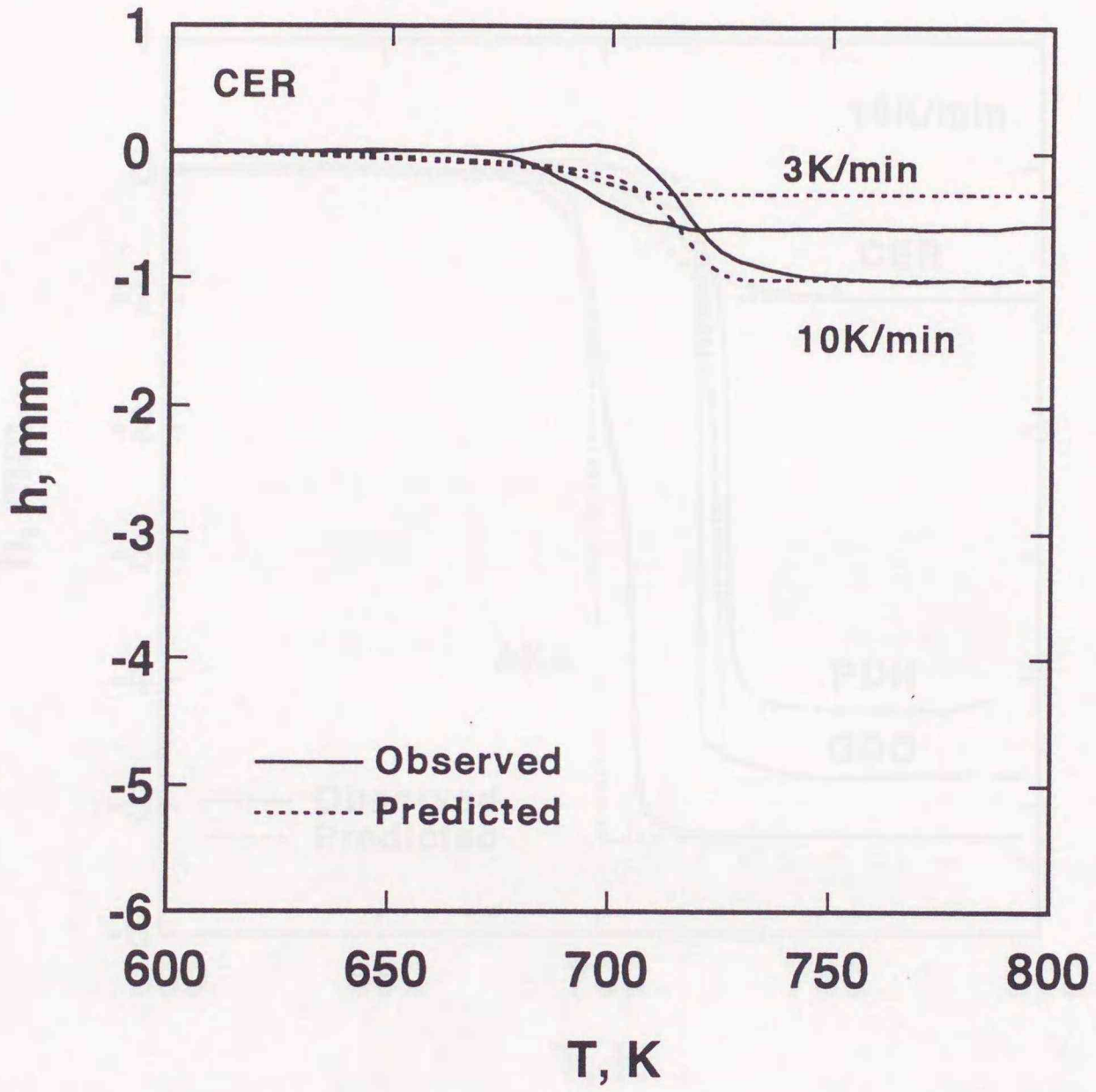

Fig. 5.9 (b) Comparison of observed needle penetration depths with those predicted for CER coal heated at different rates.

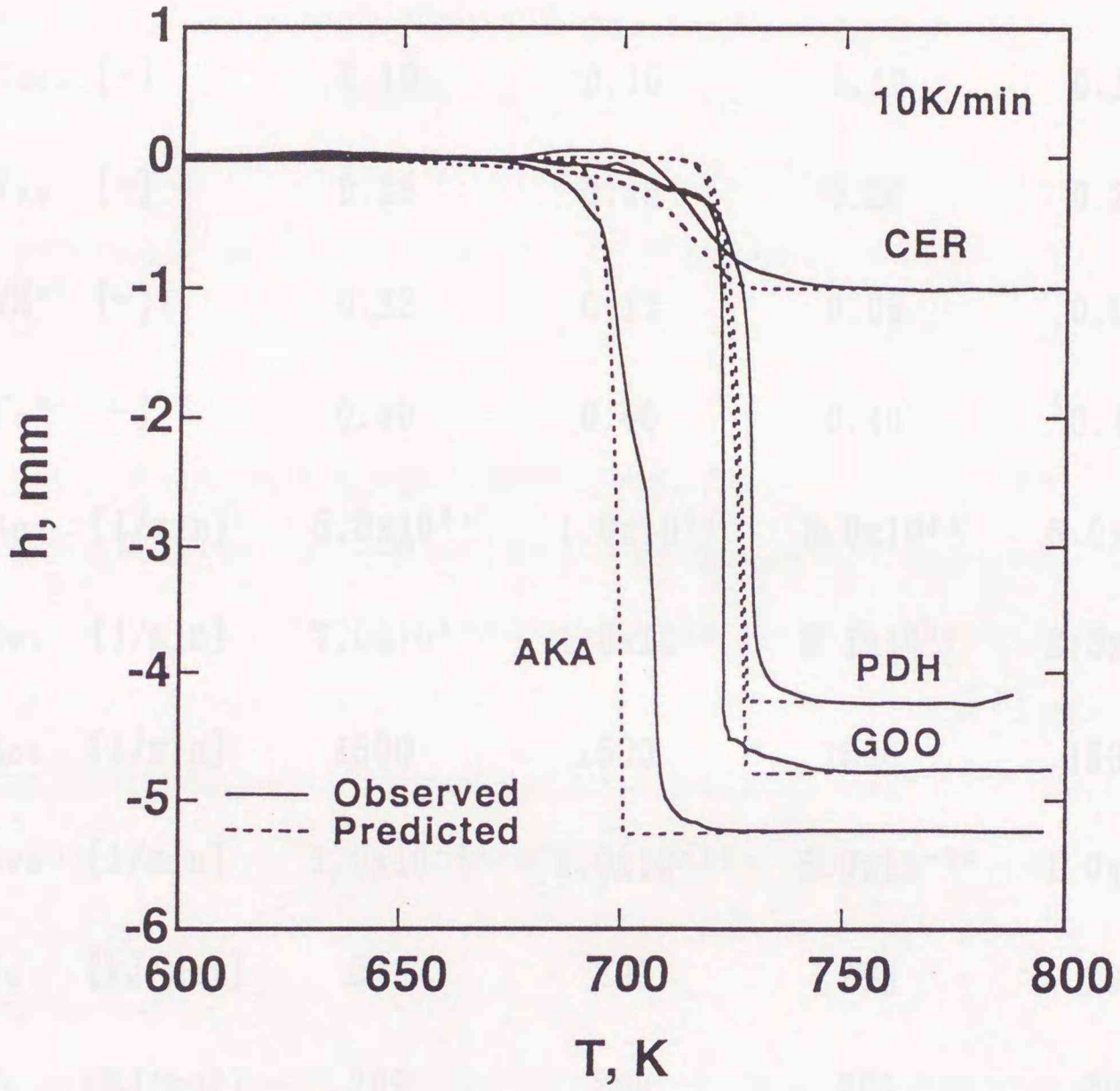

Fig. 5.9 (c) Comparison of observed needle penetration depths with those predicted for different coals heated at 10 K/min.

Table 5.1 Model parameters assumed for prediction.

	AKA	CER	GOO	PDH
Y_{CC0} [-]	0.64	0.75	0.64	0.70
Y_{CG0} [-]	0.10	0.10	0.10	0.10
Y_{P0} [-]	0.26	0.15	0.26	0.20
VM[a)] [-]	0.22	0.17	0.09	0.01
f_C[b)] [-]	0.40	0.40	0.40	0.40
k_{C0} [1/min]	5.0×10^{21}	1.0×10^{21}	8.0×10^{20}	5.0×10^{20}
k_{P0} [1/min]	7.0×10^{14}	1.8×10^{15}	2.1×10^{14}	2.8×10^{14}
k_{G0} [1/min]	1500	1500	1500	1500
k_{V0} [1/min]	1.0×10^{-21}	1.0×10^{-17}	8.0×10^{-21}	1.0×10^{-22}
E_C [kJ/mol]	293	293	293	293
E_P [kJ/mol]	209	209	209	209
E_G [kJ/mol]	63	63	63	63
E_V [kJ/mol]	251	251	251	251
k_1 [-]	19.1	4.9	19.5	15.1
k_2 [-]	0.92	0.85	0.92	0.92

a)$Y_{GC(\infty)} + Y_{GP(\infty)}$, b)$Y_{GC(\infty)}/(Y_{GC(\infty)} + Y_{GP(\infty)})$

curves using above determined parameters with those observed. It is seen that the model can explain well the observed effects of the heating rate and coal on mass fraction due to volatiles release. **Figures 5.7 (a) and (b)** show adjustment of the predicted Y_P curves to those observed. As is seen, by employing the initial values of Y_P observed as those in the prediction, the predicted results are in good agreement with those observed for all heating rates and coals. In **Figs. 5.8 (a) and (b)** comparisons are made between the predicted viscosity and that observed for GOO and CER coals heated at different rates. From Fig. 5.8 (a) it is seen that the predicted minimum viscosity disagrees with that observed. On the other hand, the predicted viscosity for CER coal which effect of the heating rate on the viscosity is less than that of GOO coal roughly agrees with that observed for different heating rates in Fig. 5.8(b). In **Figs. 5.9 (a) and (b)** the predicted needle penetration curves of GOO and CER coals (caking and weakly-caking coals) are compared with those observed at different heating rates. The model again predicts well the observed effect of the heating rate on the penetration depth. In **Fig. 5.9 (c)** the model applicability is further confirmed to the needle penetration curves for the different coals. The model explains satisfactorily well the observed effects of the heating rate and coal nature on the softening and resolidification characteristics.

5.3 Conclusions

A model is developed for description of observed effects of the heating rate and coal nature on softening and resolidification characteristics evaluated by the observed needle penetration. The model employs the equation of motion, the viscosity equation for slurry combined with that for liquid, the yield of which is described by the reaction model with the kinetic parameters independently determined from the experiments on the volatiles release and solvent extraction. The effect of the heating rate and coal nature were comprehensively described by the model on the needle penetration, volatiles release and PS formation.

References

1) D. Fitzgelard: *Fuel*, **35** (1956), 178.

2) D. Fitzgelard: *Trans. Faraday Soc.*, **52** (1956), 362.

3) D. W. van Krevelen, F. J. Huntjens and H. N. M. Dormans: *Fuel*, **35** (1956), 462.

4) W. S. Fong, Y. F. Khalil, W. A. Peters and J. B. Howard: *ibid.*, **65** (1986), 195.

5) W. S. Fong, W. A. Peters and J. B. Howard: *Rev. Sci. Instrum.*, **56** (1985), 586.

6) N. A. Frankel and A. Acrivos: *Chem. Eng. Sci.*, **22** (1976), 847.

7) H. R. Brown and P. L. Waters: *Fuel*, **45** (1966), 17.

8) T. Takanohashi, T. Yoshida, M. Iino, K. Katoh and K. Fukada: *Tetsu-to-Hagané*, **82** (1996), 366.

9) K. Ouchi, K. Tanimoto, M. Makabe and H. Itoh: *Fuel*, **62** (1983), 1227.

10) J.-i. Hayashi, T. Maezono, M. Ando, K. Kusakabe and S. Morooka: *Nenryokyokaishi*, **69** (1990), 378.

11) J.-i. Hayashi, M. Ando, K. Kusakabe and S. Morooka: *ibid.*, **69** (1990), 446.

12) P. R. Solomon, P. E. Best, Z. Z. Yu and S. Charpenay: *Energy and Fuels*, **6** (1992), 143.

13) P. R. Solomon, D. G. Hamblen, R. M. Carangelo, M. A. Serio and G. V. Deshpande, *ibid.*, **2** (1988), 405.

14) K. Matsuoka, T. Kumagai and T. Chiba: *ISIJ International*, **36** (1996), 40.

15) K. Matsuoka, H. Kawai, T. Kumagai and T. Chiba: *Tetsu-to-Hagané*, **82** (1996), 383.

16) V. Vand: *J. Phys. Colloid Chem.*, **52** (1948), 277.

17) T. Nakagawa: Rheology, 2nd ed. Iwanami Book Co., Tokyo, (1983), 118.

Chapter 6 General Summaries and Conclusions

When coal is heated over *ca.* 600 K, it undergoes pyrolysis and carbonization reactions resulting in softening and resolidification along with volatiles release. Quantitative description of these processes is an important factor for the development of novel cokemaking processes. Systematic measurements on needle penetration, mass loss and pyridine extract formation have thus been carried out as a function of the heating rate, holding temperature, gas pressure and coal natures, aiming to analyze the needle penetration characteristics and to develop a mathematical model for quantitative description of them.

In Chap. 1, the background of this study, shortcomings of existing experimental works and viscosity models as well as the purpose of the study were described.

In Chap. 2, results of systematic measurements of the needle penetration and volumetric dilation ratio with a novel needle penetrometer were described for six kinds of coals in a wide range of operating variables such as the heating rate from 1 to 50 K/min, the holding temperature from 698 to 823 K, the nitrogen gas pressure from 0.1 to 3.0 MPa. The needle penetration and dilation characteristics were found to depend on these operating variables as well as the coal nature. Especially, it was clearly indicated that the needle penetration does occur at high heating rates for coals which exhibit little softening property at low heating rates. The net needle penetration obtained from the observed needle penetration and dilation was analyzed by an equation of motion, assuming that coal behaves as a Newtonian fluid which can be solved at pseudo-steady state for a narrow temperature range. Apparent coal viscosity derived from the analysis ranged from 10^4 to 10^{12} Pa·s and was explained by the Andrade equation only within a narrow temperature range. The apparent activation energy obtained by plots arisen from Andrade's equation was over 400 kJ/mol. Such high activation energies are suggested to be due to not only physical change but also chemical reaction, namely conversion of coal to semicoke *via* a plastic intermediate.

In Chap. 3, the formation and decomposition of the intermediate were hence evaluated by different experimental methods such as a DSC, a ^{1}H NMR and solvent extraction. Increase in molecular mobility observed in the DSC was shown to correspond well to that in the yield of

pyridine extraction, implying that the extract may be responsible for the intermediate. The extract yield increased with the heating rate and the increase corresponded to decrease of the apparent viscosity. Further, the needle penetration and dilation were measured for the pellet of the extract to develop its viscosity equation. The temperature dependency of the extract was much less significant than that of the parent coal suggesting that the extract can be treated as a liquid component in softening coal and thus is defined as the intermediate.

In Chap. 4, mass loss due to volatiles release from the pellets was described, which was measured under the same conditions as the penetration experiments to determine the kinetic parameters for pyrolysis and carbonization reactions along with the needle penetration. The mass loss curves was found to shift to a higher temperature range as the heating rate increased while the total amount of volatiles release was found to be virtually independent of the heating rate. The pyrolysis model assuming that coal consists of two reactive components which convert to semicoke *via* the intermediate and directly to volatiles was shown to predict the observed mass loss curves and further explained the observed pyridine extraction yield obtained in the preceding chapter.

Chapter 5 described a needle penetration model which was developed for quantitative explanation of the observed experimental findings. The model describes the needle penetration based on the equation of motion assuming coal to behave as a Newtonian fluid. The model further assumes that pyridine extract behaves as a lubricant or liquid vehicle for solid extraction residue and ash on the basis of the observed result in Chap. 3. Thus, the softening coal is treated as a slurry and the dependency of the viscosity on solid/liquid concentration is described by Vand's equation. Furthermore, the liquid viscosity is expressed by Andrade's equation for pyridine extract as a liquid as mentioned in Chap. 3. The applicability of the present model for prediction of the needle penetration was tested, estimating the kinetic parameters independently determined from the experiment on solvent extraction and volatiles release in Chaps. 3 and 4. The effect of the heating rate and coal nature were comprehensively described by the model on the needle penetration, volatiles release and pyridine extract formation.

The needle penetration model developed in the present study contains ten parameters. Among them, eight parameters have been determined on the basis of the independent

experiments. Thus, for the moment, the two parameters, k_1 and k_2, are left as adjustable parameters in the model fitting to the needle penetration curve and a further work is needed to determine them from another independent experiment. For example, they could be determined from viscosity measurements for slurries having different concentrations of the pyridine insoluble fraction at low temperatures where pyrolysis of the pyridine extract is avoided.

As mentioned in Chap. 1, the advanced cokemaking processes aim to utilize non-caking or weakly-caking coals by blending them to caking coal. The present study can easily be extended for the blended coals and gives basic information for a proper design and optimization of the process and its operation.

Acknowledgments

The author wishes to express his highest gratitude to Prof. Tadatoshi Chiba who directed this research with the continuing suggestion which led to the completion of the research.

He thanks sincerely Profs. Kuniyoshi Ishii, Hironori Itoh and Hideshi Hattori, and Associate Prof. Jun-ichiro Hayashi for their valuable comments and advice.

He also wish to thank Dr. C.- R. Deng who initiated this research and developed the needle penetrometer.

Thanks are extended to Dr. Haruo Kumagai and Mr. Takehiko Kumagai for their daily discussion and helpful advice.

Acknowledgment is also due to the members of Prof. Chiba's Laboratory; in particular, to Messrs. Koji Kuramoto, Taihei Shimada, Hassan H. Katarambula, and Hitoshi Kawai and Daisuke Denma who carried out the experimental work.

Finally, the author wished express his great gratitude to his parents, sister and wife for their continuous encouragements, without which the present study would be impossible to be finished.

Nomenclature

a	: Pellet radius	[mm]
b	: Needle radius	[mm]
E_i	: Activation energy for reaction of i-component	[kJ/mol]
E_v	: Activation energy for viscosity	[kJ·mol^{-1}]
f_C	: = VM_C/VM	[-]
g	: Gravitational acceleration	[m·s^{-2}]
h	: Net needle penetration depth	[mm]
H	: Apparent needle penetration depth	[mm]
H_0	: Initial pellet height	[mm]
H_p	: Heated pellet height	[mm]
H_t	: Distance from bottom tip of needle to pellet bottom	[mm]
k	: = $k_P/(k_P - k_C)$	[-]
k_i	: Rate constant	[min^{-1}]
k_{i0}	: Frequency factor	[min^{-1}]
k_{V0}	: Frequency factor for viscosity	[min^{-1}]
m	: Mass of needle	[g]
P_{N2}	: Gas pressure	[MPa]
q_h	: Heating rate	[K·min^{-1}]
Q	: Relative degree of volumetric dilation	[-]
R	: Gas constant	[J·K^{-1}mol^{-1}]
t	: Time	[min]
T	: Pellet temperature	[K]
T_a	: Autoclave bottom temperature	[K]
T_s	: Holding temperature	[K]
η	: Viscosity	[Pa·s]
R	: Gas constant	[J·K mol^{-1}]
VM	: Final fraction of gas evolved	[-]

VM_i : Fraction of gas evolved from i-component [-]

W : Mass of solid residue [g]

W_{Gi} : Total mass of gas evolved from i-component [g]

Subscripts

C : Coal

CC : Coal component converted to S *via* P along with volatiles release

CG : Coal component converted to G_G

CP : Component converted from C_C to P

G : Gas

GC : Volatiles released from C_C

GG : Volatiles released from C_G

GP : Volatiles released from P

P : Intermediate

PS : Component converted from P to S

s : Steady state

S : Semicoke

0 : Initial state

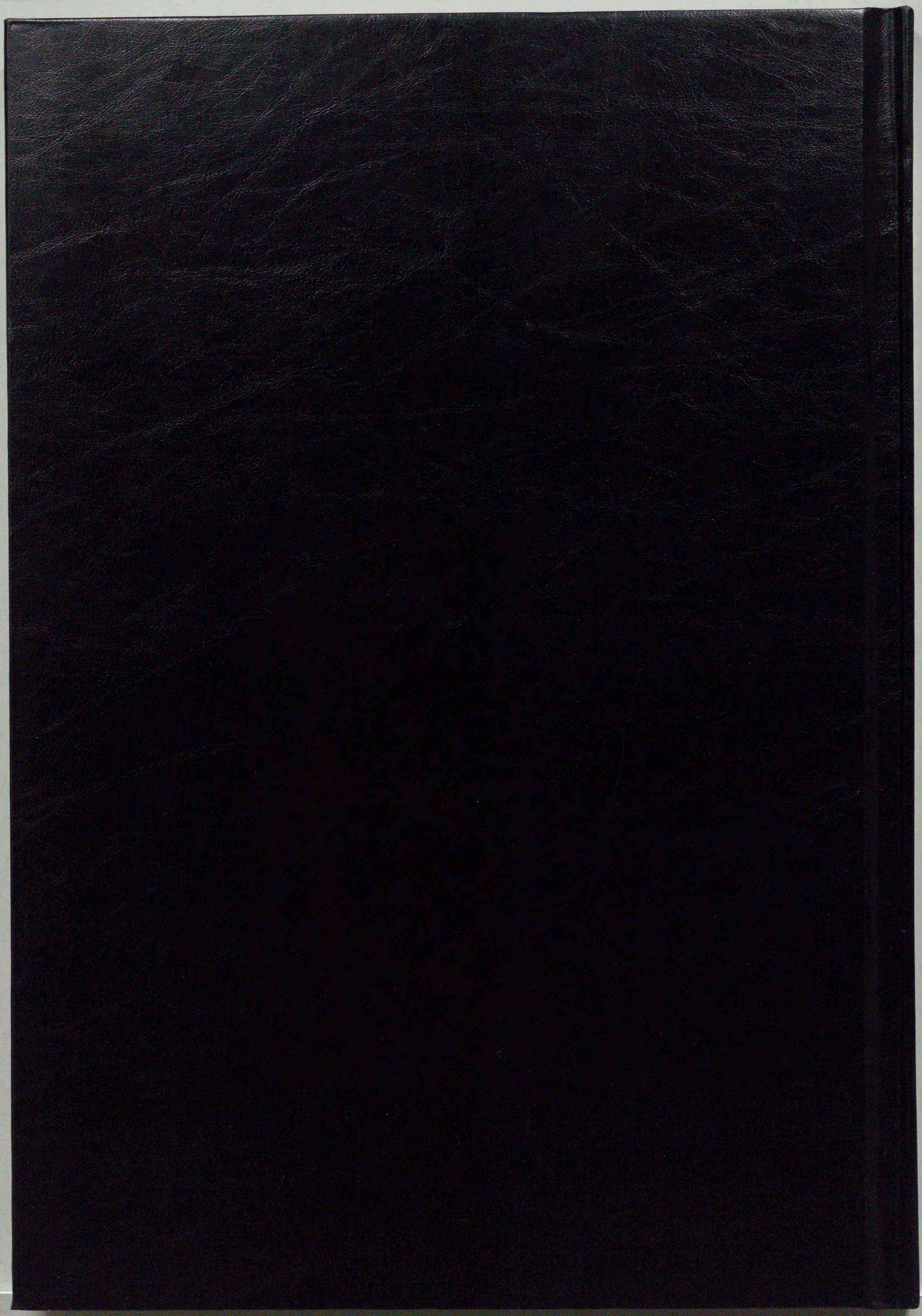

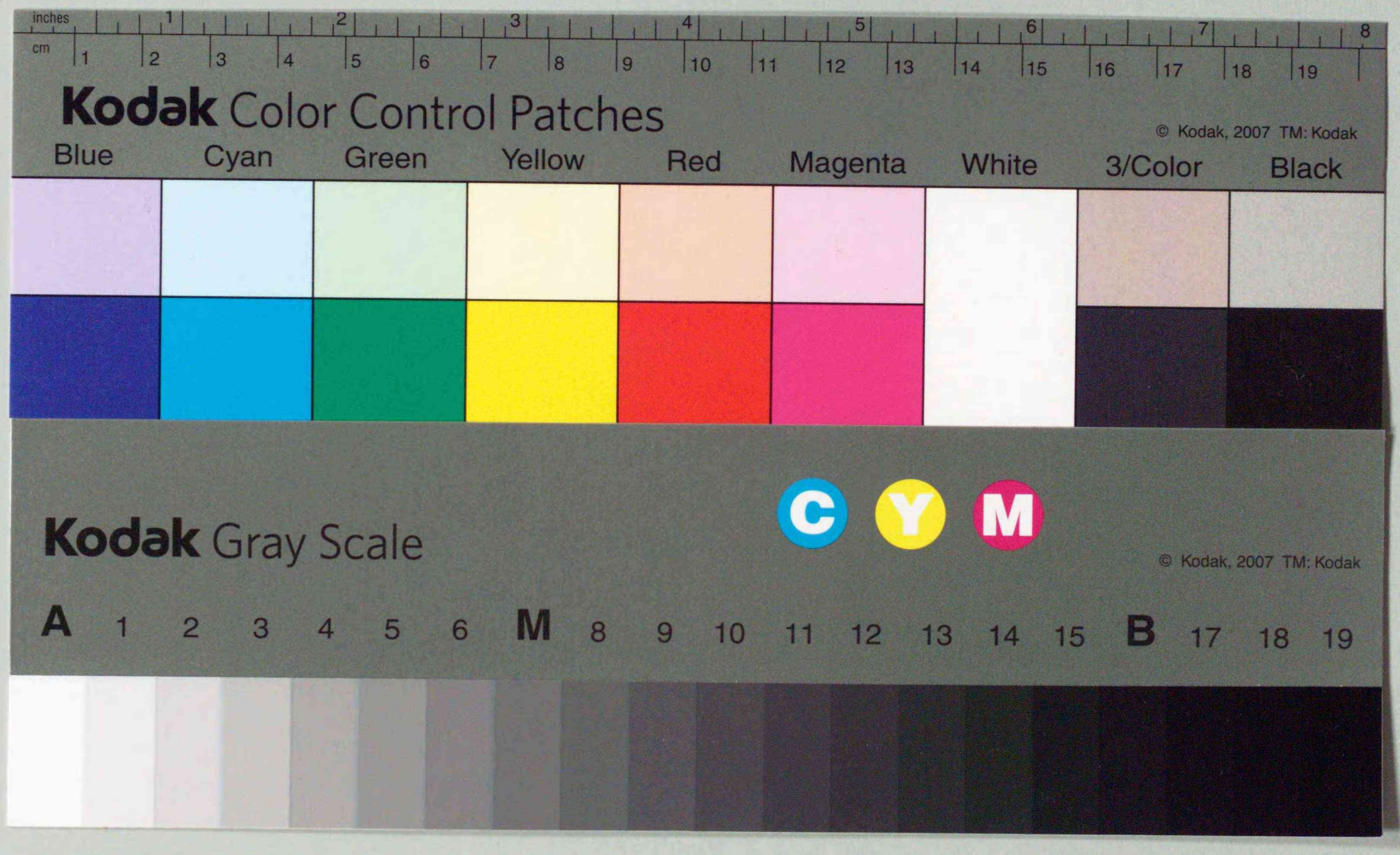
inches
cm
Kodak Color Control Patches
© Kodak, 2007 TM: Kodak
Blue
Cyan
Green
Yellow
Red
Magenta
White
3/Color
Black
Kodak Gray Scale
C
Y
M
© Kodak, 2007 TM: Kodak
A 1 2 3 4 5 6 M 8 9 10 11 12 13 14 15 B 17 18 19